Role of CXCR4 in mediating axon sprouting after local intrathecal infusion of CXCL12 in a mouse model of spinal cord injury

Inaugural-Dissertation

zur Erlangung des Doktorgrades
der Mathematisch-Naturwissenschaftlichen Fakultät
der Heinrich-Heine-Universität Düsseldorf

vorgelegt von

Federica Tundo-Lavalle
aus Maglie

Düsseldorf, Februar 2019

aus dem Labor für Molekulare Neurobiologie der Neurologischen Klinik
der Heinrich-Heine-Universität Düsseldorf

Gedruckt mit der Genehmigung
der Mathematisch-Naturwissenschaftlichen Fakultät der
Heinrich-Heine-Universität Düsseldorf

Berichterstatter:

1. Prof. Dr. Hans Werner Müller
2. Prof. Dr. Hermann Aberle

Tag der mündlichen Prüfung: 24. Mai 2019

A Mamma e Papà

SUMMARY

The regeneration of injured axons is limited in the central nervous system (CNS). The major goal of researchers is to identify the cause of CNS regenerative failure and to target these factors to promote CNS repair and regeneration, particularly, in spinal cord injured people. One therapeutic aim for example is the stimulation of regenerative axon growth of the lesioned spinal cord. The chemotactic cytokine CXCL12, also named stromal cell-derived factor 1α (SDF-1α), is disinhibitory towards CNS myelin and plays a key role during development of the nervous system. Furthermore, recent studies revealed that CXCL12 enhances sprouting of dorsal corticospinal tract (dCST) axons rostral to the lesion site in a rat spinal cord injury (SCI) model. CXCL12 reportedly interacts with two G-protein-coupled receptors, CXCR4 and CXCR7. However, which of these receptor(s) is involved in the sprouting effect is still unknown. In a pharmacological approach, by applying the CXCR4 antagonist AMD3100 on myelin cultured adult mouse DRG neurons, the involvement of the CXCR4 receptor in CXCL12 mediated neurite outgrowth *in vitro* was assessed in this study. Furthermore, the presence of the chemokine receptor CXCR4 on adult mouse DRG neurons was confirmed via immunocytochemical staining.

In order to determine the individual functional roles of the chemokine receptors in mediating the axon growth promoting and disinhibitory effects of CXCL12 after local intrathecal infusion, the initial idea of the project was to generate a mouse model with conditional knockout in the mouse dCST of CXCR4 and CXCR7 as well as the generation of receptor-deficient double mutants. As the local intrathecal infusion method is rarely used in mice due to the very thin dura mater and the narrow epidural space, a newly epidural catheterization method was established in this species. In order to investigate the sprouting effect of lesioned dCST neurons after CXCL12 treatment in conditional knockout mice, the procedure was first performed in CXCR4 wild type and ROSA floxed mice ($CXCR4_{wt/wt}$/$ROSA_{fl/wt}$). An AAV2-Cre stereotactic injection into layer V of the hind limb sensorimotor cortex to target the pyramidal neurons was used for anterograde labeling of the dCST. We found that CXCL12 infusion did neither promote sprouting of the injured dCST nor enhance functional recovery in these mice. Immunofluorescence staining of CXCR4 did not reveal presence of this receptor in the mouse dCST. In contradiction to previous publication (Opatz et al., 2009) the CXCR4 receptor could not be detected in the rat dCST. Therefore, the generation of the conditional reporter mouse was futile for the intended purpose. A subcellular localization of the CXCR4 receptor in adult mouse and rat spinal cords using immunofluorescence staining revealed that CXCR4 is expressed in the axons. According to that, CXCR4 seems to be expressed in subtypes of neurons, such as spinal motoneurons, but not in CGRP-positive sensory neurons. Furthermore, it is expressed in some glial cells, such as oligodendrocytes, but not in astrocytes. Due to the absence of a commercially available and suitable antibody directed against the second CXCL12 receptor CXCR7 the involvement of the latter could not be analyzed as planned. *In situ* hybridization studies confirmed the absence of CXCR4 receptor expression in layer V neurons of adult mouse and rat brains. However, CXCR7 and CXCL12 mRNAs were expressed in these neurons. Additionally, no injury-dependent increase was observed in the mRNA expression of CXCL12 and its receptors. Hence, the results suggest that other mechanisms rather than direct ligand-receptor interactions are responsible for CXCL12-mediated neurite sprouting in the rat spinal cord.

CONTENTS

LIST OF FIGURES

LIST OF TABLES

1. INTRODUCTION

1.1. The intact spinal cord

1.1.1 The spinal cord anatomy

The mammalian nervous system is a complex network that transmits messages between the brain and spinal cord and various parts of the body. It is divided into the central nervous system (CNS, brain and spinal cord) and the peripheral nervous system (PNS, autonomic and somatic nervous system). The brain and the spinal cord, the two main components of the CNS, are both protected within the cranial cavity of the skull and the vertebral column, respectively. The brain, as well as the spinal cord are surrounded by the meninges, which consist of three layers (Fig. 1.1 A) (Watson and Kayalioglu, 2009). The innermost pia mater, which adheres to the surface of the spinal cord, the intermediate arachnoid mater, a thin membrane named like this because of its spider web-like appearance and the outermost dura mater, a tough and dense membrane. These layers are all separated from each other by the subdural and subarachnoid spaces. The meninges enclose the cerebrospinal fluid (CSF), which circulates in the subarachnoid space and acts as cushion to protect the precious nerve tissue against damage. The spinal cord, which is divided into four regions each of which comprises several segments (Humans: cervical, C1-C7; thoracic T1-T12; lumbar L1-L5 and sacral S1-S5 / Rodents: cervical, C1-C7; thoracic T1-T13; lumbar L1-L6 and sacral S1-S4), is composed of white and gray matter. The gray matter, which contains mainly neuronal cell bodies, is arranged in the form of a “butterfly” or the capital letter “H”. The dorsally projecting arms of the gray matter are called the dorsal horns and the ventrally projecting arms are called the ventral horns (Fig.1.1 A) (Watson and Kayalioglu, 2009). The commissural gray matter, which is comparable to the cross bar of the H, contains the central canal filled with CSF. Surrounding the central canal is a single layer of cells, the ependymal cell layer, which give rise to all neurons and macroglial cells (astroglia and oligodendroglia) in the spinal cord (Saker et al., 2016). In the white matter of the spinal cord, millions of long nerve fibers, grouped together in different bundles of ascending and descending tracts, as well as propriospinal pathways, are running longitudinally connecting the brain with the rest of the body (Fig. 1.1 B). The ascending tracts transmit sensory information such as touch, pain and temperature from the sensory receptors to the brain (Kayalioglu, 2009a). In contrast, descending tracts, which carry information from the brain downwards, play an important role in the initiation of movements of the limbs and

trunk, including grasping, locomotion, respiration and posture maintenance (Watson and Harvey, 2009). The propriospinal tract axons, that originate from spinal cord gray matter interneurons and terminate on other spinal cord gray matter neurons, form local circuits and allow signal modulation in the different spinal cord segments (Conta and Stelzner, 2009). The information flow from the CNS to the muscles or target organs and *vice versa* is transmitted via spinal nerves that arise at the spinal cord at regular intervals (Fig.1.1 A) (Kayalioglu, 2009b). The spinal nerves are attached at the spinal cord by a group of ventral rootlets, which consist of axons of motoneurons and dorsal rootlets, made up of axons of sensory neurons. The cell body of each sensory neuron in the dorsal rootlet is located in the dorsal root ganglion (DRG), in close proximity to the junction of ventral and dorsal roots. These cells are pseudo unipolar primary sensory neurons that display a single axon, which divides into a peripheral branch that carries sensory information from the body to the DRG cell body and a central branch that further transfers the information from the DRG cell body to the spinal cord.

1.1.2 The descending corticospinal tract

Among mammals the anatomy of the spinal tracts is mainly conserved. The only tract that varies significantly is the biggest and main descending tract, the corticospinal tract (CST) (Fig. 1.1 B) (Watson and Harvey, 2009). The CST originates from the pyramidal corticospinal neurons in layer V of the motor cortex. In rodents, this area is not well defined as in humans, where the sensory cortex and the motor cortex are separated areas and the CST originates here from the so-called sensorimotor cortex. These neurons, which can be specifically identified through key factors, such as Fezf2 (forebrain embryonic zinc finger protein), Ctip2/Bcl11b (B-Cell CLL/ Lymphoma 11B – a transcription factor functioning downstream of Fezf2) and Sox 5 (Arlotta et al., 2005; Molyneaux et al., 2015), project their axons to the spinal cord via the pyramidal tracts. The vast majority of these CST axons cross the anatomical midline at the junction between the brainstem and the spinal cord (pyramidal decussation), terminating predominantly in the contralateral side of spinal cord. Therefore, the left side of the brain controls the right side of the spinal cord and *vice versa*. In rodents, the decussated CST is mainly located in the most ventral part of the dorsal funiculus between the dorsal horns (dorsal CST, dCST) and in rats a very small component of the un-decussated CST runs in the ventral funiculus (ventral CST, vCST) (Joosten et al., 1992). However, in higher mammals and humans, large parts of the decussated CST descend in the dorso-lateral funiculus of the spinal cord, contralateral to the hemisphere of origin (latereal CST, lCST) while uncrossed CST axons can be found in the ventral and dorso-lateral CST of the ipsilateral spinal cord (Fig. 1.1 B) (Watson and Harvey, 2009). CST axons leave the white matter to enter the gray matter and form synapses with other neurons. CST terminals are glutamatergic. In humans, pyramidal neurons terminate in the intermediate and ventral horn (Rexed's laminations V-VIII and IX), connecting in the gray matter to α-motoneurons (Watson and Harvey, 2009). In contrast, in rodents CST terminals are found mainly in the intermediate and dorsal horn of the spinal cord (Rexed's laminations I-VII). Also, contrary to primates, rodents lack the direct corticospinal connections to motoneurons, which are located in the ventral horn (namely direct cortico-motoneuronal connections). In rodents, motor commands are transmitted to motoneurons by segmental interneurons and propriospinal neurons (Alstermark et al., 2004). Apart from the CST, which particularly controls fine voluntary movements of distal musculature (e.g., fingers), motoneurons receive multiple inputs through the rubrospinal tract (RST), which

plays a role in general locomotion and in more skilled motor tasks together with the CST (Fig. 1.1 B) (Watson and Harvey, 2009).

1.1.3 Other descending and ascending tracts in the spinal cord

The RST originates from the nucleus ruber in the midbrain. Its decussated projections run in the lateral regions of the dorsal spinal cord . The RST projections terminate on gray matter interneurons in Rexed`s laminae V, VI and in the dorsal part of lamina VII (Watson and Harvey, 2009). Only a small proportion has been found to project directly onto motoneurons (lamina IX) (Küchler et al., 2002). RST axons release glutamate as neurotransmitter. Other descending tracts in the spinal cord are the reticulospinal tract (ReST), which plays a role in the preparation of movements and postural control; and the vestibulospinal tract (VeST), which is responsible for the initiation of limb and trunk extensor activity and is important for posture (Fig. 1.1 B) (Watson and Harvey, 2009). In contrast to the descending tracts in the spinal cord, which are all involved in motor control, the ascending tracts transmit somatosensory information such as pain, temperature, position sense and touch as well as pressure, pain and visceral information from internal organs from the spinal cord to the brain via axons of the DRGs (Kayalioglu, 2009a). The gracile and cuneate tracts as well as the spinothalamic tract and the spinocerebellar tract belong to the major ascending pathways in the spinal cord (Fig. 1.1 B).

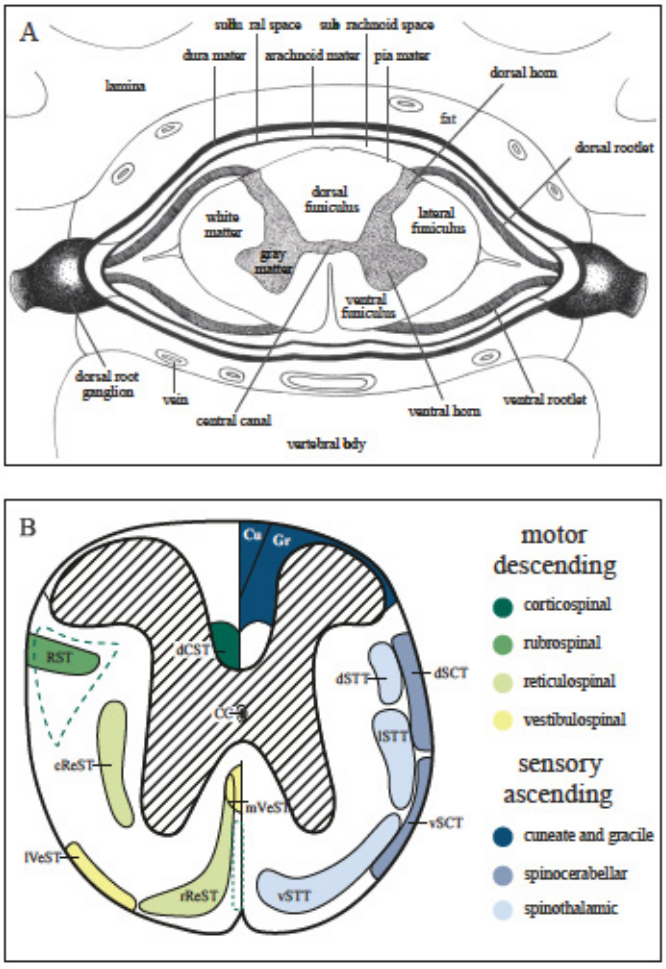

Fig. 1.1: Spinal cord anatomy.
A) Transverse section of the spinal cord surrounded by the meninges, the innermost pia mater, the intermediate arachnoid mater and the outermost dura mater. The dorsal root ganglion, where the cell body of each sensory neuron in the dorsal rootlet is located lies in close proximity to the junction of the ventral rootlet, which consists of axons of motoneurons. Modified from Kayalioglu, 2009b. **B)** Schematic representation of the major spinal cord tracts in the mouse. Transverse spinal cord section with the main the main descending motor tracts on the left and ascending sensory tracts on the right. Dashed lines indicate the location of the corticospinal tract in humans. CC, central canal; cReST, caudal reticulospinal tract; Cu, cunate fasciculus; dCST, dorsal corticospinal tract; dSCT, dorsal spinocerebellar tract; dSTT, dorsal spinothalamic tract; Gr, gracile fasciculus; lSTT, lateral spinothalamic tract; lVeST, lateral vestibulospinal tract; mVeST, medial vestivulospinal tract; rReST, rostral reticulospinal tract; RST, rubrospinal tract; vSCT, ventral spinocerebellar tract; vSTT, ventral spinothalamic tract.

1.2. The injured spinal cord

1.2.1 Demographics

A traumatic spinal cord injury (SCI) is an event that is usually sudden and unexpected. The abrupt axotomy of the nerve fiber tracts not only results in loss of sensory, motor or autonomic function below the level of injury but also directly affects the psychological well-being and the quality of life of the patients and their affiliated. The kind of disability correlates with the severity of the injury, which is determined by a five-level (A-E) American Spinal Injury Association (ASIA) impairment scale, an international standard classification (Bickenbach et al., 2013; Kirshblum et al., 2011). Thereby, level A is a complete SCI and E denotes normal sensory and motor function. Injuries at the cervical level (below the origin of the phrenic nerve) cause paralysis in both the upper and lower limbs, known as tetraplegia, whereas injuries in the thoracic region cause paralysis in the lower limb, which is called paraplegia. The majority of SCI are preventable. In developed countries, the proportion of SCI derived from motor vehicle accidences is stable/decreasing but it is increasing in developing countries due to poor infrastructure and non-standard vehicles and regulations. In regions of conflict, where the availability of weapons is high, violence, gunshot and knife injuries occur more frequently. Furthermore, as a result of an ageing population the incidence of falls in older people causing SCI is growing. Sports-related accidents, especially diving injuries belong as well to the major causes of SCI (Bickenbach et al., 2013; Lee et al., 2014). Worldwide, more than 2.5 million people suffer from paralysis caused by SCI and between 250 000 and 500 000 new injuries are reported each year (Bickenbach et al., 2013). Although the total numbers are small compared to cancer, coronary artery disease, stroke, dementia and multiple sclerosis, the economic impact of SCI on health care and the financial burden on patients is very high. During World War II, the life expectancy of SCI patients was about three month due to wound infections and long-term complications; including pressure ulcers, bladder, bowel and renal dysfunction and respiratory problems. Currently, with the recent advances in neuroscience and health care, the life expectancy of spinal cord injured patients is close to uninjured people. This however leads to long-term medication and rehabilitative care of patients which is associated with high costs for hospitalizations, home modifications and attendant care (Bickenbach et al., 2013). All these factors have driven the attention of scientists to develop regenerative therapies for SCI. Nevertheless, until now, there is no curative therapy available for SCI, but various rehabilitative, cellular and molecular therapies have been tested on animal models.

1.2.2 Rodent spinal cord injury models

In the last decades a large number of experimental animal models of SCI have been developed. Not only the comparability to human SCI is a criterion for the best choice of an SCI model, but also the experimental aim of a particular investigation plays a very important role. Parameters such as the animal species (e.g., mouse or rat), the level of injury (e.g., cervical or thoracic), the type of injury (e.g., contusion or transection), the different methods to induce a SCI (e.g., vibraknife or clip) and the injury term (acute or chronic) determine the best suitable animal model to achieve the experimental goal (Talac et al., 2004; Vogelaar and Estrada, 2016). Nevertheless, there are certain limitations when the efficacy and safety of possible SCI treatments tested in

animal models are assessed in humans. Indeed, there are many differences such as the size, gait, neuroanatomical, neurophysiological and behavioral differences as well as differences in immunological and inflammatory responses following SCI in human as compared to animals. Additionally, from the ethical point of view, it is extremely difficult to perform experiments on paralyzed human patients. Therefore, animal models are fundamental to better understand the cellular and molecular processes after SCI, and based on this information to develop new therapies. To date, it is known that most human traumatic SCI resemble a contusion/compression injury animal model. The dura mater is mostly still intact, the spinal cord is mainly compressed and lacerated; sometimes transected due to the fragments of broken bones, and hematoma and swellings start to form inside the closed vertebral canal. However, it is more convenient to study nerve regeneration in a transection injury model with a clear cut to unambiguously demonstrate regenerated axons and identify therapies, which can be afterwards tested in contusion models. If regeneration fails in a transection injury model, then it is expected to fail also in a contusion injury model. Complete transections, very reproducible injuries, are useful to investigate the effect of treatments in promoting axonal regeneration and functional recovery. Partial injury models, such as a dorsal or a lateral hemisection, are useful in assessing the effects of treatments aimed at promoting axonal regeneration and/or sprouting from spared axon tracts. This method allows the transection of individual groups of axons within the spinal cord and a less intensive postoperative animal care is needed. Compared to a complete transection, which is highly reproducible, a partial injury is inherently variable and needs an experienced surgeon. Contusions and compression injury models are considered to resemble human SCI more than transection injuries. This model is frequently used to investigate the occlusion of the central canal and the efficacy of cell transplantation (replacement) into the newly formed cyst at the lesion site, two common symptoms of SCI in human patients. Another very important parameter in the choice of a best suitable SCI model is the type of animal. Concerning the low maintenance costs, the easy animal care, the well-established functional analysis techniques and animal availability, the rat is the most commonly used animal model. Albeit cats, guinea pigs, fish, pigs and murine animal models are used in the SCI research field. Despite their small size, mice are getting more attractive as alternative to rats, since the murine genome can be easily manipulated and complex molecular events can be studied more in detail. For the present study, a dorsal hemisection of the CST was used to investigate axonal sprouting in a transgenic mouse model.

1.2.3 Pathophysiology of spinal cord injury

An initial mechanical insult of the spinal cord, such as a contusion, compression or laceration is characterized by the disruption of the neuro-glia tissue and the damage of blood vessels. The pathophysiological events after SCI are summarized in figure 1.2 A. Within minutes (acute phase) hemorrhage occurs and the spinal cord swells leading to hypotension and ischemia (deprivation of oxygen) (Mann and Kwon, 2007; Stichel and Müller, 1998). Through significant electrolytic shifts, the neurons fail to propagate action potentials along axons, contributing to spinal shock. The primary injury initiates a complex set of pathophysiological processes within minutes to weeks after injury (subacute phase), which spread further the damage and affect areas that initially were not affected in a process called secondary injury (Mann and Kwon, 2007; Stichel and Müller, 1998). The release of toxic chemicals such as glutamate and aspartate from damaged cells as well as the oxidative stress through the production of free radicals and lipid peroxidases contribute to

necrosis of cells (Bareyre and Schwab, 2003; Stichel and Müller, 1998). Additionally, infiltrating immune cells such as neutrophils, lymphocytes, macrophages and microglia, which secrete a variety of cytokines and growth factors, have both, reparative and destructive roles in the injured spinal cord. In the chronic phase, which occurs over a time course of days to years after injury, neurons and oligodendrocytes die, resulting in axonal demyelination and disruption of synaptic transmission. Astrocytes, precursor cells as well as vascular endothelial cells die too, and glial scarring, cyst formation and progressive expansion of the injury develop (Bareyre and Schwab, 2003; Stichel and Müller, 1998).

1.2.4 Neural response to injury

For many years, it was believed that lesioned CNS neurons, in contrast to PNS neurons, are incapable of regeneration leading to irreversible functional deficits (Ramón y Cajal, 1928). Several years later, the group of Aguayo in 1981 disproved this dogma, demonstrating that PNS axons fail to grow in a CNS milieu, but CNS axons are able to regenerate when the CNS environment is replaced by a peripheral nerve graft (Aguayo et al., 1981; Benfey and Aguayo, 1982; David and Aguayo, 1981; Richardson et al., 1980). In this experiment, Aguayo and his colleagues proved that CNS neurons have the intrinsic capability to regenerate, however their growth is impaired by the non-permissive local environment in the CNS. Since then much effort is spent to understand the pathophysiological mechanisms ongoing after spinal cord injury, to identify inhibiting factors responsible for axonal regeneration failure and to develop potential therapy strategies. The poor axonal regeneration is characteristic for the mammalian CNS and stands in a sharp contrast with the situation observed in fish, amphibian and the embryonic nervous system where long-distance axon regeneration and functional recovery can occur (Cohen et al., 1988; Ramón y Cajal, 1928; Sharma et al., 1993). Actually, this opposition is based on a different neuronal response of the adult CNS or PNS to traumatic SCI (Huebner and Strittmatter, 2009; Vargas and Barres, 2007). In both nervous systems, the axotomized axons, which are separated from the neurons cell bodies, undergo Wallerian degeneration (Waller, 1850). Thus, the axon is fragmented and disintegrated distal to the injury in an active process.

The first key difference between the PNS and the CNS is the time frame, within which the cell debris are removed by glial cells. In the PNS the removal of the myelin-associated inhibitory proteins by macrophages and Schwann cells is very rapid and efficient (7-14 days). In contrast, the phagocytic capacity of the microglia and oligodendrocytes in the CNS is reduced and myelin debris persists years after axon degeneration (Bosse, 2012; Vargas and Barres, 2007). Therefore, the injured neurons within CNS are exposed for a prolonged time to a growth inhibitory environment formed by oligodendrocyte derived myelin-associated inhibitors such as, NogoA (Chen et al., 2000), myelin-associated glycoprotein (MAG) (Mukhopadhyay et al., 1994), oligodendrocyte-myelin glycoprotein (OMgp) (Wang et al., 2002), Semaphorin4D (Sema4D) (Moreau-Fauvarque et al., 2003) and Ephrin B3 (Benson et al., 2005). While all these inhibitors were discovered in CNS myelin, MAG is the only one present also in the PNS myelin (Shen et al., 1998). This inhibitory environment contributes to the failure of CNS axons to regenerate. In fact, neurite outgrowth *in vitro* is inhibited when mammalian neurons are cultured on both, CNS or PNS myelin (Bähr and Przyrembel, 1995; Schwab and Caroni, 1988).

Another key difference in PNS and CNS axon regeneration is the macrophages that not only play an essential role in phagocytosis of myelin following injury, but are also responsible for the

change in the functional state of Schwann cells. Due to secretion of growth-promoting factors and stimulants by macrophages, Schwann cells are able to proliferate and to de-differentiate into non-myelinating Schwann cells, which longitudinally align to form the band of Büngner (Büngner, 1891; Lee and Wolfe, 2000; Ramón y Cajal, 1928). This structure supports axonal regeneration and guides the injured axons from the proximal into the distal nerve stump. In the CNS, oligodendrocytes fail to de-differentiate into growth supportive cells.
Additionally, another key point is that growth-inhibitory molecules of the CNS myelin, which persist at the lesion site because they were not effectively removed, promote the proliferation of reactive astrocytes (Caroni and Schwab, 1988). Astrocytes have important beneficial roles in the CNS, as they are responsible for the maintenance of the blood-brain-barrier, ion homeostasis, as well as transfer of nutrients to axons (Faulkner et al., 2004; Pekny and Nilsson, 2005). However, after CNS injury, a glial scar is formed, which is localized in the penumbra of the lesion and is characterized by a strong expression of the glial fibrillary acidic protein (GFAP). This glial scar not only forms a physical barrier to growth cones but also produces additional inhibitory extracellular matrix (ECM) molecules like, e.g. tenascin and proteoglycans that prevent axonal regeneration (Busch and Silver, 2007). Especially the members of the class of chondroitin sulfate proteoglycans (CSPG) [e.g. NG2 (Dou and Levine, 1994), neurocan (Asher et al., 2000) and phosphocan (Inatani et al., 2001) are the main inhibitory molecules found in the glial scar (Fawcett and Asher, 1999; Rolls et al., 2009; Yiu and He, 2006). Furthermore, in the lesion core, bordering the glial scar, there is the fibrous scar, which is characterized by a dense ECM network, formed mainly by collagen type IV (Col IV), but also fibronectin and laminin (Brazda and Müller, 2009; Hermanns et al., 2001; Kawano et al., 2012). Invading fibroblast, arising from the damaged meninges, astrocytes and endothelial cells sensitize Col IV. The ECM network is a supporting structure during development as well as in tissue repair and it serves as adhesive scaffold for the anchorage of different constituents (Yurchenco and Schittny, 1990). Although the components of the ECM network are per se not inhibitory to axonal regeneration (Tonge et al., 1997), inhibitory molecules, such as CSPGs, tenascin and semaphorins, which accumulate by anchoring to this network, create an inhibitory barrier of regeneration (Brazda and Müller, 2009; Hermanns et al., 2001; Klapka and Müller, 2006).
Another key difference between the PNS and CNS is, that following axotomy, PNS neurons upregulate numerous regeneration-associated genes (RAGs), such as c-Jun (Raivich et al., 2004), activating transcription factor-3 (ATF-3) (Seijffers et al., 2006), growth-associated protein-43 (GAP-43) and Cap-23 (Bomze et al., 2001). These genes are known to be important for neurite outgrowth and/or regeneration, by stabilizing and elongating the growth cone as well as by promoting axonal guidance and sprouting. No activation of these genes is found in CNS neurons (Hiebert et al., 2000; Plunet et al., 2002). Consequently, even in the absence of inhibitors, the ability to regenerate is limited due to the decreased intrinsic growth capacity of CNS neurons.

1.2.5 Experimental approaches to promote axonal regeneration after spinal cord injury

Depending on the level and severity of spinal cord injury, people living with a spinal cord injury have different hierarchies of needs. The factors that impair at the most their quality of life is oftentimes not the inability to walk, but the absence of bowel and bladder control, limitations in sexual function as well as in hand use and in breathing (Bickenbach et al., 2013). Therefore, many researchers work to identify restorative treatments. The functional outcome from the regeneration

of only few axons (5-10 %) could already improve the quality of life in a stepwise manner of people, who live with a damaged spinal cord (Blight, 1983; Fehlings and Tator, 1995). The events required for the structural and functional recovery of injured axons resembles the events that normally neurons undergo during development. After injury, if the neurons survive the insult, axon regeneration processes include the regrowth (regenerative sprouting) and the elongation in the correct direction of the damaged axons. The respective axons need to pass through the lesion site into the distal spinal cord, where the re-innervation of the normal target takes place, by forming synapses. Through the re-myelination of the regenerated axons, the former electrophysiological properties are restored and functional recovery can occur. However, as already described in the previous chapter, CNS neurons, in contrast to PNS neurons, fail to regenerate damaged axons. Neuronal apoptosis after injury, the low intrinsic regenerative capacity of adult CNS neurons, as well as the presence of regeneration barriers e.g. myelin-associated axon growth inhibitors or glial scar-associated inhibitors at the lesion site, impede CNS axon regeneration.

Furthermore, in the CNS there is a lack of growth support, due to the lack of axon growth supporting cells (glia or neural progenitor cells) and the lack of axon growth promoting molecular factors (e.g. neurotrophins, NT). The knowledge of the mechanisms underlying regeneration failure is used from researchers as working point to find new therapeutic strategies for spinal cord repair.

The first approach to promote regeneration is to activate the intrinsic regenerative capacity of CNS neurons. During postnatal development, the pro-growth genes are down regulated and the growth-inhibitor genes upregulated (Liu et al., 2011). Transcription factors that activate genes that favor axon extension emerged to be an important tool to improve neuron-intrinsic growth state (Moore et al., 2009; Moore and Goldberg, 2011; Venkatesh et al., 2018). The intrinsic neuronal capacity can also be activated for example by adenoviral alteration of RAG expression in injured central neurons. The overexpression of GAP-43 and CAP-23 in transgenic mice was shown to induce axonal regeneration in the CNS (Bomze et al., 2001). However, the long-term expression of neurotrophic factors altering RAG expression via gene therapy to promote CNS regeneration is still not an alternative to existing therapies in humans.

The second approach is to modify the non-permissive environment in the lesioned CNS tissue, either through bridging or cellular replacement strategies. Artificial bridges, out of collagen, hydrogels, nitrocellulose membranes, carbon filaments, glass filament, gelfoam and guidance tubes of different polymers, were implanted in the lesion site of the spinal cord, to provide a directional axonal growth (Bunge, 2001; Hejcl et al., 2008). Unfortunately, the outcome was not satisfying, since ingrowing axons often remained inside such an implant and did not manage to re-enter into the distal intact spinal cord stump. However, bridging the cysts or cavities in the lesioned spinal cord with cell transplantations of for example Schwann cells, olfactory ensheathing cells, peripheral nerve grafts, embryonic CNS tissue, neuronal precursor cells or stem cells, led to axonal regeneration into and through the bridges (Bunge, 2001; Li and Lepski, 2013). Axonal growth is hereby supported by replacing damaged or lost cells with new neurons or myelinating cells, by guiding regenerating axons and by providing factors to enhance the regenerative capacity. Another way to archive neuronal outgrowth through the inhibitory environment at the lesion site is to eliminate the inhibitory growth barriers for example by immunological neutralization of myelin associated inhibitors (e.g. antibody IN-1; Nogo-receptor blockade) (Buchli and Schwab, 2005; Fouad et al., 2001) or by the inhibition of the intracellular Rho signaling pathway (Fournier et al., 2003; McKerracher and Higuchi, 2006). Furthermore, also the selective enzymatic degradation of the inhibitors associated with the lesion scar e.g. chondroitinase ABC (ChABC) (Barritt et al.,

2006; Bradbury et al., 2002; Garcia-Alias et al., 2008) or the suppression of scarring to prevent the accumulation of inhibitors at the lesion site e.g. iron chelator 2,2'-bipyridine-5,5'-dicarboxylic acid (BPY-DCA) (Klapka et al., 2005; Schiwy et al., 2009; Stichel et al., 1999) are target areas for therapeutic strategies.

Furthermore, through the application of NT, which are secreted proteins that are abundant in the developing nervous system, but decrease in the adult (Ebadi et al., 1997), the lack of growth support, due to the lack of axon growth promoting molecular factors, is circumvented and axon regeneration promoted. NT, such as nerve growth factor (NGF), brain-derived neurotrophic factor

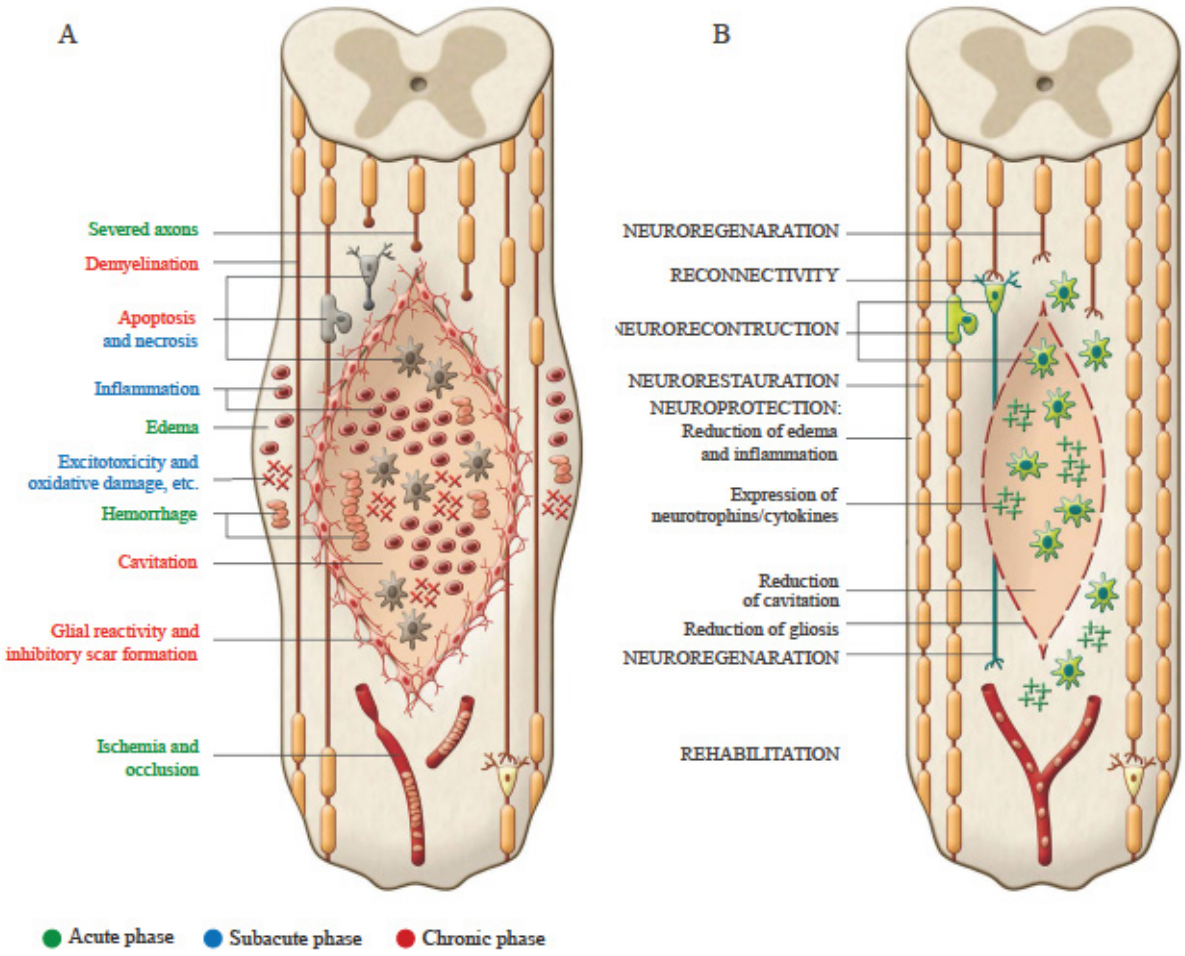

Fig. 1.2: Pathophysiological events after SCI and therapeutic strategies for spinal cord repair.
A) The diagram shows the pathophysiological events that occur after SCI, which are initiated by the primary injury and further spread through a process called secondary injury. In the acute phase, edema, hemorrhages and ischemia occur. In the subacute phase necrosis, inflammation, excitotoxicity, lipid peroxidation and electrolyte imbalance follow. During the chronic phase, the apoptosis of neurons and oligodendrocytes leads to the demyelination and disruption of synaptic transmission. Glial scarring and cyst formation result in a physical and chemical barrier to axonal regeneration. **B)** The diagram shows the therapeutic approaches to promote spinal cord repair, starting from the knowledge of the mechanisms underlying the regeneration failure. Therapeutic aims include reduction of secondary damage (neuroprotection), stimulation of regenerative axon growth and compensatory sprouting (neuroregeneration), re-myelination of axons to re-establish axonal conductivity (neurorestauration), axonal guidance and synapse formation (reconnectivity), replacement of damaged or dead cells (neuroreconstruction) and improved residual locomotor function (rehabilitation). Modified from Mothe and Tator, 2013.

(BDNF), neurotrophin-3 (NT-3) and glial cell-derived neurotrophic factor (GDNF), were applied to the injured spinal cords by different approaches. The progression of secondary injury, as well as necrotic and apoptotic cell death are prevented by this treatment, and CNS axonal growth and neuronal survival are facilitated (Blesch and Tuszynski, 2003; Koda et al., 2004; Lu and Tuszynski, 2008; Tuszynski et al., 2003). However, since not only injured, but also uninjured neurons are exposed to the broad application of NF, side effects on non-targeted cells, for example the sprouting of spinal cord sensory neurites, are caused leading to chronic pain or spasticity (Tuszynski et al., 1994).

An additional strategy, which proved to be effective in promoting neuronal regeneration, is the application of an electrical field across the lesioned spinal cord (Borgens et al., 1987; Borgens and Bohnert, 1997; Patel and Poo, 1982). Neurite sprouting and growth cone turning was observed when the electric field was applied on the nervous system and recently, epidural electrical stimulation of the lumbar spinal cord, was shown to activate the muscles, producing locomotion (Capogrosso et al., 2016). The group of Grégoire Courtine in Switzerland achieved to bypass the lesion gap by linking the cortical activity to epidural electrical stimulation of muscles, restoring gait deficits after a spinal cord injury in non-human primates. The implemented wireless control system allowed the monkeys to behave freely without any restrictions and the concept will be translated in studies with people that suffer from a spinal cord injury (Capogrosso et al., 2016).

The stimulation of axonal sprouting by therapeutic interventions would be another approach to support the extensive reorganization of the adult CNS to promote functional recovery. The chemokine stromal cell-derived factor 1α (SDF-1α), also known as CXCL12, which was intrathecally infused in a rat model of SCI for 7 days, showed to promote neurite outgrowth and therefore to be implicated in the regeneration of CNS neurons after injury. In the present study, the sprouting effect in a mouse model of SCI will be analyzed and the role of its cognate receptors, CXCR4 and CXCR7 further investigated.

Finally, the restoration of locomotor function after SCI can also occur spontaneously. Through the anatomical plasticity of damaged or spared axons, which form spontaneously collateral sprouts to bypass the lesion site and activate new intraspinal circuits, the locomotor function of injured animals can be re-established (Bradbury and McMahon, 2006; Maier and Schwab, 2006). In fact, Bareyre et al., (2004) showed that in adult rats, some transected CST axons, which would normally innervate lumbar segments, sprouted into the cervical gray matter to form connections with the propriospinal neurons, leading to a novel, indirect pathway to lumbar motor circuits.

In summary, to promote axonal regeneration after spinal cord injury,
the therapeutic aims (Fig. 1.2 B) are:

1. Neuroprotection: to reduce the secondary damage
2. Neuroregeneration: to stimulate regenerative axon growth and compensatory sprouting
3. Neurorestauration: to re-myelinate axons to re-establish axonal conductivity
4. Reconnectivity: to guide axonal growth and form synapses
5. Neuroreconstruction: to replace damaged or dead cells and
6. Rehabilitation: to improve the residual locomotor function.

The application of these single therapeutic strategies have shown to improve axonal regeneration, but the efficiency on functional recovery was modest. Since SCI is a complex multifactorial disease, in order to translate experimental research findings to clinical therapies, combinatorial (multi-component) approaches are necessary (Lu and Tuszynski, 2008; Nomura et al., 2006; Pearse and Bunge, 2006). Therefore, to improve the capacity for axonal regeneration and functional recovery

after SCI, the synergistic effects of combinatorial therapies were exploited. Several studies were performed with ChABC, a substance that breaks down inhibitory sugar chain components of CSPG molecules in the glial scar. ChABC was combined with a Schwann cell implant, to provide a growth-supportive substrate for axonal regeneration, like the Bands of Büngner in the peripheral nervous system and together with olfactory ensheathing glia to facilitate the axonal growth into the host tissue again (Fouad et al., 2005). This treatment revealed a significant improvement in regeneration and locomotor recovery of injured animals compared to the single treatment (Fouad et al., 2005). Furthermore, a highly innovative device, the mechanical microconnector system, placed in the gap of a complete transected spinal cord and able to suck both spinal cord stumps into its honeycomb structure, promoted beneficial effects on axon growth (Brazda et al., 2016; Brazda et al., 2013). With that device the tissue integrity was preserved, axonal regeneration was allowed and locomotor function improved (Brazda et al., 2016; Brazda et al., 2013). Furthermore, through micro-channels, which are connected to an osmotic minipump, the local delivery of pharmacological substances, like drugs but also substances that reduce fibrotic scar formation, like iron chelators, in the lesion center of the spinal cord is enabled. Another potential combinatorial approach is the polyethylene glycol (PEG) biopolymer treatment that showed improvements that have not been achieved bevore in severe chronic SCI (Estrada et al., 2014). After the resection of the inhibitory scar tissue, PEG filling of the resection cavity was shown to promote not only the invasion of regeneration promoting cells (endothelial and glial cells), but supported long-distance growth and myelination of axons leading to functional locomotor improvements. This highly promising approach, which can be easily combined with other molecular and cellular treatments, may further enhance its efficacy.

1.3. The chemokine CXCL12 and its cognate receptors CXCR4 and CXCR7

1.3.1 Structure and classification of chemokines and chemokine receptors

Chemotactic cytokines, shortly chemokines, are small (7-14 kDa) polypeptides, which belong to a family of proteins with high structural and functional homology, initially identified and known as key modulators of development, differentiation and trafficking of leukocytes (Rollins, 1997). In the last decades, over 50 members of the highly conserved chemokine family, as indicated by their expression in mammals, chicken, zebrafish, sharks, jawless fish and *Caenorhabditis elegans*, were identified in humans (DeVries et al., 2005; Zlotnik et al., 2006). Their functions, that extend far beyond leukocyte physiology, could be revealed using healthy and diseased organisms (Gerard and Rollins, 2001; Murphy et al., 2000; Proudfoot, 2002; Rossi and Zlotnik, 2000). Despite their role as activators and chemoattractants for leukocyte subpopulations and some non-hematopoietic cells, chemokines are also involved in the regulation, development and maintenance of the innate and adaptive immune response and are, therefore, also involved in acute and chronic inflammatory events (Campbell et al., 2005; Moser and Loetscher, 2001; Murdoch and Finn, 2000). Furthermore, they can act on angiogenesis and cell migration enforcing their role in tumor growth and metastasis (Müller et al., 2001; O'Hayre et al., 2008; Rempel et al., 2000; Strieter et al., 1995). The development of tissues and organs, wound healing as well as viral

pathogenesis (HIV-strains) belong also to the highly divergent functions of chemokines (Feng et al., 1996). Despite this diversity in functionality, chemokines can be subdivided by their function in two main groups, the inflammatory chemokines and the homeostatic chemokines (Jaerve and Muller, 2012; Moser et al., 2004). The inflammatory chemokines are responsible to recruit leukocytes to inflamed and injured tissue as well as tumors. In contrast, homeostatic chemokines are constitutively expressed and guide leukocytes during hematopoiesis in the bone marrow and thymus, during the initiation of the adaptive immune response in lymphoid organs and finally in the peripheral tissue.

The characteristic fold of chemokines consists of three β strands, a carboxy (C) terminal helix and a flexible amino (N) terminal region, which exhibits four conserved cysteine-motifs that form two characteristic disulphide bridges between the first and third, and between the second and forth cysteine, respectively (Baggiolini et al., 1997; Murphy et al., 2000). Chemokines can, therefore, also be structurally subdivided into four subfamilies, according to the number of conserved cysteine-motifs in the mature protein and the spacing in between these two cysteines. The CC and CXC subfamilies include the majority of chemokines. These two subfamilies differ one from another only by one additional amino acid, which separates the two adjacent cysteines. The other two families are exceptions, where two cysteines are lacking (as in XCL1 or Lymphotactin) or three amino acid residues instead of one occur in between the two adjacent cysteines (Fractalkine, CX3C-chemokine) (Imai et al., 1997; Kelner et al., 1994).

Chemokines mediate their effects through the binding to chemokine receptors. To date, up to 23 distinct chemokine receptors have been identified in humans (Arimont et al., 2017; Nomiyama et al., 2011). They are divided into four different families, according to the four previously described chemokine subfamilies they bind (Murphy et al., 2000). The chemokine receptors belong to the rhodopsin family of seven transmembrane domain receptors, which are coupled to the Gαi class of heterotrimeric G-proteins, making them members of the large protein family of G-protein-coupled receptors (GPCRs) (Murdoch and Finn, 2000; Zhu et al., 2013). The typical tertiary structure of a chemokine receptor, which has a molecular weight of approximately 40 kDa and a common length of 340-370 amino acids, includes an extracellular N-terminal sequence, seven helical transmembrane domains with three intracellular and three extracellular loops, and an intracellular C-terminus (Fig. 1.3 A) (Arimont et al., 2017; Bajetto et al., 2002). The N-terminal sequence of the chemokine receptor is important for ligand specificity, while the C-terminal sequence, couples the G-proteins relevant for intracellular signaling (Brelot et al., 2000; Cai et al., 2004; Xu et al., 2013). The chemokine receptor signal transduction mechanisms will be described in detail for the CXCL12 and CXCR4 axis in the following chapters.

1.3.1.2 The chemotactic cytokine CXCL12

The stromal cell derived factor-1 (SDF-1), also known as chemokine CXCL12, is a constitutively secreted and ubiquitously expressed chemokine, that owes its name to the fact, that stromal cells, such as macrophages, adipocytes, osteoblasts and endothelial cells, were shown to produce and to secrete CXCL12. In fact, CXCL12 was cloned from a murine cell line from bone marrow stromal cells and was initially characterized as a pre-B-stimulatory factor (PBSF) (Nagasawa et al., 1994; Tashiro et al., 1993). CXCL12 has a single open reading frame of 282 nucleotides encoding not only one polypeptide, but through splicing events of one single gene, six further isoforms, the so called CXCL12α, CXCL12β, CXCL12γ, CXCL12δ, CXCL12ε and CXCL12θ are generated in

humans (De La Luz Sierra et al., 2004; Nagasawa et al., 1996b; Yu et al., 2006). In contrast, only three splicing isoforms (α, β and γ) were described in mice and rats (Gleichmann et al., 2000; Nagasawa et al., 1996b). However, the sequence homology between *Homo sapiens* and *Mus musculus* is very high and accounts for 99 %. CXCL12α, the predominant and smallest isoform, encodes for a protein of 89 amino acids and consists of three exons. All the other splicing variants of CXCL12 share the same three exons and have additionally a forth exon at the C-terminus. Unlike the majority of the CXC chemokines, which can be mapped to human chromosome 4 (murine chromosome 10), the genes of ancient and conserved chemokines, as the gene coding for CXCL12, have a distinct, unique chromosomal location, namely the human chromosome 10 (murine chromosome 6) (Shirozu et al., 1995; Zlotnik et al., 2006). The similarity of the CXCL12 protein between the species as well as the unusual chromosomal location underlies the importance and the critical function of the CXCL12 chemokine, which must be conserved throughout evolution. Indeed, CXCL12 has a crucial role in developmental processes, including hematopoiesis, cardiogenesis, vascular formation, neurogenesis as well as the maintenance of tissue stem cells (Aiuti et al., 1997; Nagasawa et al., 1996a; Sugiyama et al., 2006; Tachibana et al., 1998; Zou et al., 1998). In support of the singularity of CXCL12 among the other members of the chemokine family, in which several chemokines within one subclass are able to bind to a single receptor or a single chemokine binds to several receptors, CXCL12 mediates its effect only through the binding to two different receptors: CXCR4 and CXCR7. The essential role of the chemokine CXCL12 and its receptors was further confirmed by the perinatal death of animals lacking CXCL12 or the two receptors (Nagasawa et al., 1996a; Sierro et al., 2007; Tachibana et al., 1998; Zou et al., 1998).

1.3.1.2 The chemokine receptor CXCR4

The chemokine receptor CXCR4, also known as LESTR (Leukocyte-expressed seven transmembrane-domain receptor) or Fusin, is a G-protein-coupled seven transmembrane domain receptor (Fig. 1.3 A), that was cloned from a human blood monocyte cDNA library (Loetscher et al., 1994). The CXCR4 gene (located on chromosome 2 in humans and chromosome 1 in mice), which encodes a protein of 352 amino acids, contains two exons separated by an intron (Caruz et al., 1998). This receptor was identified as a co-receptor of CD4+ T-lymphocytes, required to enable HIV-1 (human immunodeficiency virus-type 1) cell fusion and entry (Feng et al., 1996). So far, it is known that CXCR4 function is regulated on multiple levels, namely via transcriptional processing (alternative splicing events), posttranslational modifications (glycosylation, sulfation, phosphorylation etc.) and receptor dimerization (Deng et al., 2014; Levoye et al., 2009; Mueller et al., 2013; Salanga et al., 2009). After an extended testing of a large number of chemokines, the CXCL12 was discovered as the natural ligand of CXCR4 (Bleul et al., 1996; Oberlin et al., 1996). Recently, the cytokine macrophage migration inhibitory factor (MIF) and extracellular ubiquitin were identified as non-cognate ligands for CXCR4 (Bernhagen et al., 2007; Saini et al., 2011). The binding of CXCL12 to CXCR4 activates tissue dependent signaling pathways involved in chemotaxis, cell survival and proliferation, as well as increase in intracellular calcium and gene transcription, through heterotrimeric G-proteins (Fig 1.3 B) (Busillo and Benovic, 2007; Teicher and Fricker, 2010; Zhu et al., 2013). Chemokine receptors are predominantly coupled to the Gαi class of heterotrimeric G-proteins and as such, pertussis toxin inhibits receptor-dependent activation of Gi proteins. Directly after receptor activation, the Gαi subunit mediates

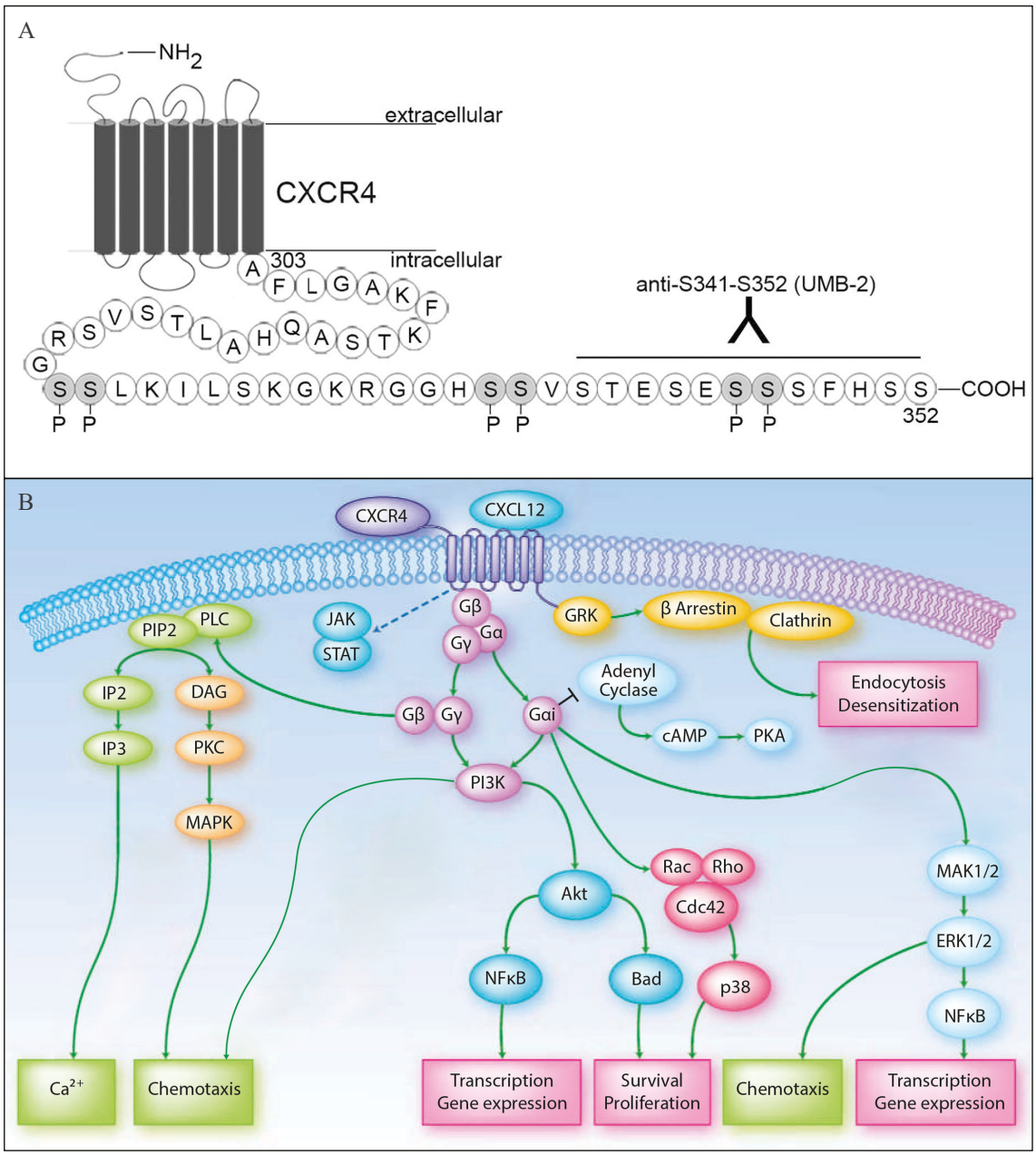

Fig. 1.3: CXCL12/CXCR4 intracellular signaling transduction pathways.
A) Schematic representation of the human G-protein-coupled receptor CXCR4 with its typical tertiary structure including an extracellular N-terminal sequence, seven helical transmembrane domains with three intracellular and three extracellular loops and an intracellular C-terminus. Detailed amino acid sequence of the C-terminal tail of CXCR4 showing the epitope of the UMB2 antibody and the serine cluster 346-347, which is phosphorylated upon ligand binding. Modified from Mueller et al., 2013. **B)** Schematic diagram showing the major CXCL12/CXCR4 signaling pathways related to chemotaxis, cell survival and proliferation as well as increase in intracellular calcium and gene transcription. CXCL12 binding to CXCR4 leads to the activation of G-protein-coupled signaling. The Gβγ-subunit activates the PLC/PIP2/IP3 cascade for Ca^{2+} mobilization and the PLC/PIP2/MAPK pathway for the process of chemotaxis. Furthermore, chemotaxis is also activated by the PI3K pathway and through the Gαi-subunit, which activates the MAPK-pathway. The PI3K/AKT pathway regulates cell survival and proliferation. In addition, after ligand binding the CXCR4 receptor is rapidly phosphorylated at the c-terminus by GRK and internalized via β-arrestin/clathrin endocytosis. Modified from Teicher and Fricker, 2010.

the inhibition of the adenylyl cyclase, while the Gβγ-subunit stimulates the activation of the phospholipase C (PLC). PLC hydrolyzes phosphatidylinositol 4, 5-biphosphate (PIP2) to form two second messengers, namely diacylglycerol (DAG) and inositol 1,4,5-triphosphate (IP3). DAG thereby activates the protein kinase C (PKC) and initiates the mitogen-activated protein kinase (MAPK) pathway mediating the chemotaxis process, while IP3 elevates the cytosolic concentrations of free Ca^{2+} mainly by depleting the intracellular stores. The raise in calcium flux after chemokine binding is often used to measure the chemokine activity and is attributed to Gβγ-subunit activation. The process of chemotaxis can also be stimulated through the activation of the PI3K pathway and the subsequent phosphorylation of several components of the focal adhesion complex (proline-rich tyrosine kinase-2, Pyk2; focal adhesion kinase, FAK; paxillin, and Crk) by both, the Gβγ-subunit and the Gαi-subunit and by the Gαi-subunit alone through the activation of the Erk1/2 signaling pathway. Furthermore, the Gαi-subunit can also activate the PI3K/AKT pathway and regulate cell survival and proliferation of tumor tissue by post-translational inactivation of cell death machinery (Akt-Bad pathway; p38 pathway) or increasing the transcription of cell survival-related genes using NF-Kb as transcription factor. Changes in the gene expression occur also through the activation of the MAPK/ERK cascade by the Gαi-subunit. Upon ligand binding, the intracellular C-Terminal sequence of the CXCR4 receptor is rapidly phosphorylated at serine sites by G-protein receptor kinases (GRK) and internalized via β-arrestin and clathrin-mediated endocytosis (Busillo et al., 2010; Krupnick and Benovic, 1998; Mueller et al., 2013). After internalization the CXCR4 receptor can be either degraded or recycled back to the plasma membrane (Marchese et al., 2003). Sustained stimulation of the CXCR4 receptor with CXCL12 causes lysosomal degradation of the receptor (Marchese and Benovic, 2001). The antibody most commonly used is the knockout validated rabbit monoclonal anti-CXCR4 antibody clone UMB-2, which recognizes its epitope within the amino acid residues 341-352, located in the intracellular C-Terminal sequence of the receptor (Fig. 1.3 A) (Fischer et al., 2008; Mueller et al., 2013). The UMB-2 antibody recognizes the receptor only in its inactive state, when the serine-cluster 346-347 is not phosphorylated (Mueller et al., 2013). Upon ligand binding, this serine-cluster is rapidly phosphorylated and the UMB-2 antibody does not recognize the phosphorylated epitope of the activated CXCR4 receptor any more. Furthermore, CXCR4 receptors can form homodimers or heterodimers with other chemokine receptors, and with this modulate the signal transduction (Salanga et al., 2009). However, the functional consequences of homo- or heterodimerization are still not well understood. Dimerization has been suggested to result in G-protein-independent signaling through the JAK/Stat signaling pathway (Teicher and Fricker, 2010), others postulate a more robust and more potent response of CXCR4 to CXCL12 (Zhu et al., 2013) while some groups describe an impairment in CXCR4 receptor typical G-protein signaling through the dimerization of CXCR4 (Levoye et al., 2009). The CXCL12-CXCR4 axis is highly conserved between the species and the importance of it was confirmed by the dramatic embryonic developmental consequences of CXCL12 and CXCR4 deletion experiments. CXCL12 deficient mice die perinatally because of severe deficits in the ventricular septum of the heart, disturbed hematopoiesis and lymphopoiesis (Ma et al., 1998; Nagasawa et al., 1996a). CXCR4 receptor knockout animals displayed a similar phenotype (Ma et al., 1998; Tachibana et al., 1998; Zhu et al., 2009; Zou et al., 1998). Additionally, CXCR4 deleted mice, had developmental abnormalities in neuronal networks in the CNS, especially in the architecture of the cerebellum, the hippocampal dentate gyrus and in the spinal cord. Also the blood vessel development in the gastrointestinal tract of CXCR4 deficient mice was defective.

1.3.1.3 The chemokine receptor CXCR7

The chemokine receptor CXCR7, also known as ACKR3 (atypical chemokine receptor 3), the second CXCL12 receptor identified in 2005 (Balabanian et al., 2005; Graham et al., 2012), is a G-protein-coupled seven transmembrane domain receptor originally cloned from a canine cDNA library (Libert et al., 1990). The evolutionary conserved CXCR7 gene, which is located on chromosome 1 in mice and on chromosome 2 in humans and thus lies in close proximity to the gene encoding for CXCR4, encodes a protein of 362 amino acids (Bachelerie et al., 2014). CXCR7 was primarily believed to act as a receptor for vasoactive intestinal peptide (Sreedharan et al., 1991), but this possibility was later dismissed when CXCR7 was shown to exert CXC-chemokine receptor function (Balabanian et al., 2005; Cook et al., 1992; Nagata et al., 1992). In fact, the chemokine CXCL12, which was considered to bind only to CXCR4, interacts and signals also through CXCR7. In contrast to CXCR4, which binds CXCL12 in a monogamous manner, CXCR7 is able to additionally bind also the chemokine CXCL11 (interferon-inducible T-cell α chemoattractant, ITAC) (Burns et al., 2006). Furthermore, compared to CXCR4, CXCR7 displays a 10-fold higher affinity to CXCL12 (Balabanian et al., 2005; Burns et al., 2006). This, and the fact that the cell surface expression of CXCR7 is highly dynamic, support the overall idea of a crucial role for CXCR7 in regulating the availability of CXCL12 for CXCR4, serving as a CXCL12-scavenger (Burns et al., 2006; Naumann et al., 2010; Sanchez-Alcaniz et al., 2011). The internalization of the receptor, which is initiated through C-terminal phosphorylation, continued by β-arrestin recruitment and binding, and finally concluded by clathrin-mediated endocytosis, is independent of the ligand, but the process can be accelerated through CXCL12 binding (Hoffmann et al., 2012; Naumann et al., 2010). After internalization, the CXCR7 receptor can be either degraded or recycled back to the plasma membrane, whereas the internalized CXCL12 is immediately degraded (Mahabaleshwar et al., 2012). The rapid uptake and degradation of CXCL12, as well as the G-protein coupling and receptor stability was shown to be influenced by the C-terminus of the CXCR7 receptor (Hoffmann et al., 2012). Unlike CXCR4, CXCR7 is unable to activate typical signal transduction pathways via Gαi-proteins that would result in GTP hydrolysis and calcium elevation (Burns et al., 2006). Therefore, CXCR7, is not a typical GPCR, since it belongs as the name implies to the subfamily of atypical chemokine receptors (Graham et al., 2012). While CXCR4 desensitizes the CXCL12/CXCR4 pathway by ligand-dependent internalization and G-protein coupling, CXCR7 is postulated to sequester CXCL12 in order to silence, inhibit or regulate CXCL12-CXCR4-induced signal transduction (Naumann et al., 2010; Sanchez-Alcaniz et al., 2011; Shimizu et al., 2011). However, as already mentioned for CXCL12 and CXCR4 depleted animals, CXCR7 deficiency is also perinatally lethal, due to severe cardiac defects and impairment in vascularization and angiogenesis, suggesting a critical role of the receptor in embryogenesis (Gerrits et al., 2008; Sierro et al., 2007; Yu et al., 2011). However, in contrast to CXCR4 and CXCL12 deficient animals, CXCR7 knockout mice have no impairment in hematopoiesis and show normal development of the cerebellum and hippocampus, implicating that CXCR7 is involved in several but not all CXCL12 functions (Sierro et al., 2007).

1.3.2 Role of CXCL12 and its receptors in the developing *versus* the adult CNS

Besides the role of CXCL12 in the immune system, where it exerts its function in chemotaxis, inflammation and hematopoiesis, its role in the cardiovascular system, in the vascularization and angiogenesis, as well as its crucial role in developmental processes, the importance of the CXCL12-CXCR4 axis in the central nervous system first became obvious in studies that used knockout animals. In these animals, the abnormal morphology of the cerebellum or the hippocampus is due to the defective migration of progenitor cells (cerebellar granule and Purkinje neurons) to their target area (Lu et al., 2002; Ma et al., 1998; Zou et al., 1998). Axonal growth cones of migrating neurons select the direction of migration in response to chemotactic cues as they get chemoattracted or chemorepelled. CXCL12 itself was shown not to exhibit chemoattracting or repelling effects, but it acts as a modulator to reduce the effectiveness of many axonal repellents, a requisite important for normal axon pathfinding (Chalasani et al., 2003; Chalasani et al., 2007). Also the assembly and sensory pathfinding of olfactory neurons (Miyasaka et al., 2007) as well as facial motoneurons (Sapede et al., 2005) are regulated by the CXCL12-CXCR4 signaling pathway. Moreover, the latter is also required for migration and axon pathfinding of ventral motoneurons (Lieberam et al., 2005), retinal ganglion cells (Li et al., 2005) and dorsal root ganglion cells (Odemis et al., 2005). Furthermore, also the tangential migration of interneurons and their final distribution in the neocortex and other brain areas is controlled by the CXCL12-CXCR4 axis (Zhu and Murakami, 2012). Indeed, both, projection neurons of the cortex (Stumm and Hollt, 2007; Tiveron et al., 2006; Tysseling et al., 2011) and the meninges (Stumm et al., 2007) express CXCL12 and are responsible for the regulation of the tangential migration of the interneurons (Lopez-Bendito et al., 2008). As mentioned above, in contrast to CXCR4 knockout animals, CXCR7 depleted animals show normal development of the cerebellum and hippocampus (Sierro et al., 2007). However, recently detailed analysis revealed that the migratory and subsequent positioning of cortical interneurons is disturbed in these animals, too (Sanchez-Alcaniz et al., 2011). These defects were attributed to the modulation of the CXCL12-CXCR4 axis via the scavenger receptor CXCR7. In physiological conditions CXCR7 prevents the over-accumulation of CXCL12 in the cortex, which would lead to the desensitization and degradation of CXCR4, thereby ensuring a sufficient amount of CXCR4 protein to be present to mediate chemokine response (Sanchez-Alcaniz et al., 2011). On the other hand, another group suggests distinct functions of the two receptors in regulating interneuron migration (Wang et al., 2011). Also the migration of gonadotropin-releasing hormone (GnRH) neurons is influenced indirectly by CXCR7 through regulation of CXCL12 availability (Memi et al., 2013). Altogether, the CXCL12-CXCR4/CXCR7 axis regulates essential processes for the establishment of a neuronal network, such as neuronal migration, guidance and axon pathfinding. The importance of this role is also supported by the developmental pattern of expression of CXCL12 and its receptors. CXCL12 is highly and selectively expressed in the developing and mature brain of rodents. In the developing nervous system, CXCL12 is present already at the earliest stages of differentiation (McGrath et al., 1999). In contrast to the expression in cerebellum and olfactory bulb, where CXCL12 is progressively down regulated within the first two weeks after birth, the expression in neurons of other brain regions, like neurons in the thalamus, granule neurons of the hippocampus and pyramidal neurons of the cortical layer V, is low at birth but gradually upregulated during the first two postnatal weeks (Daniel et al., 2005; Tham et al., 2001; Tissir et al., 2004). The CXCL12 receptor CXCR4 is highly expressed in brain regions that are associated with adult neurogenesis,

such as the olfactory bulb, throughout the ventricular system and within the subgranular zone of the dentate gyrus as well as in cortical GABAergic interneurons (Lu et al., 2002; Stumm et al., 2002; Stumm et al., 2003; Tissir et al., 2004). Although CXCR4 expression decreases progressively during development (Schonemeier et al., 2008a; Tissir et al., 2004), the chemokine receptor is still detectable in subpopulations of mature neurons and is occasionally present in astrocytes and microglial cells (Banisadr et al., 2002; Lipfert et al., 2013; Stumm et al., 2002; Trecki et al., 2010). In contrast to CXCR4, CXCR7 is upregulated during postnatal development. It is expressed in neurons, such as those of the cortical layer V, in cortical interneurons and in the hippocampus, in astrocytes, meningeal cells and endothelial cells of brain blood vessels, resembling the expression pattern of CXCL12 (Schonemeier et al., 2008a; Shimizu et al., 2011; Tissir et al., 2004).

1.3.3 Implication of CXCL12 and its receptors in spinal cord injury

The CXCL12-CXCR4 axis is also extremely relevant in CNS homeostasis and, therefore, plays an important role in neurogenesis and neuromodulation. Actually, neuronal migration, process formation and elongation and synaptogenesis require changes in neuronal shape, which in turn need the rearrangement of the cytoskeleton (Tanaka and Sabry, 1995). In cultured cerebellar granule cells, CXCL12 stimulates axonal elongation via a Rho-dependent pathway, which is linked to actin cytoskeletal signaling mechanisms (Arakawa et al., 2003). However, in hippocampal neurons, CXCL12 reduces axonal elongation but stimulates axonal branching (Pujol et al., 2005). This differential regulation has been proposed to correlate with a compartment-selective trafficking of CXCR4 (Baudouin et al., 2006). Additionally, CXCL12 exerts disinhibitory effects by reducing the sensitivity of axonal growth cones of postnatal DRG neurons as well as mature retinal ganglion cells (RGC) towards CNS myelin and other repellent axon guidance factors, stimulating neurite outgrowth (Chalasani et al., 2003; Chalasani et al., 2007; Heskamp et al., 2013; Opatz et al., 2009). The antirepellent activity of CXCL12 was shown to act through the elevation of intracellular cAMP levels via a pertussis toxin-sensitive G-protein-coupled signaling pathway (Chalasani et al., 2003), despite the fact, that paradoxically the activation of Gαi class typically inhibits adenylate cyclase and therefore induces decreased cAMP levels. Hence, it was shown, that multiple G-protein subunits work together to produce the cAMP levels required for CXCL12's antirepellent activity (Twery and Raper, 2011). The elevation of cAMP leads to the upregulation of regeneration-supporting genes such as Arginase I, a key enzyme in the synthesis of polyamines, molecules implicated in nervous system development, axonogenesis and regeneration (Cai et al., 2002; Chu et al., 1995). Elevated neuronal cAMP levels *in vivo* result in regeneration of mature spinal axons (Neumann et al., 2002; Qiu et al., 2002) and play a role in the spontaneous regeneration of neonatal spinal cord axons after injury (Cai et al., 2001). CXCL12 has also an important role in CNS injury. It is reflected in the upregulation of CXCL12 upon injury, which is mostly associated with reactive astrocytes (Hill et al., 2004; Miller et al., 2005) and the formation of a gradient that guides immune and stem cells towards the injury site (Sanchez-Martín et al., 2011; Tysseling et al., 2011). Hence, this cell recruitment via CXCL12/CXCR4 signaling is an important element in regulating spinal cord responses to injury. The local intrathecal infusion of CXCL12 into the lesioned rat spinal cord enhanced the sprouting of dCST axons rostrally to the lesion (Jaerve et al., 2011; Opatz et al., 2009). Additionally, also serotonergic (5-HT) and tyrosine hydroxylase (TH) positive fibers sprouted after rat spinal cord

injury (Jaerve et al., 2011). However, the exact mechanisms underlying these beneficial effects of CXCL12 are still unknown. Recently, the group of Zendedel et al. (2012) investigated the functional recovery of rats after intrathecal infusion of CXCL12 in a spinal cord contusion model. They demonstrated that CXCL12 improved locomotor recovery and this outcome was correlated with higher numbers of neuronal cell bodies and lower numbers of apoptotic cells, indicating a neuroprotective effect of CXCL12. Furthermore, CXCL12 induced angiogenesis, augmented microgliosis and astrocytosis (Zendedel et al., 2012). Whether axonal sprouting or regeneration was involved in functional recovery was not analyzed by this group, who referred in this respect to the publication of Opatz and colleagues published in 2009.

1.4 Aim of this thesis

Spinal cord injury (SCI) is a life changing event for the patient and their affiliated. This topic has a high economic relevance since the patients have almost a life expectancy close to uninjured people and have to live their whole life with disability. The major goal of researchers is to identify the causes of regenerative failure in the central nervous system (CNS) and to target these factors to promote CNS repair and regeneration in spinal cord injured people. Various causes of CNS regenerative failure were exploited in the last decades and both single therapeutic strategies and combinatorial approaches were applied in experimental animal models to improve axonal regeneration. One therapeutic aim is the stimulation of axon regeneration or compensatory sprouting of the lesioned spinal cord axons. The chemotactic cytokine CXCL12, also named stromal cell-derived factor 1α (SDF-1α), is known to stimulate neurite outgrowth *in vitro* as well as axonal sprouting in an *in vivo* rat spinal cord injury model. The aim of this thesis was to investigate the functional role of CXCL12 in axon sprouting, and the identification of the functional receptors CXCR4 and CXCR7 mediating the effects of CXCL12. For this purpose, conditional (floxed) CXCL12 receptor knockout mice receiving a transection of the dorsal corticospinal tract (dCST) were used. Due to the absence of a commercially available and suitable (i.e., specific) antibody against the second CXCL12 receptor CXCR7, the involvement of this receptor was not included into this study. In particular, the following aspects were addressed in this work:

- Testing if CXCL12 is a growth promoting and disinhibitory factor for adult mouse DRG neurons *in vitro* and *in vivo*.
- Investigation of the involvement of the cognate receptor CXCR4 in CXCL12-mediated signaling using pharmacological as well as genetic approaches.
- Establishment of a local spinal epidural-catheterization method for mouse spinal cord injury models, which allows unrestricted local drug infusion and avoids catheter induced spinal cord compression for reliable conclusions about the treatment efficacy.
- Establishment of an experimental mouse spinal cord injury as well as anterograde labeling of the dorsal corticospinal tract using AAV2-Cre transduction.
- Efficacy of intrathecally infused CXCL12 in stimulating neurite outgrowth of the injured dorsal corticospinal tract and in the induction of locomotor recovery after SCI in wildtype and conditional CXCL12 receptor knockout mice.
- Identification of the CXCR4 receptor expression on protein level in spinal cord sections via immunofluorescence and on mRNA level in brain sections using *in situ* hybridization in spinal cord lesioned and unlesioned mice.

2. MATERIALS AND METHODS

2.1 Buffers, solutions, antibodies and primer

2.1.1 Buffers and solutions

Buffers and solutions	Composition/Manufacturer
AMD3100 (Octahydrochloride hydrate); 5 µM	Sigma-Aldrich
Baytril (15 mg/kg, s.c.)	Bayer
BSA (Bovine Serum Albumin - fraction V)	Sigma-Aldrich
Collagenase type IA; 0,3 %	Sigma-Aldrich
Cryoprotect solution	620 mg NaH2PO4 x H2O (Merck) 2.18 g Na2HPO4 (Merck) 18 g NaCl (Merck) Ad 400 ml *aq. bidest.* Ph titration to 7.3 600 g sucrose (Sigma-Aldrich) 20 g Polyvinyl pyrolidone (mW 40 kD) (Sigma-Aldrich) Ad 1400 ml *aq. bidest.* 600 ml ethylene glycol (Sigma-Aldrich)
CXCL12, recombinant (human); 10 µM	250 µg CXCL12 (1x Vial without stabilizer, Peprotech) ad 3.139 ml 1 % BSA/PBS buffer Pumping rate: ~ 40 ng/0.5 µl/h Cell culture: 500 ng/ml
DAPI (4,6-Diamino-2-phenylindole) 1:10000	Roche Diagnostics

Buffers and Solutions	Composition/Manufacturer
DMEM high glucose	GIBCO, Thermo Scientific
DMEM low glucose	GIBCO, Thermo Scientific
DPX	Fluka
DS (Donkey Serum), 5%	Serotec
Ethanol	Sigma-Aldrich
Evans Blue Dye 5 % in PBS	Sigma-Aldrich
FBS (Fetal bovine serum)	GIBCO, Thermo Scientific
Fluoromount G for tissue mounting	Southern Biotech
Forene 100 % (v/v)	AbbVie
Gelatine	1 g Gelatine (Merck) 0.1 g Chrom(III)-potassium sulfate dodecahydrate (Merck) ad 200 ml *aq. bidest.* and sterile filter
HBSS, no calcium, no magnesium	GIBCO, Thermo Scientific
Kapa2G™ Fast DNA Polymerase	Peqlab Biotechnologie
Laminin L2020, (20 mg/ml)	Sigma-Aldrich
Massons Trichrome:	Merck
Solution A	0.5 % fuchsin acid 0.5 % xylidine ponceau 1 % acetic acid
Solution B	1 % molybdatophosphoric acid hydrate
Solution C	2 % light green SF yellowish 2 % acetic acid in *aq. bidest.*
Methanol	Sigma-Aldrich
2-Methylbutan	Sigma-Aldrich
NGS (Normal Goat Serum), 10 % in PBS	Vector Laboratories
Nissl	1.6326 g Sodium acetate (Merck) 2.88 ml acetic acid (Merck) 100 mg cresyl violet (Sigma-Aldrich) ad 300 ml *aq. bidest.*

Buffers and Solutions	**Composition/Manufacturer**
Papain	Worthington
PB (phosphate buffer), 0.2 M, pH 7.4	28.8 g Na2HPO4 (Merck) 5.2 g NaH2PO4 (Merck) ad 1000 ml *aq. bidest.*
PBS (phosphate buffer saline), 0.1 M, pH 7.4	50 ml 0.2 M PB 9 mg NaCl (Merck) ad 1000 ml *aq. bidest.*
PBS (phosphate buffer saline) cell culture	GIBCO, Thermo Scientific
Penicillin/Streptomycin 500 U/m, 2%	Merck
PFA (Paraformaldehyde), 4 %, pH 7.4	40 g PFA powder (Merck) ad 1000 ml 0.1 M PB Ph titration with 5 M NaOH
Poly-D-lysine (molecular weight 300,000 kDa) (0.1 mg/ml)	Sigma-Aldrich
2-propanol	Sigma-Aldrich
Protease inhibitor cocktail	Merck
QuickExtract™ DNA Extraction Solution 1.0	Epicentre an Illumina® company
Rimadyl (4mg/kg; s.c.)	Pfizer
RotiHistol®	Roth
Sucrose	Sigma-Aldrich
Sudan Black 0.3 % in EtOH	Fluka
Tissue Tek®; O.C.T. compound	VWR
Triton X-100, 0.3 %	30 µl Triton X-100 (Sigma- Aldrich) ad 10 ml PBS
Trypsin-EDTA, 0.25%	GIBCO, Thermo Scientific

2.1.2 Antibodies

2.1.2.1 Primary antibodies

Antibody	Class	Antigen	Dilution	Manufacturer
Anti-HA (H6908)	rb IgG	Hemagglutinin	1:500	Sigma-Aldrich
CGRP (1720-9007)	gt IgG	Calcitonin gene-related peptide	1:500	Serotec
Ctip2 (ab28448)	rb IgG	Ctip	1:200	Abcam
GFAP (MAB3402)	ms IgG	Glial fibrillary acidic protein	1:500	Chemicon
MBP (Clone SMI-94)	ms IgG	Myelin basic protein	1:500	Biolegend
NeuN (MAB377)	ms IgG	Neuronal nuclei	1:500	Chemicon
NeuN (ABN 78)	rb IgG	Neuronal nuclei	1:1000	Chemicon
PAM311-NP (SMI-311R)	ms IgG	Pan-Axonal Neurofilament Marker (non-phosphorylated)	1:500	Covance
PAM312-P (SMI-312R)	ms IgG	Pan-Axonal Neurofilament Marker (phosphorylated)	1:500	Covance
Tuj1 (MMs-435P)	ms IgG	Neuronal Class III ß-Tubulin	1:500 (IHC) 1:1000 (ICC)	Covance
UMB2 (ab124824)	rb IgG	C-terminus of CXCR4	1:400	Abcam

2.1.2.2 Secondary antibodies

Antibody	Class	Dilution	Manufacturer
Alexa Fluor® 488 anti-rabbit	gt IgG	1:500	Molecular Probes
Alexa Fluor® 594 anti-rabbit	gt IgG	1:500	Molecular Probes
Alexa Fluor® 488 anti-rabbit	dk IgG	1:500	Molecular Probes
Alexa Fluor® 594 anti-rabbit	dk IgG	1:1000	Molecular Probes
Alexa Fluor® 594 anti-mouse	gt IgG	1:500	Molecular Probes
Alexa Fluor® 488 anti-mouse	dk IgG	1:1000	Molecular Probes
Alexa Fluor® 488 anti-goat	dk IgG	1:500	Molecular Probes
Alexa Fluor® 488 anti-rat	gt IgG	1:500	Molecular Probes

2.1.3 Primer Table

Primer Type	Primer Sequence 5`→3`	manufacturer
ROSA wt forward	AAG GGA GCT GCA GTG GAG TA	Sigma – Aldrich
ROSA wt reverse	CCG AAA ATC TGT GGG AAG TC	Sigma – Aldrich
ROSA mutant forward	CTG TTC CTG TAC GGC ATG G	Sigma – Aldrich
ROSA mutant reverse	GGC ATT AAA GCA GCG TAT CC	Sigma – Aldrich
CXCR4 forward	CCA CCC AGG ACA GTG TGA CTC TAA	Sigma – Aldrich
CXCR4 reverse	GAT GGG ATT TCT GTA TGA GGA TTA GC	Sigma – Aldrich

2.2 Animals

2.2.1 Animals

Adult, 4-8 weeks old female $CXCR4_{wt/wt}/ROSA_{fl/wt}$ mice (B6.Cg-$Cxcr4_{tm2Yzo}$/J Gt(ROSA)$26Sor_{tm14(CAG-tdTomato)Hze}$/J) (Jackson Laboratory, USA) were housed in a specifically pathogen-free environment under standard conditions on a 12 h light/dark cycle with *ad libitum* access to pelletized dry food and germ-free water. All animals were bred in the animal facility (Zentrale Einrichtung für Tierversuche und Tierschutzaufgaben, ZETT) of the Heinrich-Heine-University, Düsseldorf. Institutional guidelines for animal safety and comfort were adhered to. All surgical interventions and pre- and post-surgical animal care were performed in compliance with the German Animal Protection law (State Office of Environmental and Consumer Protection of North Rhine-Westphalia, LANUV NRW). The animal proposal with the following reference number 84-02.04.2013.A444 was used for experimental procedure.

2.2.2 Genotyping

The DNA was extracted from mouse tail tip biopsy using the QuickExtract DNA Extraction Solution (Epicentre) according to the manufacturer's instructions. The PCR for CXCR4 and ROSA was performed using the Kapa2G Fast ReadyMix PCR Kit (Kapabiosystems), ROSA and CXCR4 forward and reverse Primer (see table 2.1.3, The Jackson Laboratories, Stock number: 008767) and the PCR System (Mastercycler Pro, Eppendorf) according to manufacturer's protocol. DNA was amplified using following PCR protocol: initial denaturation at 95 °C for 3 min, denaturation at 95 °C for 15 sec, annealing at 60 °C for 15 sec and extension at 72 °C for 1 min. Denaturation, annealing and extension steps were repeated for 34 cycles. Final extension at 72 °C for 10 min.

2.3 Cell culture

2.3.1 Preparation of astrocytes conditioned medium

Astrocyte conditioned medium (ACM) is widely used to support the growth of neurons in cell culture. For the production of ACM astrocytes of postnatal (P0/1) rats were isolated as previously described (Schmalenbach and Müller, 1993). Briefly, cerebral hemispheres were dissected and the meninges were carefully removed. The tissue was dissociated by gentle trituration through fire – polished Pasteur pipettes, filtered through 60 µm gauze and subsequently rinsed with serum-containing DMEM medium (10 % FCS, 2 mM glutamine, 2 % Penicillin/Streptomycin). Cells were seeded in tissue culture flasks and incubated for up to 12 days in a growth medium containing DMEM supplemented with 10 % FCS in a 10 % CO_2 and 95 % humidity at 37 °C. Medium was replaced every 4 days. To reduce contamination by non-astroglial cells, the confluent cultures were shaken overnight on a rotary platform at 180 rpm. The supernatant, which mainly contains neurons, microglia and oligodendroglial cells was discarded. To prepare serum-free ACM the confluent grown astroglial cells were rinsed with PBS (3x10 min) and then further cultured in

N2 medium, containing 75 % DMEM, 25 % HAM's F12, 5 µl/ml insulin, 100 µg/ml transferrin, 2 mM glutamine, 20 nM progesterone, 100 µM putrescin, 30 nM sodium – selenite. After 48 h incubation, the primary astrocyte culture secreted enough essential factors and nutrients into the N2 medium, which are useful to support neuronal growth. The supernatant was collected by centrifugation at 2100 rpm for 10 min at 4 °C and then aliquoted into sterile falcon tubes and frozen at - 80 °C for further use, like the cultivation of cerebral cortical neurons from mouse embryo.

2.3.2 Dissociation of cerebral cortical neurons from mouse embryo

An appropriately timed pregnant C57BL/6 wild type female mouse (16.5 days) was anaesthetized and sacrificed via cervical dislocation. The abdominal cavity was opened and the uterus, containing the embryos was removed. The embryos were isolated and then decapitated. The skull was opened and the brain was removed and placed into a separate dish. Carefully the brain was separated into two hemispheres, the meninges were removed and the cortex was isolated from the midbrain and hippocampus. The cortices of both hemispheres were cut into small pieces, and digested in a 0.05 % trypsin/EDTA-solution at 37 °C for 10 min. The digestion step was stopped by adding serum-containing Glutamax (10 % FCS, 2 mM glutamine and 2 % Penicillin/Streptomycin) to the cells, which were then collected by centrifugation at 2000 rpm for 1 min. After the addition of DNase solution (80 µg/ml DNase in Glutamax) the cells were triturated through fire–polished Pasteur pipettes, filtered through 60 µm gauze and subsequently rinsed with serum-containing Glutamax medium to stop DNase activity. After a last centrifugation step at 1500 rpm for 5 min, the resulting pellet was resuspended into ACM (see 2.3.1). Cells were plated on Poly-D-lysine (1.0 mg/ml; molecular weight 300,000 kDa) and laminin (13 µg/ml) coated cover slips of 24 well plates (Greiner) and cultured at 37 °C and 5 % CO_2 for 2 days.

2.3.3 CXCR4 antibody validation

To validate the CXCR4 antibody, either human CXCL12 (500 ng/ml dissolved in a 1 % PBS/BSA solution) or control solution (PBS/BSA) was added to the medium of dissociated mouse cerebral cortical neuron cultures. After 24 h in culture cerebral cortex neurons, were fixed with 4 % PFA, and then immunocytochemically stained with an antibody against the axonal marker βIII-tubulin, and against the chemokine receptor CXCR4 (see table 2.1.2.1 and 2.1.2.2). For quantitative analysis, images were taken by the Cellomics™ ArrayScan VTI (Thermo Fisher Scientific). The quantification of CXCR4 and accordingly Tubulin positive neurons per well as well as the quantification of the nucleus count were automatically performed with the Cellomics software to avoid quantification bias. For each protein a separate protocol was used. Average neuron counts per group were normalized to control groups as indicated. Data are presented as the mean ± SEM. N = three replicate wells from four separate experiments.

2.3.4 Dissociation of dorsal root ganglion cells

DRG neurons of $CXCR4_{wt/wt}/ROSA_{fl/wt}$ mice were obtained under sterile conditions as described previously (Gobrecht et al., 2014; Scott, 1977). In brief, mice were anaesthetized, decapitated and the DRG neurons (T8-L6) were harvested, cut into sections, digested in a collagenase-trypsin

mixture (0.3 % collagenase type IA, 0.25 % trypsin/EDTA, serum-free low glucose DMEM) at 37 °C for 45 min and mechanically dissociated. After digestion of all ganglia, the trypsin was inactivated by adding serum-containing DMEM and the DRGs were collected by centrifugation at 900 g for 10 min. The resulting pellet was resuspended in low glucose DMEM containing 10 % FBS (fetal bovine serum) and 2 % Penicillin/Streptomycin (500 U/ml). Cells were plated on Poly-D-lysine (0.1 mg/ml; molecular weight 300,000 kDa) and laminin (20 mg/ml) coated 96 well plates (Becton Dickinson) and cultured at 37 °C and 5 % CO_2 for 2 days. For myelin coating, CNS myelin extract from adult rat brain (see 2.3.4.1) was left to dry on Poly-D-lysine/ laminin coated wells overnight at room temperature at a pre-optimized concentration.

2.3.4.1 Preparation of CNS Myelin

Inhibitory central myelin extract was prepared according to earlier publications (Ahmed et al., 2006; Sengottuvel et al., 2011). In brief, Sprague-Dawley rat brains were mechanically homogenized in 0.32 M sucrose and centrifuged at 800 x g for 10 min (4 °C) to collect cell debris. The supernatant was kept, the cell pellet again homogenized in 0.32 M sucrose and centrifuged as described above. Both supernatants were combined and centrifuged at 13,000 x g for 20 min (4 °C). The supernatant was discarded and the pellet resuspended in 0.32 M sucrose. 0.9 M sucrose was pipetted in a tube and overlain with the resuspended solution thoroughly. The tube was then centrifuged at 20,000 x g for 60 min (4 °C). After the centrifugation step, the white myelin extract is between the two phases. It was carefully collected, resuspended in 0.32 M sucrose solution and centrifuged at 13.000 x g for 25 min (4 °C). Subsequently, the pellet was resuspended in water and kept on ice for 30 min. After final centrifugation at 20,000 x g for 25 min (4 °C), the supernatant was discarded and the CNS myelin extract was resuspended in water in the desired volume, aliquoted and subsequently stored at -80 °C. The concentration of CNS myelin extract used for further experiments was optimized for each lot by testing different concentrations in cell culture for its inhibitory potential. The CNS myelin was kindly provided by the group of Prof. Dr. Dietmar Fischer.

2.3.5 Neurite outgrowth assay

For the neurite outgrowth assay, either human CXCL12 (500 ng/ml dissolved in a 1 % PBS/BSA solution) or control solutions (PBS or PBS/BSA) was added to the medium of dissociated mouse DRG cultures. The CXCR4 antagonist AMD3100 was added at 5 µM. The pharmacological inhibitor was used either alone or in combination with CXCL12 or BSA respectively. After 2 days in culture DRG neurons, were fixed with 4 % PFA and then immunocytochemically stained with an antibody against βIII-tubulin, an axonal marker and a neuronal nuclei marker, NeuN (see table 2.1.2.1 and 2.1.2.2). For quantitative analysis 6 x 6 images were taken by the Pathway 855 microscope system (Becton Dickinson). The quantification of total axon length and neuron numbers per well were automatically performed with the Attovision software, avoiding bias of quantification. Average neurite length per neuron and neuron counts per group were normalized to control groups as indicated. Data are presented as the mean ± SEM. N = six replicate wells from three to five separate experiments.

2.4 Surgical procedures

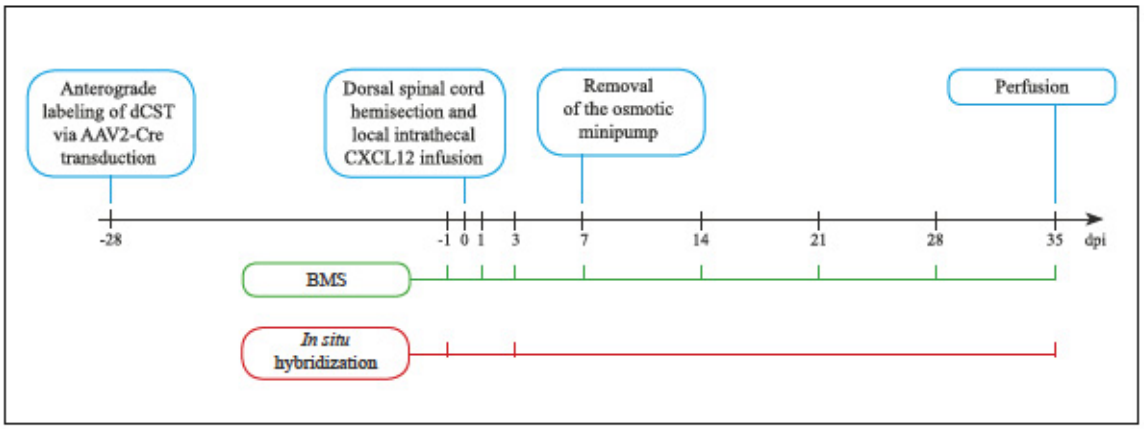

Fig. 2.1: Experimental design.
Schematic illustration of the experimental timeline. AAV2-Cre transduction of pyramidal neurons of the layer V in the hind limb region of the sensorimotor cortex of CXCR4wt/wt/Rosa/- mice leads to the anterograde labeling of the dorsal corticospinal tract, which expresses the reporter gene tdTomato. After four weeks, a dorsal spinal cord hemisection was performed and CXCL12 was intrathecally infused via an osmotic minipump. One week later, the osmotic minipump was removed in an additional surgery. Five weeks after SCI the mice were perfused. The open field BMS locomotor test was evaluated at day -1 and 1, 3, 7, 14, 21, 28 and 35 days post injury (dpi) to analyze functional recovery. For *in situ* hybridization, samples were taken from control and from 3 dpi and 35 dpi injured animals.

2.4.1 Preparation of AAV2

For AAV2 (adeno-associated virus of serotype 2) production, the pAAV-MCS plasmid (Stratagene, USA) carrying the cDNA for Cre-HA (Hemagglutinin epitope-tagged Cre-Recombinase; kindly provided by Dr. Zhigang He) downstream of the CMV promoter (cytomegalovirus promoter) was used. To generate recombinant AAV, pAAV-RC (Stratagene, USA) that encodes the AAV genes rep and cap and the helper plasmid (Stratagene, USA) that encodes E2A, E4 and VA were used for co-transfection in 293T cells (Stratagene, USA). Purification of virus particles was performed as described previously (Park et al., 2008; Zolotukhin et al., 1999). The viral solutions had titer of about 1 x 109 GC/ml, which lead to a RGC transduction rate of up to 90 %. The preparation of the AAV2 was kindly performed by the group of Prof. Dr. Dietmar Fischer.

2.4.2 Anterograde labeling of corticospinal tract axons

Four weeks prior to spinal cord lesioning, the dCST was anterogradely traced via injections of AAV2-Cre into the layer V of the hind limb sensorimotor cortex of four weeks old $CXCR4_{wt/wt}/ROSA_{fl/wt}$ mice (Fig. 2.1). As this virus serotype is highly neurotropic, mainly neurons are transduced upon stereotaxic injection of AAV2 (Baek et al., 2010; Jara et al., 2012; Park et al., 2008). In CXCR4/ROSA mice, transduced neurons can be visualized without immunofluorescence staining since the transduction of neurons with AAV2-Cre leads to a strong cytoplasmatic expression of the red fluorescent reporter protein tdTomato. The transcription of the reporter protein is normally inhibited via a floxed stop-sequence, which is localized in the

ROSA26 locus lying prior to the tdTomato gene (Fig. 2.2 A). AAV2-Cre transduced neurons express the HA-tagged Cre-Recombinase, which leads to the excision of the floxed stop-sequence, thereby allowing the transcription of the red fluorescent protein. Through the transduction of the pyramidal neurons in layer V of the sensorimotor cortex, which project their axons into the CST, this method was used to anterogradely trace the dCST. Mice were anesthetized with isoflurane (Abbvie, 1.5-2 % in O_2 and NO_2 at a ratio of 1:3), and the skull of the animals was shaved and disinfected. Then, the head was fixed in the stereotactic frame (Stoelting Co., USA) at both external *acoustic meati*. A midline incision over the skull was made to reveal the reference skull mark bregma, defined as the midpoint of the curve of best fit along the transverse suture (Fig. 2.2 B) (Paxinos and Franklin, 2001). To expose the sensorimotor cortex, two small openings in the skull were made as shown in Fig 2.1 C with a microdrill (Micromot 40/E NO28515, Proxxon, Germany) and 0.5 mm drill head (Fine Science Tools, USA). The injection coordinates of the hind limb sensorimotor cortex were calculated using bregma as reference and the mouse brain atlas in stereotaxic coordinates (Paxinos and Franklin, 2001). A total of 2 µl of AAV2-Cre was injected

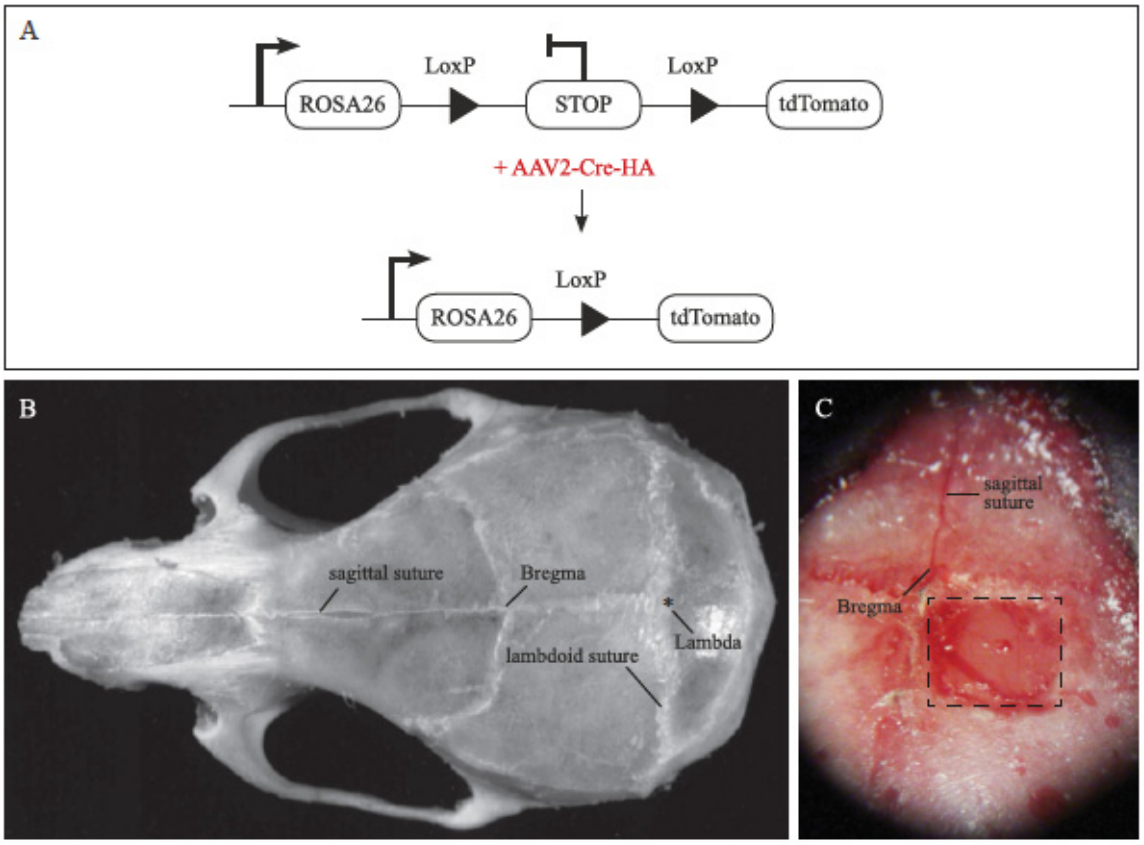

Fig. 2.2: Generation of anterogradely labeled corticospinal tract axons via AAV2-Cre transduction. **A)** The transcription of the reporter gene, tdTomato, which is localized in the ROSA26 locus, is normally inhibited by a floxed stop sequence. The transduction of pyramidal neurons in layer V of the sensorimotor cortex via AAV2, which express the HA-tagged Cre-Recombinase leads to the excision of the floxed stop-sequence, thereby allowing the transcription of the red fluorescent protein and therefore the anterograde labeling of the dCST. **B)** Photographic representation of the dorsal surface of the mouse skull with the stereotaxic reference points: bregma, lambda, the sagittal and lambdoid suture (Paxinos and Franklin, 2001). **C)** Image of the dorsal surface of a mouse skull during the surgery, which reveals the reference skull point bregma and the sagittal suture. Framed area indicates the small opening, which was made to expose the sensorimotor cortex on the right side.

into the sensorimotor cortex at three sites pro hemisphere through a glass capillary (Ø 40-60 µm) attached to a nanoliter injector (Model 701 RN, Drummond Scientific Company, USA). The coordinates were as follows (coordinates from bregma in mm): anterior-posterior/medial-lateral/dorsal-ventral, 0.0/1.5/0.5, − 0.5/1.5/0.5, − 1.0/1.5/0.5). The capillary was left in place for 1 min before moving to the next coordinate. After all coordinates were injected with the AAV2-Cre, the exposed brain area was covered with PBS soaked Gelfoam (Gelastypt, Sanofi Aventis, Denmark) and the skin was sutured.

2.4.3 Filling and priming of osmotic minipumps

The osmotic minipump Alzet pump model 1007D was chosen for the experiments, since it was the smallest in physical size, ideal for the small mice and endowed with a release rate of 0.5 µl/h for a duration of 7 days. The pumps were filled and primed in advance to the surgery according to the manufacturer's instructions. The empty pump together with its flow moderator was weighed. Then the pump was slowly filled with the respective solution using a supplied blunt-tipped filling tube connected to a syringe. The pump was held in an upright position and the reservoir was filled, allowing air to escape around the filling tube. Afterwards, the flow moderator was inserted and the filled minipump was weighed again. The difference in the weights obtained before and after filling gives the net weight of the solution loaded and is a measurement for complete filling of the minipump. Prior to *in vivo* implantation, the filled minipumps were primed in sterile 0.9 % saline at 37 °C *in vitro* for at least two to four hours. Priming is essential when immediate pumping is required and a catheter is used with the pump. Thus, a constant pumping rate was guaranteed at implantation time point.

2.4.4 Dorsal hemisection and epidural catheterization

For spinal lesioning and epidural catheterization, mice were anesthetized with isoflurane (Fig. 2.1). Then, the back of the animals was shaved and disinfected. A midline incision over the dorsal processes of T8-T12, exposing the underlying paravertebral muscles, was made using sharp ended scissors. The adipose tissue between the shoulder blades was detached from the muscles and retracted by a clamp (Fine science tools, USA). The muscles above T8-T12 were cut laterally of the vertebrae and forced apart by a muscle retractor (Fine science tools, USA). After exposure of the above mentioned vertebrae a complete laminectomy of T9 and T11 was performed (Fig. 3.4 A, B1-B2). A surgical thread (Ethicon 9-0, USA) was knotted around the tip of a 32G PU intrathecal catheter (Alzet Mouse Intrathecal Catheter: outer Ø: 0.23 mm; inner Ø: 0.09 mm; Charles River Laboratory), which was then guided epidurally from below T10 towards T9 as illustrated in Fig. 3.4. One end of the surgical thread was kept in the epidural space, while the other end was pulled out on the caudal side of T10. Above T10, both ends of the surgical thread were knotted together to secure and lift the catheter (Fig. 3.4 B3). To ensure a centered position of the catheter over the lesion, the spinous process of T10 was removed in advance. For stabilization of the catheter fixation, the surgical thread was additionally glued with Histoacryl® tissue glue (B. Braun Surgicals, Germany) between two cushions of autologous fat tissue covering the exposed spinal cord area of T11 as well as the vertebra T10 (Fig. 3.4 A, B4). The cushions were glued to surrounding adipose and muscle tissue. After catheter filling, the catheter was connected to the subcutaneously placed primed (37 °C) osmotic minipump preloaded with 100 µl of either

control solutions (PBS or PBS/BSA) or treatment solution (10 µM CXCL12, in 1 % PBS/BSA). Subsequently, a T9 dorsal hemisection lesion (Fig. 3.4 A, B5) was performed similar to that described previously by Zheng et al. and Liu et al. (2010). First, the dura mater at T9 was opened in close proximity to the catheter tip with a pair of microscissors (Fine Science Tools, USA) and then a bilateral cut of the dorsal spinal cord was made to a depth of 0.8 mm with an ultra-fine micro knife (Fine Science Tools, USA). Finally, the lesion area was covered with a piece of Nescofilm® (Alfresa Pharma Corporation, Japan) to avoid intense catheter adhesion to the surrounding tissue. The overlying muscles and skin were sutured in layers. The substances were infused for 7 days at an infusion rate of 0.5 µl/h. One week after the spinal cord injury, the osmotic minipump was removed in an additional surgery (Fig. 2.1). Briefly, the sutures above T12 were re-opened, the catheter was cut at this level and it was removed together with the connected osmotic minipump. The skin was re-sutured and the mice were kept for an additional 4 weeks before they were sacrificed (Fig. 2.1, see 2.4.7).

2.4.5 Examination of catheter fixation and catheter-induced compression

To examine the mouse catheter fixation, 5 % Evans Blue dye was intrathecally infused for 7 days to visualize the liquid distribution, starting immediately after dorsal hemisection. Seven days post-lesion, mice were sacrificed and the spinal cord tissue was cut with a cryostat (see 2.5.1). To analyze catheter-induced spinal cord compression, spinal cord sections were stained for Masson`s trichrome (see 2.6.1).

2.4.6 Postoperative care

Immediately after surgery, the mice received 1 ml of physiological saline and pain relief by subcutaneous injection of 4 mg/kg Rimadyl (Pfizer). Individual caging on a warming blanket (37 °C) and with soft bedding was provided until full recovery from anesthesia. Animals were then returned to their home cages with *ad libitum* access to food and water. Post-operative care included prophylactic treatment with antibiotics (Baytril®; Bayer Healthcare, 15 mg/kg) for 1 week, manual bladder emptying until normal function returned, and pain relief (Rimadyl) for 2 days post-lesion. If there was blood in the urine the antibiotic was additionally administrated for further 3 days and in case of automutilation the affected area was covered daily with Alu-Spray (Selectavet).

2.4.7 Animal sacrifice and perfusion

Seven days after surgery (examination of catheter fixation and catheter-induced compression) or 5 weeks after SCI (quantification of axonal sprouting) mice were deeply anesthetized (isoflurane) and then transcardially perfused using a peristaltic pump (Fig. 2.1) (Ministar, World Precision Instruments). The chest of the mice was opened, a needle inserted into the left ventricle and the right atrium was opened with a scissor. With a pump rate of 4 ml/min, the blood within the circulatory system was washed out with cold PBS for 1 min. Then the PBS was replaced by a chemical fixative, 4 % PFA for 5 min. The spinal cords and brains were dissected, post-fixed in 4 % PFA at 4 °C for 24 h and subsequently cryoprotected for 3 days in 30 % sucrose, until the tissue was fully saturated with sucrose solution and sunk to the bottom of the vial.

2.5 Tissue preparation

2.5.1 Cryostat sectioning of frozen spinal cord tissue

After cryoprotection the spinal cords were trimmed to the required size and region, e.g. for the testing of catheter fixation and catheter-induced compression: spinal cord lesion core area; sprouting quantification and axonal counting: spinal cord segment 5 mm rostral to the lesion area. The tissue molds (Sakura Finetek, VWR, USA) were filled with O.C.T. compound and the spinal cord segments were gently transferred into the molds and oriented as desired. The molds were placed on a flat level surface of a block of dry ice and let freeze slowly. The embedded spinal cord segments were stored at -80 °C. Tissue sectioning was performed using a cryostat (CM3050S, Leica Biosystems, Germany). For transverse or parasagittal sectioning of spinal cord, the tissue molds were transferred into the cryostat 30 min prior the cutting, to allow equilibration to the respective temperature (chamber temperature: -15 °C; specimen temperature: -20 °C). Then, the frozen tissue blocks were freeze-mounted onto the cryostat specimen chuck with O.C.T. compound. Serial sections of 20 µm thickness were collected on adhesive microscope slides (Star Frost) and let dry before storing them in micro slide boxes (VWR, Germany) at -20 °C.

2.5.2 Microtome sectioning of frozen brains

After cryoprotection, the brains were placed on a paper towel to remove excess liquid surrounding the tissue. Then, the brains were slowly frozen in isopentane at a temperature of - 32 °C to - 27 °C and stored at - 80 °C. For transverse sectioning of frozen brains, the tissue was freeze-mounted onto the microtome cutting area with O.C.T. compound. Serial sections of the hind limb region of the primary sensorimotor cortex of 20 µm thickness (mouse) or 30 µm (rat), respectively, were cut (cutting temperature: - 30 °C), collected in 24 well plates (Costar) prefilled with cryoprotect solution and stored at - 20 °C.

2.6 Histochemical staining protocols

2.6.1 Masson trichrome staining

Masson`s trichrome staining is an easy and fast staining method for connective tissue in histological samples. It was chosen to reveal catheter induced spinal cord compressions. The staining procedure was described by Bancroft et al. (1996) and consists of three different solutions. The dyes in solution A (0.5 % fuchsin acid, 0.5 % xylidine ponceau, 1 % acetic acid) stain muscles, fibrin, cytoplasm and erythrocytes red. Fibers like collagens are colored green by solution C (2 % light green SF yellowish, 2 % acetic acid). Solution B (1 % molybdatophosphoric acid hydrate) is essential for the differentiation of the staining. The trichrome staining procedure was started by washing the spinal cord sections in PBS and then *aq. bidest.* The sections were then immersed in solution A for 5 min and subsequently rinsed with *aq. bidest.* Afterwards, the sections were incubated in solution B for 3 min and subsequently rinsed in *aq. bidest.* Last, the sections were

immersed for 5 min in solution C and rinsed again in a last rinsing step in *aq. bidest.* The tissue sections were dehydrated with an ascending ethanol sequence (50 %, 70 %, 90 %, 2 x 100 %, each 1 min). Afterwards, the sections were transferred to RotiHistol® (2 x 1 min) and embedded in DPX mounting medium.

2.6.2 Nissl staining

The Nissl staining is a commonly used method for the identification of the basic neuronal structure in brain or spinal cord tissue. It stains the Nissl body in the cytoplasm of neurons purple-blue. It was chosen to reveal the spinal cord injury area in transverse and sagittal spinal cord sections of injured mice. The tissue sections were stained in a cresyl violet solution (1.6326 g sodium acetate, 2.88 ml acetic acid, 100 mg cresyl violet ad 300 ml *aq. bidest.*) for 5-10 minutes and warmed up to 37 °C in an oven to enhance the staining. The sections were then rinsed with *aq. bidest.* Afterwards, sections were dehydrated with an ascending ethanol sequence (50 %, 70 %, 90 %, 2 x 100 %, each 1 min). Finally, the sections were transferred to RotiHistol® (2 x 1 min) and embedded in DPX mounting medium.

2.7 Immunofluorescence staining protocols

2.7.1 Visualization of AAV2-Cre transduced cerebral pyramidal neurons

Immunofluorescence staining is not required for the visualization of the projecting axons of AAV2 transduced pyramidal neurons in the sensorimotor cortex since the transduction of neurons with AAV2-Cre leads to a strong cytoplasmatic expression of the red fluorescent protein tdTomato in these cells (Fig. 2.2 A, see 2.4.1). Therefore, after washing the 20 µm thick transverse spinal cord sections 5 mm caudal to the lesion site with PBS (3 x 10 min), sections underwent a 0.3 % Sudan Black staining, to reduce background staining. After further washing steps, they were coverslipped with Fluoromount G.

2.7.2 CXCR4 immunofluorescence staining of spinal cord sections

The immunofluorescence staining of CXCR4 in 20 µm thick transverse spinal cord cryosections was started by washing the sections with PBS (3 x 10 min). Then, sections were blocked with 10 % normal goat serum, 2 % BSA in PBS for 1 h at room temperature (RT) followed by primary antibody incubation over night at 4 °C. All antibodies were diluted in blocking solution. The chemokine receptor CXCR4 was co-stained either with one of the neuronal markers PAM311-NP, PAM312-P, Tuj1, NeuN and CGRP, or co-stained with a glial marker such as GFAP or MBP. Afterwards, sections were rinsed with PBS (3 x 10 min) and incubated for 2 h at room temperature with the respective secondary antibody (see table 2.1.2.2). Cell nuclei were labeled with 4,6`-diamidino-2-phenylindoline (DAPI). Finally, the sections were rinsed again in PBS (3 x 10 min), and the sections were additionally stained with 0.3 % Sudan Black dye to reduce background staining. After further washing steps they were coverslipped with Fluoromount G.

2.7.3 Staining of brain sections

The immunofluorescence staining of 20 µm thick (rat: 30 µm) transverse brain sections was started by washing the free-floating sections with PBS (3 x 10 min). Then, sections were blocked with 10 % normal goat serum, 1 % BSA in PBS for 1 h at RT followed by primary antibody (Ctip2 and Anti-HA, see table 2.1.2.1) incubation over night at 4 °C. All antibodies were diluted in blocking solution. Afterwards, sections were rinsed with PBS (3 x 10 min) and incubated for 2 h at RT with the respective secondary antibody (see table 2.1.2.2). Cell nuclei were labeled with DAPI. Finally, the sections were rinsed again in PBS (3 x 10 min) and to reduce background staining, they were additionally stained with 0.3 % Sudan Black dye. After further washing steps they were carefully transferred into gelatin and then mounted on adhesive microscope slides and coverslipped with Fluoromount G.

2.8 Analysis of tissue sections

2.8.1 Image acquisition

For the histochemical staining the digital, bright field images were taken with the Keyence BZ-8100E microscope under a 10 x (Masson Trichrome staining) or a 2 x (Nissl staining) objective. However, the image acquisition of the fluorescence staining occurred via a fluorescence mode of Keyence BZ-8100E microscope under a 40 x objective. All digital images were merged by the BZ Analyzer software from Keyence.

2.8.2 Axonal counting and sprouting quantification in spinal cord sections

The quantification of the rostral sprouting in mice that received a dorsal hemisection and the infusion of either control solutions (PBS or PBS/BSA) or treatment solution (10 µM CXCL12, in 1 % PBS/BSA) through an osmotic minipump for 7 days, was performed according to Liu et al. (2010) and Kim et al. (2003). Animals were sacrificed 5 weeks after spinal cord injury. To quantify the sprouting axons 5 mm rostral to the lesion site, a vertical line was drawn through the central canal of transverse sections in images using Adobe Photoshop software. At a distance of 50 µm parallel to this line additional vertical lines (I, II, III etc.) were drawn. The sprouting fibers on one-half of the gray matter that cut these lines were counted using the Photoshop counting tool. The resulting numbers were averaged over five sections per animal and then normalized against the total number of labeled axons in the dCST. This latter number was established by counting the labeled CST axons in five transverse sections at the thoracic level in two rectangular areas (50 µm x 50 µm). Data are presented as the mean ± SEM. N = four PBS control animals, five BSA control animals and six CXCL12 treated animals.

2.8.3 Quantification of CXCR4 expression in spinal cord sections

The images were directly merged by the BZ Analyzer software from Keyence. The quantification was performed using Image J software (https://imagej.nih.gov/ij). The borders of the transverse spinal cord section were marked and the Bernsen auto local threshold was applied over five sections per animal and then normalized to the values obtained from the analysis of control groups as indicated. The immunoreactivity of CXCR4 was calculated. Data are presented as the mean ± SEM. N = four control unlesioned animals and 11 lesioned animals.

2.9 Behavioral Testing

2.9.1 Open field Basso Mouse Scale locomotor test

Locomotor hind limb function was assessed using the Basso Mouse Scale (BMS) (Basso et al., 2006). This scale has been shown to be more sensitive, reliable and valid for assessing mouse behavior following SCI than the original open field Basso, Beattie and Bresnahan (BBB) locomotor test designed for rats (Basso et al., 1995). Prior to injury, the animals were trained every day for 4 min over one week. While walking in an open field (60 x 9 x 43 cm) the hind limb movements of the mice were observed by two examiners blinded to the treatment groups. The BMS scale ranges from 0 (no hind limb movement) to 9 (consistent, coordinated gait with parallel paw placement and normal trunk stability) and the subscore ranges from 0-11. The examiners assigned the BMS score based on the following parameters: ankle movement, plantar placing, weight support, stepping, coordination, paw position, trunk stability, and tail position). Mice were evaluated at day -1 and 1, 3, 7, 14, 21, 28 and 35 days post injury (Fig. 2.1). The left and the right paws were analyzed separately. Data are presented as the mean ± SEM. N = four PBS control mice and five CXCL12 treated mice.

2.10 *In situ* hybridization

In situ hybridization uses a radiolabeled complementary RNA strand to localize a specific DNA or RNA sequence in a tissue section. The technique was used to localize the mRNA of *Cxcl12*, *Cxcr4* and *Cxcr7* in brain sections of control and injured [3 days post injury (dpi), 5 weeks post injury (wpi)] mice and rats (Fig. 2.1). The CXCL12 probe was transcribed from full-length mouse CXCL12α cDNA. Probes for mouse and respectively rat CXCR4 and CXCR7 correspond to the coding regions of the receptors (Sanchez-Alcaniz et al., 2011; Stumm et al., 2002). Riboprobes were generated from the linearized vector constructs by *in vitro* transcription. Construction of ^{35}sulphur-[^{35}S]-radioactively labeled riboprobes was done using [^{35}S]-uridine ([^{35}S]-UTP) and [^{35}S]-cytidine triphosphate ([^{35}S]-CTP). Purification of the riboprobes was performed using P-30 micro Bio-Spin® columns. The riboprobes were diluted in hybridization buffer to 100.000 counts/µl, and stored in aliquots at -20 °C until hybridization. *In situ* hybridization was performed as described previously (Stumm et al., 2002). The brains were dissected, immediately

frozen in -25 to -35 °C cold 2-methylbutane and stored at -80 °C until further use. Brains were embedded frontally in Tissue-Tek® O.C.T. and sectioned coronally using a Leica CM1850 Cryostat at -20 °C. The 20 µm thick brain sections were mounted on HistoBond® glass slides, air-dried and stored at -80 °C until prehybridization. Fixation of slide-mounted frozen sections was performed in phosphate-buffered 4 % paraformaldehyde for 60 min. After washing in PBS, the slides were incubated for 10 min in 0.4 % Triton X-100, rinsed in distilled water, and incubated for 10 min in 0.1 M triethanolamine, pH 8.0 containing 0.25 % v/v acetic anhydrate. The slides were rinsed twice in PBS and then dehydrated in 50 and 70 % 2-propanol. The air dried sections were stored at -20 °C. For the application of the riboprobes, frozen prehybridized sections were thawed and dried. 40 µl of the probe-hybridization mix were spread on a 40 mm coverslip, which was subsequently applied to the respective sections. Bubbles formation was strictly avoided. Hybridization was performed overnight (14-36 h) at 60 °C. The slides were washed in 2x saline sodium citrate buffer and then further washing steps with a series of reducing concentrations of sodium citrate were performed. After washing in water, the tissue was dehydrated in 50 and 70 % 2-propanol. Detection of the probe's signal was done by radiographic films and subsequent photographic emulsion coating. Slides were exposed to x-ray film for 46 hours. For high-power bright- and dark-field microscopic analysis, autoradiographic detection of ^{35}S was performed with NTB-2 nuclear emulsion. Exposure times were 21 days. Cresyl violet was used as counterstain. The *in situ* hybridization was kindly performed by the group of Prof. Dr. Ralf Stumm at Friedrich-Schiller-University, Jena.

2.11 Statistical Analysis

Due to the small sample size, it was not possible to check normality of volume parameter. Tests for normality (like for example Shapiro-Wilk-Test) are known to be too liberal with this small sample size. Additionally it is not possible to have a reliable interpretation of the distribution with graphical methods like Q-Q-Plots with this small data set. Since parametric methods are not robust enough for deviations from normality when sample size is so small, non-parametric methods needed to be applied in this study. Non-parametric significant tests do not have strict requirements, neither on the distribution of the data nor on sample size. Hence, the non-parametric Mann-Whitney-U-Test was applied to compare two unpaired groups for significant difference in the parameter of interest. The non-parametric Wilcoxon Test was applied to compare two paired groups for significant difference in the parameter of interest. The non-parametric Kruskal-Wallis Test was applied to compare more than two unpaired groups for significant difference in the parameter of interest. All analyses were conducted using GraphPad Prism 7 software. Statistical consulting through Daniela Keller (www.statistik-und-beratung.de).

3. RESULTS

3.1. Role of the CXCL12-CXCR4 axis in cultured DRG neurons

3.1.1 *In vitro* validation of the CXCR4-UMB2 antibody

Upon ligand binding, the intracellular C-Terminal sequence of the activated CXCR4 receptor is phosphorylated and cannot be recognized any more from the most commonly used knockout validated rabbit monoclonal anti-CXCR4 antibody clone UMB-2 (Fig. 1.3) (Busillo et al., 2010; Krupnick and Benovic, 1998; Mueller et al., 2013). This antibody recognizes the receptor only in its inactive state, when the C-Terminal is not phosphorylated (Fischer et al., 2008; Mueller et al., 2013). After internalization the CXCR4 receptor can be either degraded or recycled back to the plasma membrane (Marchese et al., 2003). However sustained stimulation of the CXCR4 receptor with CXCL12 causes lysosomal degradation of the receptor (Marchese and Benovic, 2001). In order to confirm the specificity of the CXCR4-UMB-2 antibody and to verify that human CXCL12 is able to bind mouse CXCR4, the immunocytochemical expression of CXCR4 was analyzed in embryonic mouse cerebral cortex neurons that were subjected to either recombinant human CXCL12 (500ng/ml) for 24 h or to the control solution BSA. CXCR4 was identified in a subset of embryonic mouse cortical neurons, most likely interneurons, already after 24 h (Fig. 3.1 A, C). The receptor was expressed in the soma, in the neurites and in the growth cones. After treatment with the recombinant human CXCL12, the CXCR4-UMB-2 antibody did not recognize the phosphorylated epitope of the activated CXCR4 receptor anymore and the immunoreactivity disappeared (Fig 3.1 A, C). High-content analysis with the Cellomics™ Array Scan, which combines fluorescence microscopy, image processing and automated cellular measurements, confirmed the loss of more than 50 % of CXCR4 positive neuron staining after CXCL12 treatment in cell culture (Fig 3.1 C). However, the number of nuclei in the CXCR4 and Tubulin Cellomics protocol (Fig. 3.1B) as well as the number of βIII-tubulin positively stained neurons (Fig. 3.1 C) remained unchanged upon CXCL12 treatment.

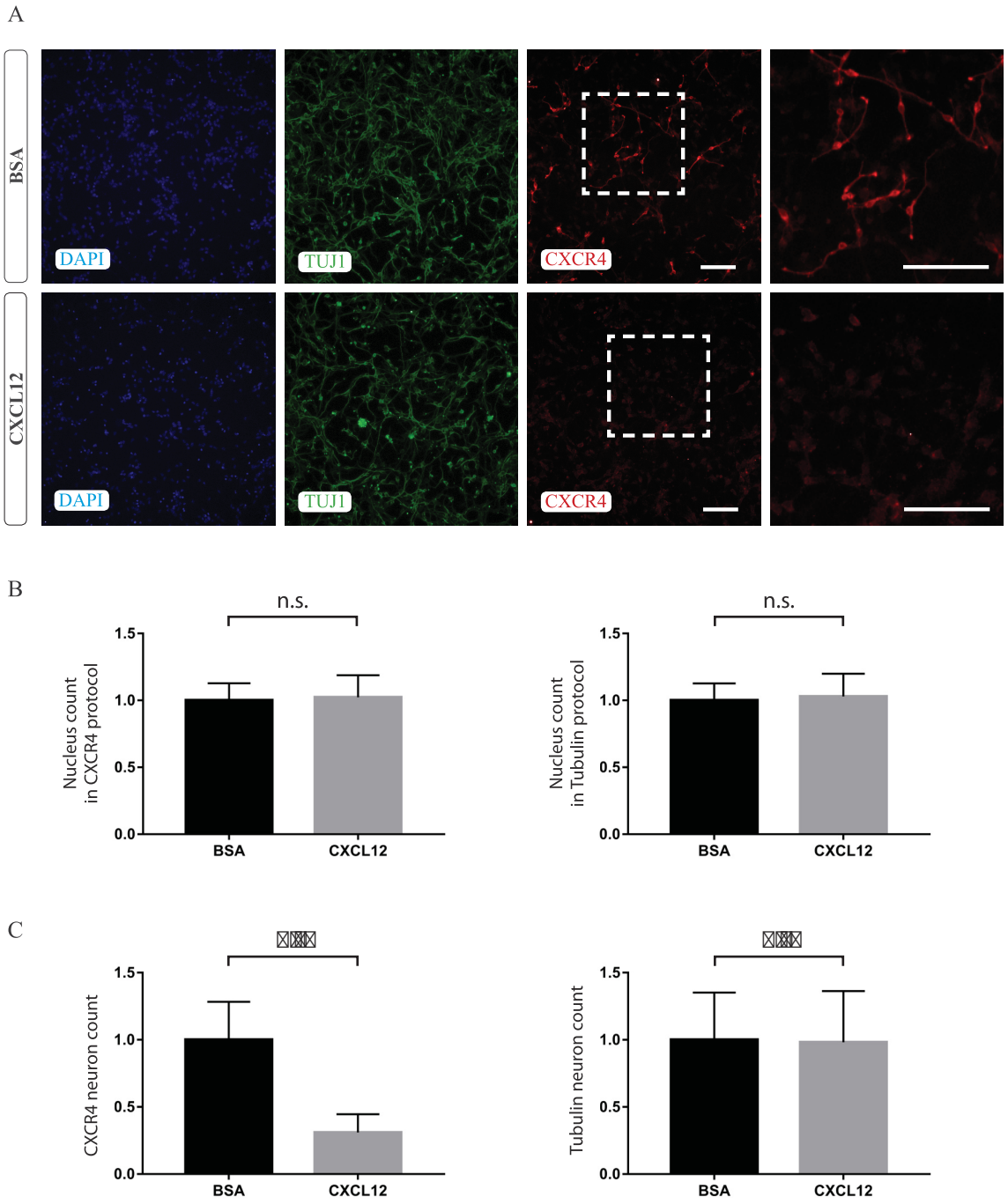

Fig. 3.1: CXCR4-UMB2 antibody validation.
A) Embryonic mouse cerebral cortical neurons were stained for nuclear DAPI (blue staining), axonal βIII-tubulin (green staining) and CXCR4 receptor (red staining) after exposure for 24 h to either control solution (PBS/BSA) or CXCL12 (500 ng/ml in 1% PBS/BSA). Framed areas indicate higher magnification on the right site. Scale bar: 50 µm. **B)** Quantification of the CXCR4 cells with positively stained DAPI nuclei and of the tubulin cells with positively stained DAPI nuclei in either control or treatment solution. Values were normalized to the control group with an average number of 62749 cells/well (CXCR4) and 61423 cells/well (tubulin) (24 well plate). **C)** Quantification of the CXCR4 and tubulin, respectively positively stained neurons in either control or treatment solution. Values were normalized to the control group with an average number of 8421 µm/cell (CXCR4) and 32443 µm/cell (tubulin) (24 well plate). Data are presented as the mean ± SEM. N = three replicate wells from four separate experiments. The non-parametric Wilcoxon test was applied to compare the two paired groups for significant difference in the parameter of interest.

3.1.2 CXCL12 does not improve neurite outgrowth of adult dorsal root ganglion cells

It has been previously described that CXCL12 stimulates axonal elongation and branching in cultured cerebellar granule cells, hippocampal neurons and adult retinal ganglion cells (RGC) (Arakawa et al., 2003; Heskamp et al., 2013; Pujol et al., 2005). In order to investigate the effect of CXCL12 on neurite outgrowth of adult mouse DRGs, neurons were dissociated, plated on laminin-coated dishes and exposed to CXCL12 (500ng/ml) in the highest concentration tested for adult RGC, which yielded the strongest neurite outgrowth. After two days in culture, the axon growth of βIII-tubulin positive DRG neurons was measured automatically by the Attovision software. CXCL12 did not promote enhanced axon outgrowth of DRG neurons that were grown on laminin coated plates (Fig.3.2 A, C).

3.1.3 Neurite outgrowth of adult DRG neurons is impaired on CNS myelin

One of the major obstacles of neuronal regeneration of CNS axons is the presence of myelin. The growth inhibitory environment formed by oligodendrocyte derived myelin-associated inhibitors such as NogoA, myelin-associated glycoprotein (MAG), oligodendrocyte-myelin glycoprotein (OMgp), Semaphorin4D and Ephrin B3 contributes to the failure of CNS axons to regenerate (Bähr and Przyrembel, 1995; Benson et al., 2005; Chen et al., 2000; McKerracher et al., 1994; Moreau-Fauvarque et al., 2003; Wang et al., 2002). In fact, as previously published for postnatal rat DRGs (Opatz et al., 2009) and adult rat RGCs (Heskamp et al., 2013), axon growth of cultured adult mouse DRG neurons plated on myelin-coated dishes was impaired in comparison to control DRG neurons plated on laminin (Fig. 3.2 A, C). In the presence of myelin not only the axon length, but also the number of branching events was reduced compared to laminin controls. However, the number of outgrowing neurons on myelin was not reduced compared to the cell number of growing neurons on laminin (Fig. 3.2 D).

3.1.4 CXCL12 exerts disinhibitory effects towards CNS myelin stimulating neurite outgrowth of adult dorsal root ganglion cells

As previously published, in cultured rat postnatal (P6) DRG neurons as well as in adult rat RGCs, plated on a myelin substrate, the administration of CXCL12 mediated an extensive, concentration-dependent axon outgrowth (Heskamp et al., 2013; Opatz et al., 2009). CXCL12 was sufficient to mediate overcoming of myelin-induced outgrowth inhibition. In order to examine the disinhibitory effect of CXCL12 on adult mouse DRGs, neurons were dissociated, plated on laminin-, and on myelin-coated dishes and exposed to CXCL12 (500 ng/ml) in the highest concentration tested for adult RGCs and P6 DRG neurons, which yielded the strongest axon outgrowth. After two days incubation time, the axon length of βIII-tubulin positive DRG neurons was measured automatically by the Attovision software. CXCL12 was able to exert disinhibitory effects toward CNS myelin in DRG neurons and promoted axon outgrowth, comparable to the axon outgrowth of control DRG neurons, grown on laminin-coated dishes, while the nucleus number remained unchanged (Fig 3.2 A, C-D). Not only the axon length, but also the number of branching events was increased in CXCL12 treated DRG neurons.

3.1.5 CXCL12 mediates neurite outgrowth and disinhibitory effects on myelin grown DRG neurons via the chemokine receptor CXCR4

CXCL12 mediates its effect through the binding to two different seven-transmembrane receptors, CXCR4 and CXCR7, which are expressed in the nervous system of developing and adult rodents, but also in a variety of different other tissues (Bleul et al., 1996; Chalasani et al., 2003; Nagasawa et al., 1996b). To assess the involvement of CXCR4 in CXCL12 mediated neurite outgrowth a pharmacological approach by applying the CXCR4 antagonist AMD3100 was used (Hatsea et al., 2002). Adult DRG neurons were dissociated and plated on either laminin- or myelin-coated dishes. The neurons were either exposed to AMD3100 (5 μM) alone or in combination with CXCL12 (500 ng/ml) or to BSA, respectively. The CXCR4 antagonist AMD3100 did not interfere with the DRG culture plated either on laminin or on myelin. In fact, like the results in absence of AMD3100, CXCL12 did not promote enhanced axon outgrowth of DRG neurons that were grown on laminin coated plates and axon growth was impaired for cells that were grown on myelin, while the nucleus number remained unchanged (Fig. 3.2 B, E-F). The CXCL12 mediated disinhibitory effect on DRG neurons grown on myelin was reduced following AMD3100 treatment, emphasizing the implication of CXCR4 in CXCL12 mediated growth promotion (Fig. 3.2 B, E). To verify whether CXCL12 mediates its neurite promoting effects through CXCR4, the presence of the chemokine receptor in adult mouse DRG neurons was assessed via immunocytochemistry. CXCR4 was expressed in the soma, axons and growth cones of DRG neurons (Fig. 3.3). Since a specific antibody against CXCR7 was not found and so far, no specific signal could be detected via immunocytochemistry or immunohistochemistry when commercially available antibodies to CXCR7 were used, the presence of CXCR7 on adult DRG neurons could not be verified.

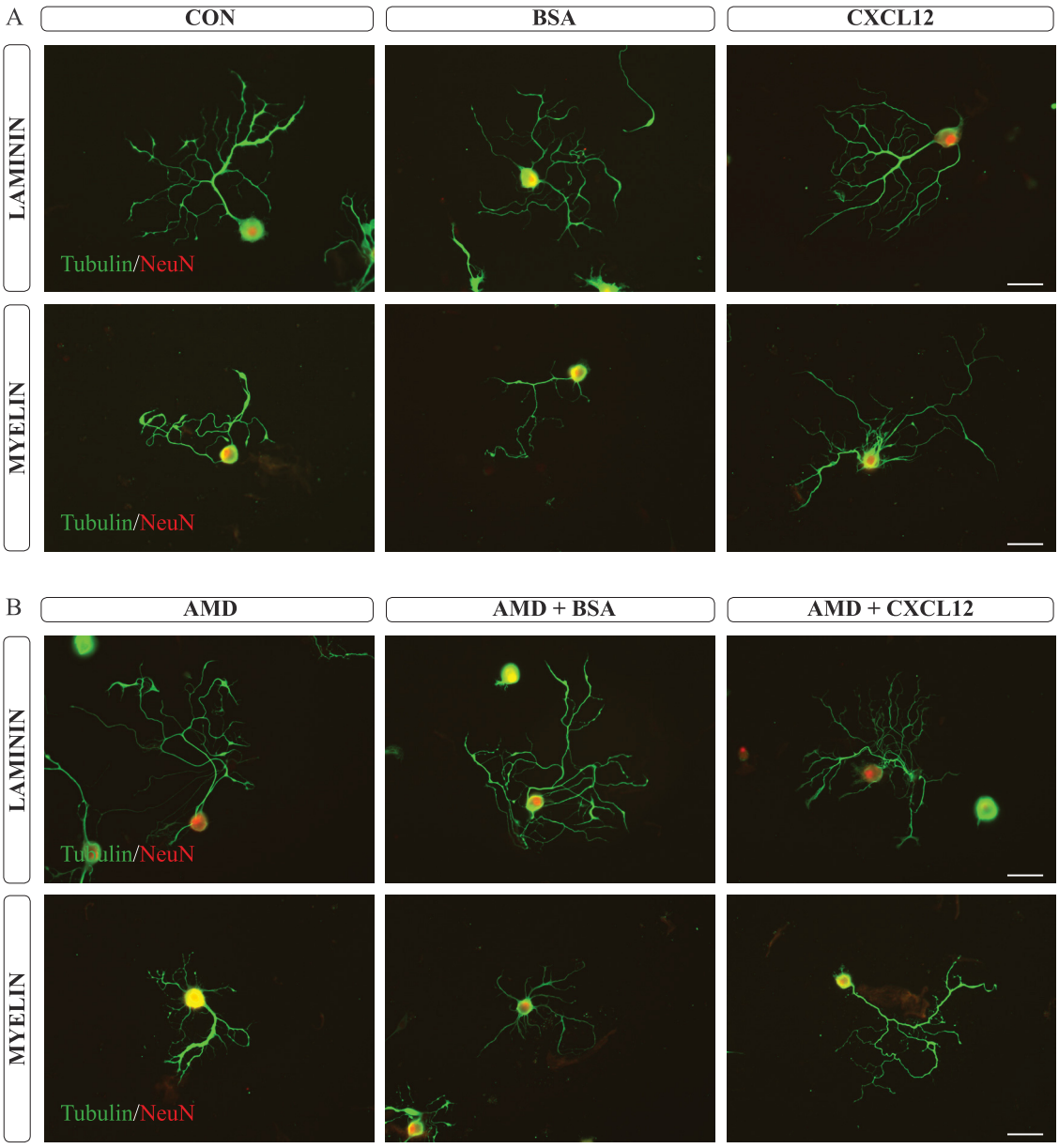
A
CON
BSA
CXCL12
LAMININ
MYELIN
Tubulin/NeuN
Tubulin/NeuN
B
AMD
AMD + BSA
AMD + CXCL12
LAMININ
MYELIN
Tubulin/NeuN
Tubulin/NeuN

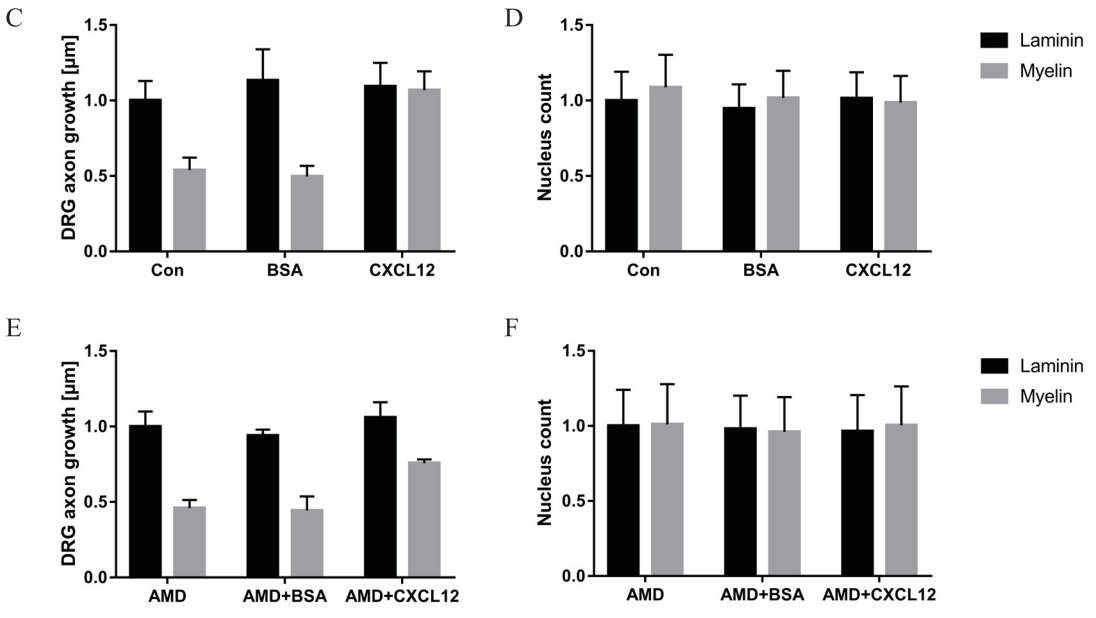
C
DRG axon growth [µm]
1.5
1.0
0.5
0.0
Con
BSA
CXCL12
D
Nucleus count
1.5
1.0
0.5
0.0
Con
BSA
CXCL12
Laminin
Myelin
E
DRG axon growth [µm]
1.5
1.0
0.5
0.0
AMD
AMD+BSA
AMD+CXCL12
F
Nucleus count
1.5
1.0
0.5
0.0
AMD
AMD+BSA
AMD+CXCL12
Laminin
Myelin

Fig. 3.2: CXCL12 mediates axon outgrowth and disinhibitory effects on myelin grown DRG neurons via the chemokine receptor CXCR4.
Adult mouse dorsal root ganglion cells were dissociated and plated on **A)** laminin or on **B)** myelin coated cell culture dishes. Cells were incubated with vehicle (con), BSA, CXCL12 (500 ng/ml), AMD3100 (AMD, 5µM), AMD3100 + BSA (AMD + BSA) and AMD3100 + CXCL12 (AMD + CXCL12) for 2 days. DRGs were stained for βIII-tubulin (green) and NeuN (red) after fixation. Scale bar: 50 µm. **C)** Quantification of axon growth of dissociated adult mouse DRG neurons plated either on laminin (black bars) or laminin + central myelin extract (myelin, gray bars) and incubated with vehicle (con), BSA and CXCL12. Axon growth was normalized to the untreated control on laminin with an average neurite axon length of 228 µm/DRG neuron. **D)** Quantification of the nucleus number of dissociated adult DRG neuron plated either on laminin (black bars) or laminin + central myelin extract (myelin, gray bars) and incubated with vehicle (con), BSA and CXCL12. DRG nucleus count was normalized to the untreated control on laminin with an average nucleus number of 85 DRGs/well (96 well plate). **E)** Quantification of axon growth of dissociated adult mouse DRG neurons plated either on laminin (black bars) or laminin + central myelin extract (myelin, gray bars) and incubated with AMD, AMD + BSA and AMD + CXCL12. Axon growth was normalized to the untreated control on laminin with an average neurite axon length of 173 µm/DRG neuron. **F)** Quantification of the nucleus number of dissociated adult DRG neuron plated either on laminin (black bars) or laminin + central myelin extract (myelin, gray bars) and incubated with AMD, AMD + BSA and AMD + CXCL12. DRG nucleus count was normalized to the untreated control on laminin with an average nucleus number of 92 DRGs/well (96 well plate). Data are presented as the mean ± SEM. N = six replicate wells from three (E-F) to five (C-D) separate experiments. The non-parametric Wilcoxon Test was applied to compare two paired groups for significant difference in the parameter of interest.

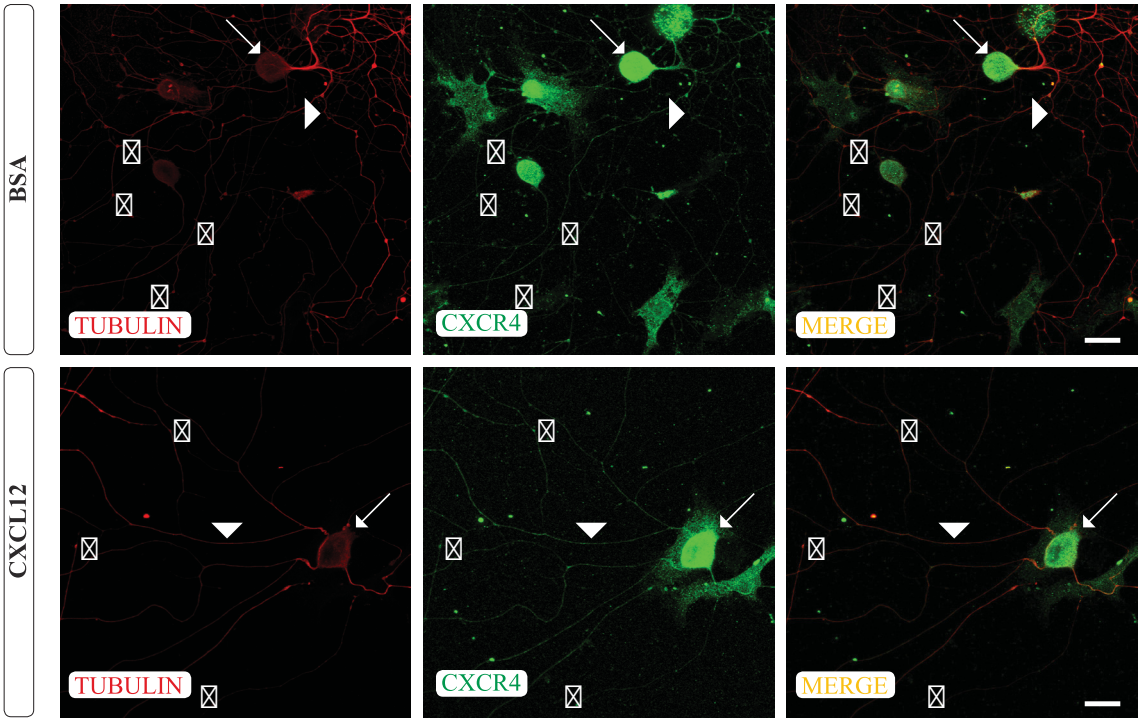

Fig. 3.3: CXCR4 expression on dorsal root ganglion cells.
Adult mouse dorsal root ganglion cells were dissociated and plated on laminin coated cell culture dishes. Cells were incubated for 2 days with BSA and CXCL12, respectively. DRGs were stained for βIII-tubulin (red) and CXCR4 (green) after fixation. CXCR4 is expressed in the soma (arrow), axons (arrowhead) and growth cones (asterisk) of DRG neurons. Scale bar: 25 µm.

3.2 Role of CXCR4 in mediating axon sprouting after local intrathecal infusion of CXCL12 in a mouse model of spinal cord injury

3.2.1 Fixation of mouse catheter for local intrathecal infusion via an osmotic minipump

Intrathecal infusion is a commonly used delivery method of drugs into the subarachnoid space, which is used not only in the clinic but also for experimental approaches in laboratory animals. This method for long term drug application allows local and continuous delivery of substances to the spinal cord and avoids fluctuating drug levels in case of repetitive injections, which also imply frequent surgical interventions and physical stress. The catheterization method used in this thesis is the optimized procedure of the rat catheterization protocol established in our laboratory. The dura suturing is a very important step in the catheter fixation method in the rat. However, the very small size of the mouse in contrast to the rat makes this technically not feasible. Therefore, the rat catheter fixation procedure had to be adapted to the mouse spinal cord injury model. The attachment of the epidural mouse catheter to the base of vertebra T10 with a surgical thread resulted in a stable catheter fixation in the mouse (Fig. 3.4 A, B3). Thereby, the catheter could be secured, lifted and positioned with the tip directly over the spinal cord lesion, to ensure local distribution of the substance (Fig. 3.4 A, B3). Additionally, another essential step for stable catheter fixation was to remove the spinous process of T10 to avoid shifting of the catheter to either the right or left side, and to fix the surgical thread between two autologous fat cushions to increase fixation (Fig. 3.4 A, B4). In order to demonstrate the stability of this catheter fixation, mice were intrathecally infused with Evans Blue dye for 7 days via an osmotic minipump connected to the mouse catheter, starting directly after dorsal hemisection. The Evans Blue staining, used for the visualization of the distribution of the infused liquid, showed the most intense blue staining in the lesion center, while the staining intensity decreased in rostral and caudal direction in all Evans Blue dye infused mice (n =5) (Fig. 3.4 C-D). The strong blue staining at the lesion site suggests that no catheter retraction occurred and thus confirms the stable intrathecal catheter fixation and local intrathecal drug infusion over seven days post-lesion in a mouse model of spinal cord injury.

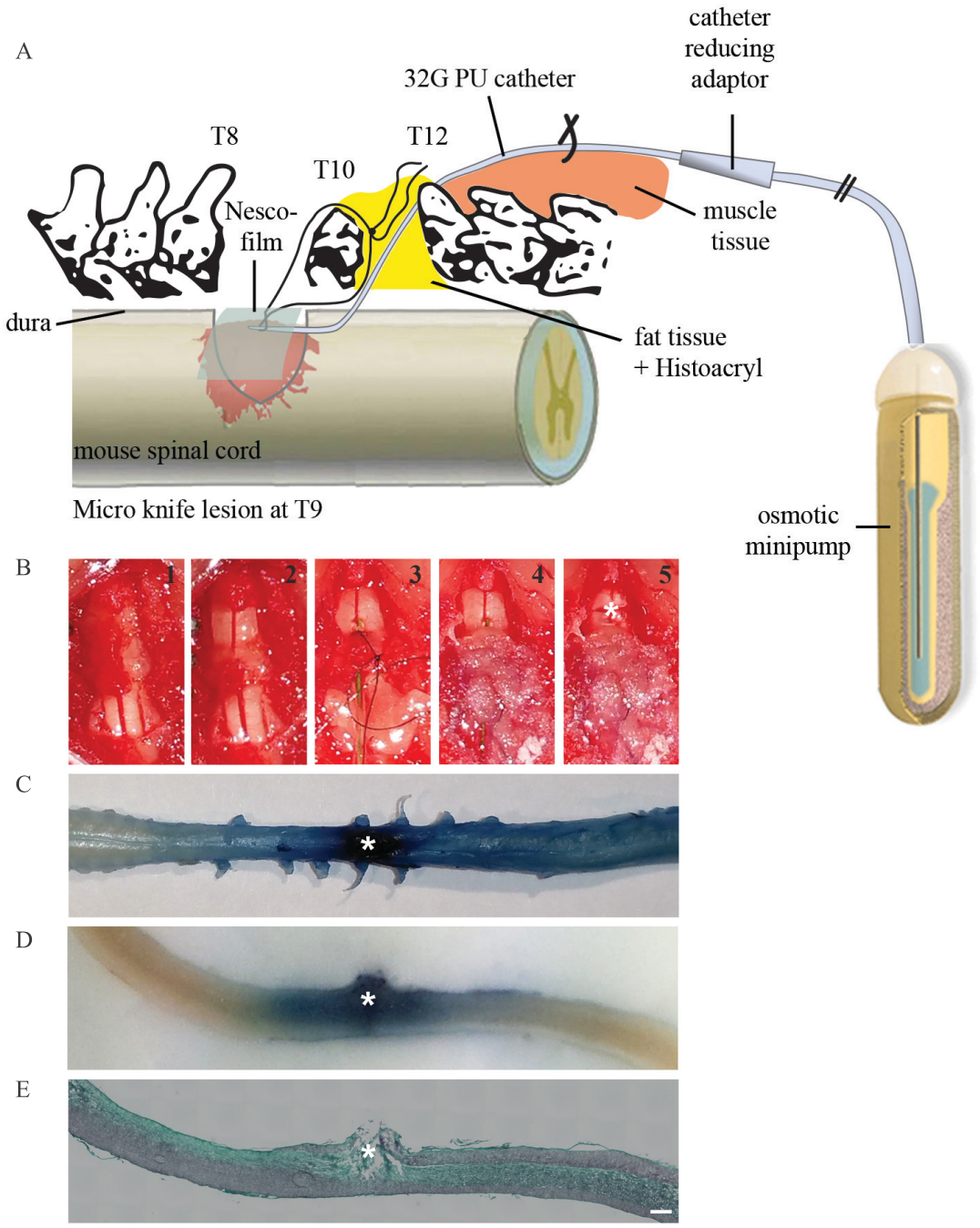

Fig. 3.4: Fixation of mouse catheter for local intrathecal infusion via an osmotic minipump in a mouse SCI model.

A) Schematic illustration of the intrathecal catheter application after dorsal hemisection of a mouse spinal cord at thoracic level T9. As dura suturation is not possible in the mouse, the catheter was guided epidurally towards the lesion site then fixed to T10 via a thread and glued to autologous fat cushion at T11. Further details of the catheter application method are described in the text. **B)** Photographic *in vivo* images of the mouse microsurgery. Laminectomy at T11 (B1) and T9 (B2), catheter fixation (B3) and stabilization with tissue glue (B5) and spinal cord injury (B5). C-D) Lesioned mouse spinal cords from animals with intrathecal catheters and osmotic minipumps filled with Evans Blue to validate local intrathecal drug application. **C)** Dorsal view of the lesioned mouse spinal cord and **D)** parasagittal section of the spinal cord show rostral and caudal distribution of Evans Blue staining. **E)** Parasagittal sections of the lesioned mouse spinal cord stained with trichrome to evaluate catheter-induced compressions of the spinal cord 7 days post lesion. Asterisks in B5, C, D and E indicate the lesion center. Scale bar: 500 µm. Orientation in B1-B5, caudal = down, with view on the dorsal side of the cord. Orientation in C-E, caudal = right.

3.2.2 Optimized mouse epidural catheterization prevents catheter-induced spinal cord compression

The very narrow subdural and subarachnoid space in rodents, especially in mice, is still a challenging issue for the intrathecal catheterization method, since scarring and compression of the spinal cord can occur. To avoid compression events, a complete laminectomy of T11 was performed as another key step of the optimized mouse epidural catheterization method. Analogous to the rat catheter fixation method, a total laminectomy of T11 was necessary to insert the catheter in a smooth angle, avoiding sharp bending of the catheter and pressure on the spinal cord in this area (Fig. 3.4 A, B2). Furthermore, covering the exposed spinal cord with autologous fat cushions at T11 and lifting the mouse catheter using the surgical thread that attached the catheter to the base of T10 are also key steps to avoid compression of the mouse spinal cord (Fig. 3.4 A, B3-B4). In order to verify if the optimized mouse epidural catheterization method leads to catheter induced compression, a trichrome staining of the mice spinal cords was performed. The staining revealed that none of the animals received any compression of the caudal spinal cord nor compressions in the area of T10/11 seven days post lesion (Fig. 3.4 E). This demonstrates that the optimized epidural catheterization method prevents catheter-induced spinal cord compression in mice.

3.2.3 Experimental spinal cord injury in the mouse – thoracic dorsal hemisection

Several spinal cord lesion models have been developed in the last decades and the choice of the best suitable correlates with the experimental aim. Since the focus of the experiments described here lies on the sprouting events of CNS axons and on the locomotor recovery after CXCL12 infusion, a partial injury in the form of dorsal hemisection was chosen. This spinal cord lesion transects the dorsal columns, including the dCST and the dorsal grey matter. The dorsal hemisection was applied at the thoracic spinal cord level. However, since the spinal cord in the adult mouse is significantly shorter than the vertebral canal (Sakla, 1969), it is very important to mention which spinal cord segment was finally injured. Vertebral landmarks, such as anatomical landmarks of the vertebral processes and the presence of a central blood vessel between the thoracic vertebrae 6 and 7, were used for the accurate identification of the target vertebrae for the laminectomy and later on the spinal cord injury (Harrison et al., 2013). In conclusion, a complete laminectomy of vertebra T9 was performed and the corresponding T11 spinal cord segment was injured using a pair of microscissors and an ultra-fine micro knife. In order to determine and verify the depth of the desired extension of the lesion, Nissl staining of transverse (Fig. 3.5 A-C) and sagittal spinal cord sections (Fig. 3.5 D) was done. The Nissl substance is granules of rough endoplasmic reticulum found in the cytoplasm of neurons. Therefore, the gray matter, which is composed of neuronal cell bodies, was stained in its butterfly shape, while the white matter, made up of axons, was not. Staining of transverse spinal cord sections rostrally, throughout and caudally to the spinal cord injury site illustrate the extent of the lesioned area (Fig. 3.5 A-C). The central canal and the area ventral to it were not injured during the dorsal hemisection. The RST was not included by the injury, too since the lesion was not extended so far laterally. Directly above the spinal cord injury site, the callus was prominent and it decreased in rostral and caudal direction. The depth of the lesion was also visualized by the Nissl staining of parasagittal spinal cord sections (Fig. 3.5 D). In a more central section, the visible cut defines the injured region of the gray matter

and shows the spared ventral part of the spinal cord, again confirming, that the depth of the dorsal hemisection was adequate, since only the dorsal columns and not the tissue ventral to the central canal was injured.

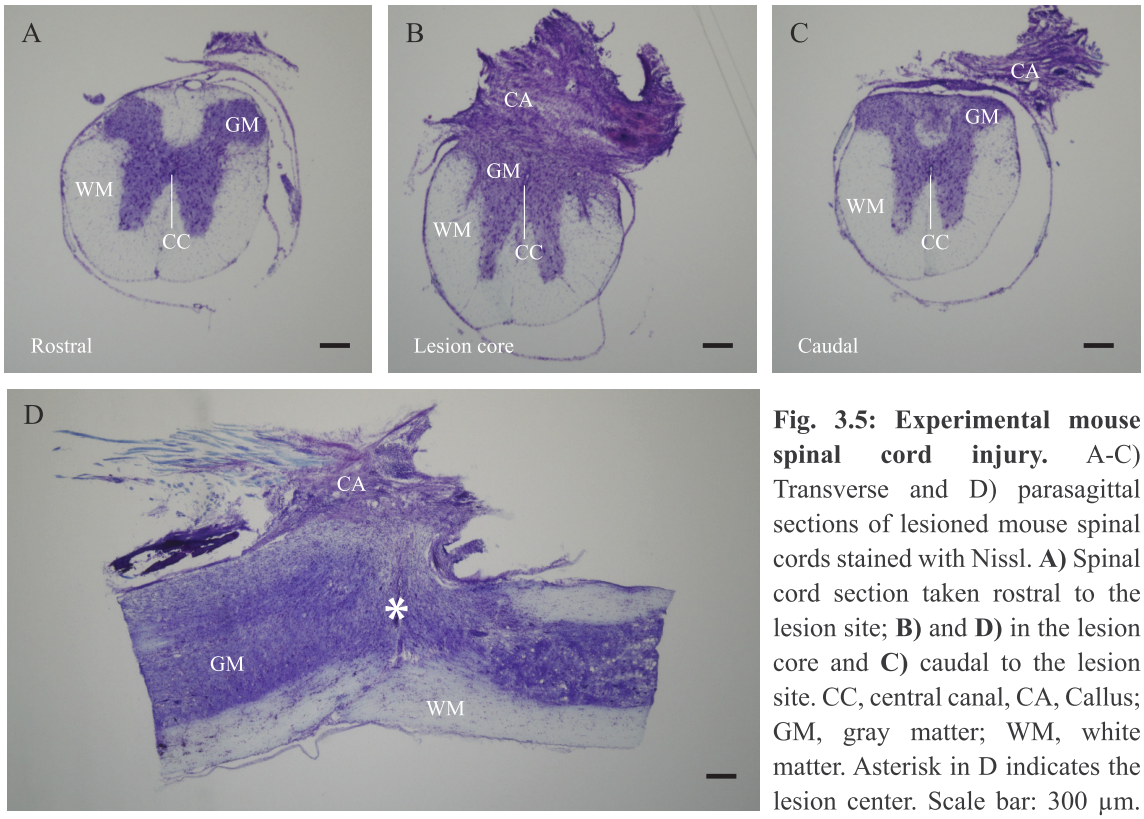

Fig. 3.5: Experimental mouse spinal cord injury. A-C) Transverse and D) parasagittal sections of lesioned mouse spinal cords stained with Nissl. **A)** Spinal cord section taken rostral to the lesion site; **B)** and **D)** in the lesion core and **C)** caudal to the lesion site. CC, central canal, CA, Callus; GM, gray matter; WM, white matter. Asterisk in D indicates the lesion center. Scale bar: 300 µm.

3.2.4 AAV2 transduced corticospinal tract neurons express Cre-Recombinase and consequently the red fluorescent protein tdTomato, used for anterograde labeling

To analyze the sprouting effect of the lesioned dCST axons, neurons of this tract were anterogradely traced by stereotactic injections of the adeno-associated virus serotype 2 (AAV2) into the layer V of the hind limb sensorimotor cortex of four weeks old $CXCR4_{wt/wt}/ROSA_{fl/wt}$ mice (Fig. 2.1). The ROSA reporter mouse carries the ROSA26 locus, which contains a floxed stop-sequence that inhibits the transcription of the red fluorescent protein tdTomato (Fig. 2.2 A). The excision of the floxed stop sequence was mediated by the expression of the Cre-Recombinase (Cre) via the AAV2 construct. This tracing method leads to a specific red fluorescent staining of the AAV2-Cre transduced neurons that can be visualized without immunohistochemical staining. In order to verify the CST tracing, transverse sections of a mouse brain were stained for Cre. Virus-transduced pyramidal cells that expressed the reporter gene tdTomato also expressed the HA-tagged Cre-Recombinase in the sensorimotor cortex (Fig. 3.6 A). Furthermore, transverse brain sections stained with Ctip2, a cellular marker for layer V neurons, co-localized with tdTomato positive neurons, confirming the right depth of the stereotactic injections of the AAV2-Cre construct (Fig. 3.6 B). The successfully transduced pyramidal neurons in layer V project their axons into the dCST. To validate the stereotaxic coordinates and to test if the axons of the virus-transduced pyramidal neurons in the brain express the red fluorescent reporter protein also in the spinal

cord, transverse spinal cord sections at the thoracic level were analysed. Indeed, the axons of the successfully transduced neurons in the brain were positively stained with the red fluorescent protein tdTomato also in the spinal cord (Fig. 3.6 C). Many small red stained dots were visible in the spinal cord in between of the two dorsal horns, in a well-defined area in the dorsal funiculus, exactly where the dCST is located. In conclusion, the stereotaxic coordinates used were suitable for successful anterograde labeling of the dCST via AAV2-Cre transduction of layer V neurons in the sensorimotor cortex of ROSA reporter mice.

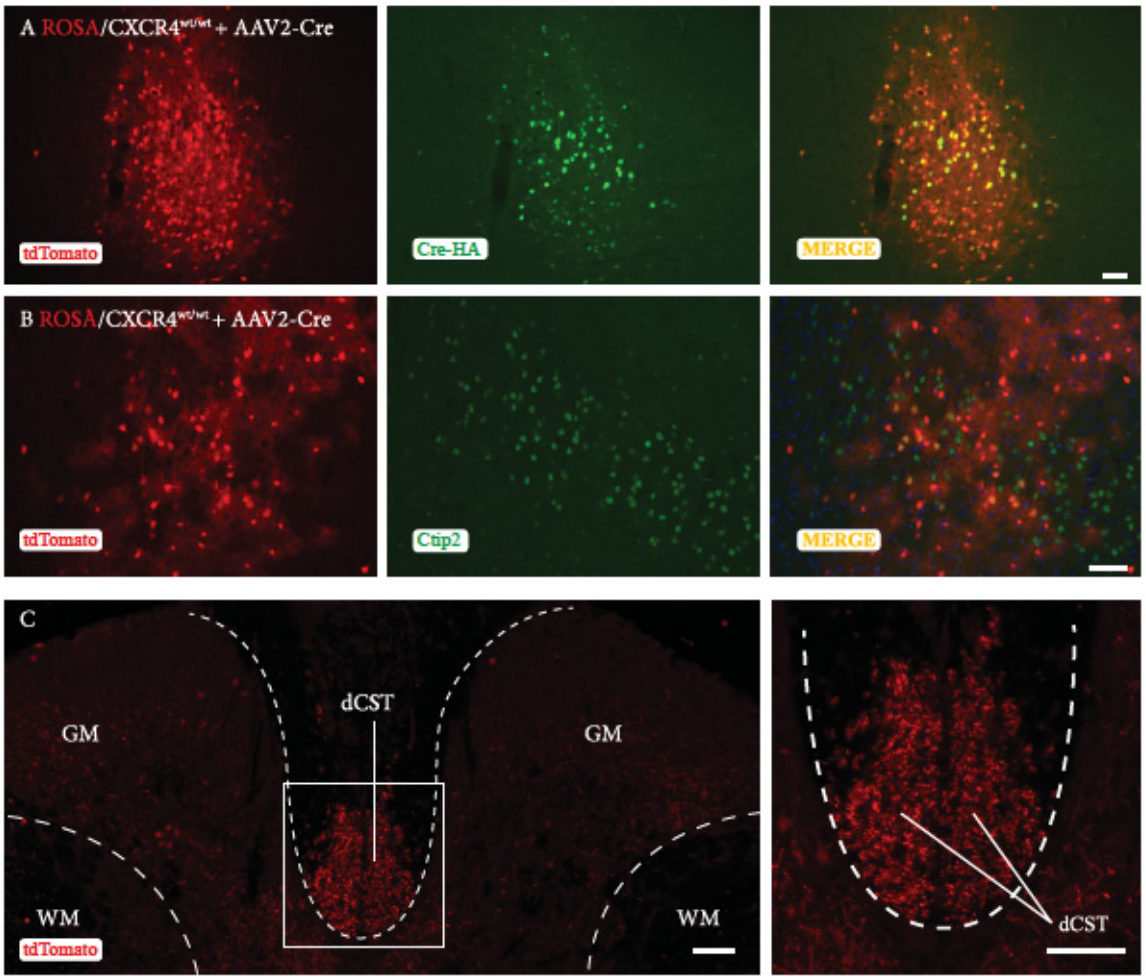

Fig. 3.6: Anterograde labeling of the corticospinal tract using AAV2-Cre transduction.
A) Transverse sections of an adult mouse brain show virus transduced neurons in the sensorimotor cortex that express the red reporter gene tdTomato. Sections were stained for Hemagglutinin epitope-tagged Cre-Recombinase (green) and **B)** for Ctip2 (green), a marker for pyramidal neurons (layer V) of the sensorimotor cortex. Scale bar: 50 µm. **C)** Transverse section of the mouse spinal cord at thoracic level showing the anterograde labeling of the dCST. The successfully transduced pyramidal neurons in the transverse brain section (A-B), which express the tdTomato project their axons into the dCST. Dashed line indicates the shape of the butterfly and separates the gray matter (GM) from the white matter (WM) in the spinal cord. Framed area indicates higher magnification. Scale bar: 50 µm.

3.2.5 Local intrathecal infusion of CXCL12 into the lesioned mouse spinal cord does not promote sprouting of corticospinal tract axons

As previously published for cultured postnatal (P6) rat DRG neurons as well as adult rat RGCs, and confirmed in this thesis for adult mouse DRG neurons, the neurite outgrowth of these cells grown on inhibitory CNS myelin was increased after the application of CXCL12 *in vitro* (Heskamp et al., 2013; Opatz et al., 2009). Furthermore, in an *in vivo* study, the local intrathecal infusion of CXCL12 into the lesioned rat spinal cord was shown to promote sprouting of dCST axons (Opatz et al., 2009). In order to confirm the CXCL12 mediated neurite outgrowth and the disinhibitory effect also in a mouse *in vivo* model, the chemokine was intrathecally applied in the lesioned mouse spinal cord. Therefore, four weeks prior to the spinal cord lesion, the dCST was anterogradely traced via stereotactic injections of AAV2-Cre into the layer V of the sensorimotor cortex of mice (Fig. 2.1 and 3.6). Then, mice underwent a dorsal hemisection of the spinal cord, which included the lesion of the dCST, followed by local intrathecal infusion of either human CXCL12 (dissolved in a PBS/BSA solution), or control medium as BSA or PBS via an osmotic minipump over a period of 7 days (Fig. 2.1 and 3.4). Five weeks after injury, the animals were sacrificed and the rostral sprouting of the traced dCST was quantified as described in material and methods. Little spontaneous sprouting of the dCST axons was observed in the PBS control group which could not be significantly increased, neither by the BSA control- nor the CXCL12 treatment, although a slight trend towards CXCL12 mediated sprouting was visible in the treatment group (Fig. 3.7). In conclusion, CXCL12 seems to exert neither disinhibitory nor neurite promoting effects in an *in vivo* model of mouse spinal cord injury. The chemokine seems to act in a species-specific way in mice, which seems to differ from the effects, which were previously described for rats (Opatz et al., 2009).

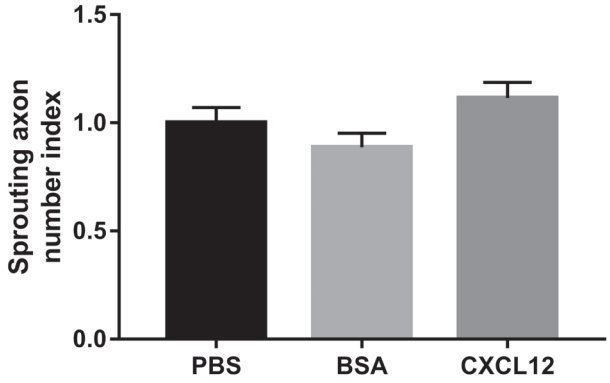

Fig. 3.7: Axonal sprouting of injured dCST axons is absent in the mouse spinal cord after local intrathecal infusion of CXCL12.
Quantification of CXCL12 induced rostral axon sprouting of the lesioned dCST following local intrathecal chemokine infusion. Mice received a dorsal hemisection and the infusion of either control solution as PBS or BSA (PBS/BSA) or treatment solution (10 µM CXCL12 in 1% PBS/BSA) through an osmotic minipump for 7 days. Animals were sacrificed 5 weeks after SCI and the sprouting quantification was performed on spinal cords segments 5mm rostral to the lesion area. The number of sprouting fibers was normalized against the total number of labeled axons in the dCST. Complete values were normalized to the control group with an average number of 173. Data are presented as the mean ± SEM. N = four PBS control animals, five BSA contral animals and six CXCL12 treated animals. The non-parametric Kruskal-Wallis Test was applied to compare the three unpaired groups for significant difference in the paramteter of interest.

3.2.6 No improvement in functional behavior after CXCL12 infusion in injured mice – Basso Mouse Scale (BMS)

In a contusion model of rat spinal cord injury, the local intrathecal infusion of CXCL12 for 28 days via an osmotic minipump led to an improved motor recovery (Zendedel et al., 2012). In the open field test, the behavioral scores were significantly higher in CXCL12 treated animals compared to control groups. Unfortunately, neither sprouting nor the disinhibitory effects of CXCL12 were investigated in that publication and therefore, they were not correlated with the improved motor recovery of the rats (Zendedel et al., 2012). In order to investigate whether CXCL12 has beneficial effects on the motor recovery of spinal cord injured mice, regardless mediating neuronal sprouting, mice were subjected to the open field Basso Mouse Scale locomotor test (BMS) (Basso et al., 2006). Over one week prior to injury, mice were handled every day for 4 minutes to get acclimatized to the open field. After dorsal hemisection, mice were intrathecally infused with either CXCL12 or PBS for 7 days (Fig. 2.1). Locomotor function of the left and right hind paws were assessed separately one day prior the SCI and at day 1, 3, 7, 14, 28 and 35 days post injury, respectively (Fig. 2.1). The following parameters were evaluated for the mouse hind limbs: ankle movement, plantar placement, weight support, stepping, coordination, paw position, trunk stability and tail position. All mice started with the highest BMS score of 9, which relates to consistent, coordinated gait with parallel paw placement and normal trunk stability (Fig. 3.8). One day after injury in both the control group and the treatment group the mean BMS score dropped to 4 for the left hind limb (Fig. 3.8 A) and 5 for the right hind limb (Fig. 3.8 B), reflecting the spinal shock phase. Between the first and the seventh day post injury the mice started improving their locomotor function and reached a plateau at a mean BMS score of 6, which relates to frequent or consistent plantar stepping and some coordination (Fig. 3.8 A-C). After the spinal shock phase, the mice treated with CXCL12 showed a faster recovery compared to the control animals (Fig. 3.8 A-C). Indeed, starting from the 7th till the 35th day post injury, CXCL12 treated animals recovered faster in relation to day 1 post injury as compared to control animals. They regained most coordination and only mild trunk instability was observed. In contrast, control animals gained only some coordination back and revealed severe trunk instability. To detect differences between groups that have similar BMS scores on the main scale, an additional subscore was calculated for animals that have achieved the score of frequent stepping in the BMS scale (Fig. 3.8 D). The analysis of the subscore confirmed that the fine motor control was not significantly improved in CXCL12 treated animals, although they showed slightly higher subscores compared to control groups. In conclusion, CXCL12 did not significantly improve locomotor function in spinal cord injured mice as compared to control mice. However, the faster recovery after SCI, reflected by slightly higher BMS scores in CXCL12 treated animals emphasizes a light trend towards a CXCL12-mediated effect.

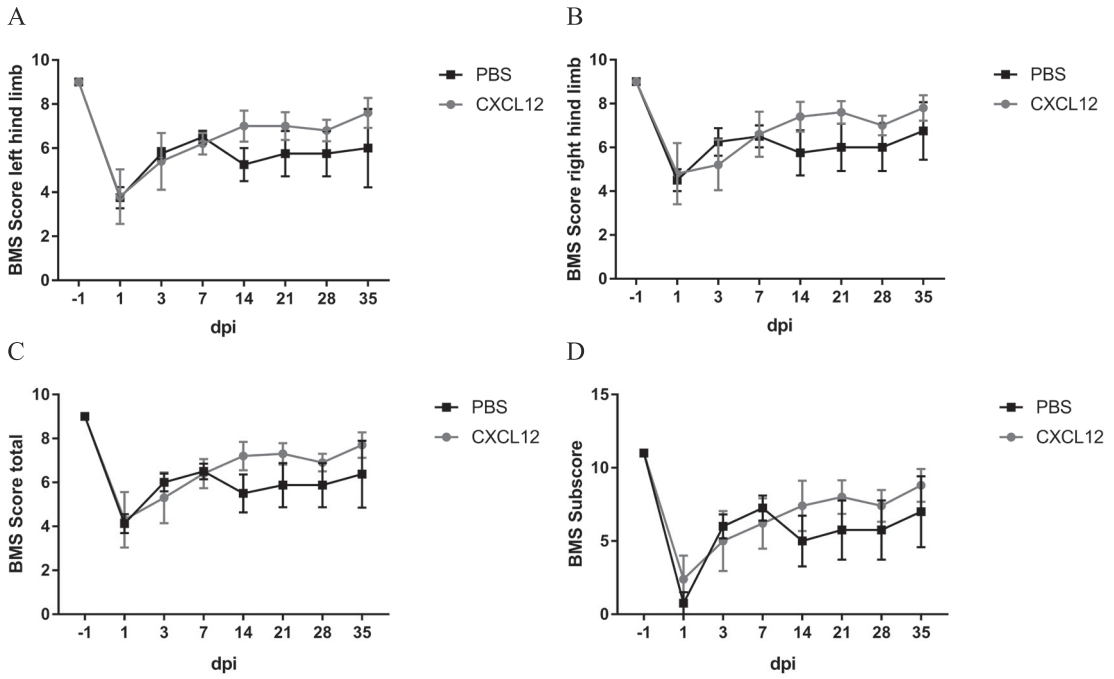

Fig. 3.8: Locomotor behavior is not significantly improved in injured mice after CXCL12 local intrathecal infusion.
Locomotor hind limb function of spinal cord injured adult mice was assessed using the Basso Mouse Scale (BMS). Mice received a dorsal hemisection and the infusion of either control solution as PBS (black rectangle) or treatment solution (gray circle, 10 µM CXCL12 in 1% PBS/BSA) through an osmotic minipump for 7 days. Mice were evaluated at -1 and 1, 3, 7, 14, 28 and 35 days post injury. The locomotor function of the left **A)** and right **B)** hind limb were assesed separately. The total BMS for both hind limbs is shown in **C).** The BMS scale ranges from 0 (no hind limb movement) to 9 (consistent, coordinated gait with parallel paw placement and normal trunk stability). For animals that achieved the score of frequent stepping in the BMS scale an additional subscore **D)** was calculated that ranges from 0-11. Data are presented as the mean ± SEM. N = four PBS control animals and five CXCL12 treated animals. The non-parametric Mann-Whitney-U-Test was applied to compare the two unpaired groups, animals infused with control solution and the one with treatment solution at the different time points for statistical differences. The non-parametric Wilcoxon Test was applied to compare the recovery within the group for statistical differences.

3.3 Expression of the chemokine receptor CXCR4 in the mouse and rat nervous system

3.3.1 CXCR4 is not expressed in the dorsal corticospinal tract of mice and rats

The CXCL12 receptor CXCR4 is highly expressed in the mouse and rat brain: in the olfactory bulb, throughout the ventricular system, in the dentate gyrus, and in cortical interneurons (Lu et al., 2002; Stumm et al., 2002; Stumm et al., 2003; Tissir et al., 2004). In rats, CXCR4 was described to be also present in the spinal cord along the axons of layer V neurons in the dCST, in the ventral horn cell population, possibly in motoneurons, and very strongly in the ependymal cell layer around the central canal (Jaerve et al., 2011; Opatz et al., 2009). In order to investigate if there are species-specific differences in the expression of CXCR4 in the mouse spinal cord, transverse sections were immunofluorescent stained against CXCR4 (Fig. 3.9 A). Furthermore,

since the CXCR4 antibody used in Opatz et al., (2009) was discovered to bind unspecifically, transverse sections of the rat spinal cord were also subjected to CXCR4 immunofluorescence staining (Fig. 3.9 B) (Fischer et al., 2008). In mouse spinal cord, the ependymal cell layer was positively stained for CXCR4 (Fig. 3.9 A). Moreover, the dorsal funiculus, the area between the two dorsal horns, was also positively stained for CXCR4, However, the dCST, did not show any immunoreactivity for CXCR4. Furthermore, in the ventral and lateral funiculus, where many motor and sensory axons pass through, the CXCR4 expression was very high (Fig. 3.9). Mainly the area flanking the anterior median fissure and the outer area in the lateral funiculus, but not the adjacent part to the gray matter were positively stained for CXCR4. Similar findings were observed in the rat spinal cord. However, the CXCR4 staining was more intense than in the mouse (Fig. 3.9 B). In contrast to the previously published data, CXCR4 was found not to be expressed in the dCST of the rat spinal cord, but only in the dorsal funiculus and additionally in the white matter of the ventral and lateral funiculus. The ependymal cell layer around the central canal was also positively stained for CXCR4 in both, rat and mouse.

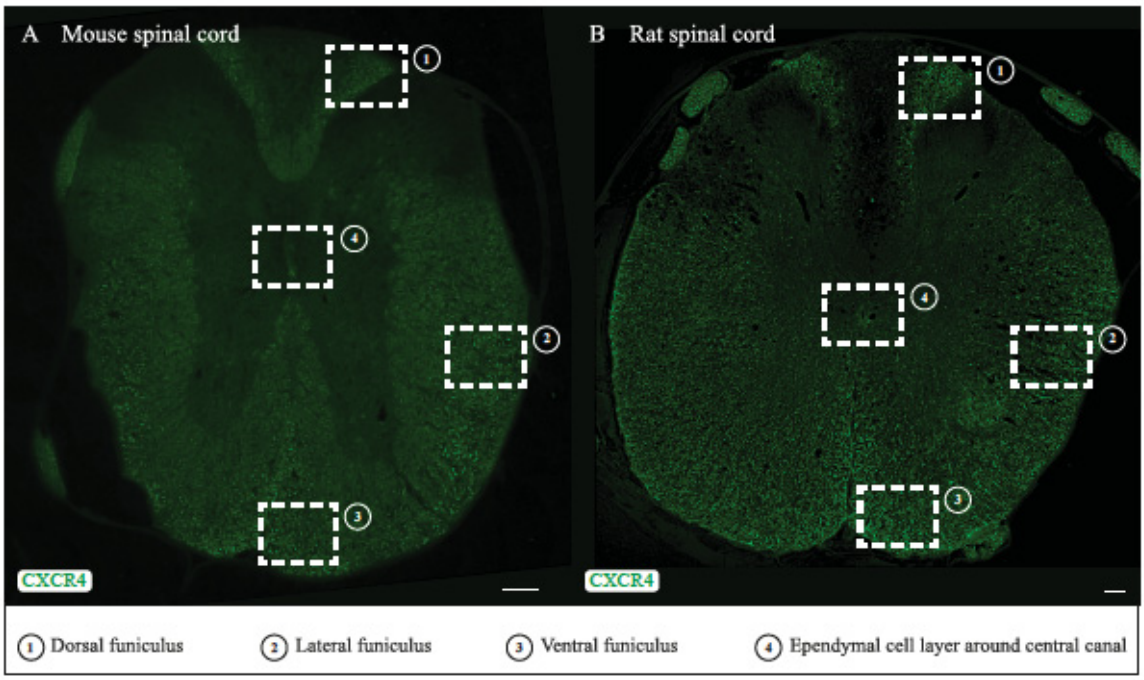

Fig. 3.9: Immunofluorescence staining of CXCR4 is not present on the dCST of mice and rats. Transverse sections of **A)** mouse and **B)** rat spinal cord stained with CXCR4-UMB2 antibody (green). Dashed rectangles indicate CXCR4 expression in (1) dorsal funiculus, (2) lateral funiculus, (3) ventral funiculus and (4) ependymal cell layer araound central canal. Scale bar: 100µm.

3.3.2 CXCR4 is expressed on axons of neurons located in the dorsal, lateral and ventral funiculus, on motoneurons but not on CGRP positive neurons

In order to verify if the staining seen in the dorsal, lateral and ventral funiculus of the mouse spinal cord correlates with the expression of CXCR4 in neurons, co-localization studies on transverse spinal cord sections with different immunofluorescent neuronal markers in combination with CXCR4 were performed. First, the neuronal marker neurofilament was used to test if CXCR4 has an axonal staining pattern. Neurofilaments are intermediate filaments in neurons, which comprise

the major part of the neuronal cytoskeleton. Their function is to support axonal structure and to regulate axon diameter. Based on their molecular mass there are three different neurofilament subunits (heavy, medium and light) (Szaro et al., 1990). The antibody preparation used for this study is a cocktail of antibodies recognizing all three chains. Additionally, the medium and the heavy neurofilaments can be phosphorylated *in vivo* (Szaro et al., 1990). The antibody PAM312-P reacts with phosphorylated epitopes of neurofilaments and recognizes thick and thin axons. In contrast, PAM311-NP reacts with nonphosphorylated epitopes and this antibody recognizes only thick axons. Indeed, compared to PAM312-P (Fig. 3.11, 3.15), where smaller and bigger dots and consequently more neurons were detected, immunofluorescence staining of PAM311-NP (Fig. 3.10, 3.14) visualized less but thicker neurons in transverse mouse and rat spinal cord sections, hence validating the neurofilament staining. As previously published, antibodies that detect the nonphosphorylated form of neurofilament do not stain the cuneate tract in rats, while antibodies that detect phosphorylated neurofilaments do so (Szaro et al., 1990). In mice, PAM311-NP did not show any immunoreactivity in the cuneate tract, too (Fig. 3.10), while PAM312-P stained it extensively (Fig. 3.11). In the rat spinal cord sections, PAM311-NP stained the cuneate tract (Fig.3.14), but not as strong as PAM312-P did (Fig. 3.15). Finally, the CXCR4 receptor co-localized with axons stained by both neurofilament antibodies in the dorsal, lateral and ventral funiculus proving that CXCR4 was expressed on neurons, more exactly on their axons, in both the mouse and the rat spinal cord (Fig. 3.10, 3.11, 3.14, 3.15). The second neuronal marker tested was β-III Tubulin, a structural component of the cytoskeleton, which is involved in mitosis, meiosis and intracellular transport. The clone Tuj1 is highly neuron specific and does not identify β-III Tubulin in glial cells. In transverse spinal cord sections, CXCR4 co-localizes with Tuj1-stained cells, again confirming a neuronal and axonal expression of the receptor in mice and rats (Fig. 3.12, 3.16). In order to analyze, if CXCR4 is expressed on neuronal cell bodies, the co-localization with the neuronal marker Neuronal Nuclei (NeuN) was tested. NeuN is a protein involved in the regulation of mRNA splicing and exclusively expressed by neurons. It plays a role in regulating neural cell differentiation and nervous system development (Kim et al., 2009; Mullen et al., 1992). In the gray matter, where all the cell bodies of spinal neurons were located, a high expression of NeuN was found (Fig. 3.13, 3.17). In contrast to the ventral horn, where only few big neuronal cell bodies were located, many little and medium sized cell bodies were stained with NeuN in the dorsal horn of the mouse and rat spinal cord. In the dorsal horn, no co-localization with CXCR4 was found on neuronal nuclei, while CXCR4 was faintly present in the cell population of the ventral horn, most likely motoneurons (Fig. 3.13, 3.17). These data correlate with the previously published data obtained from rat (Jaerve et al., 2011). Lastly, in order to further characterize the CXCR4-positive cell population right above the dorsal horn, an antibody against the Calcitonin Gene-Related Peptide (CGRP), a neuropeptide involved in pain transmission, was tested. CXCR4 was not co-expressed with this neuronal marker in the mouse and rat spinal cord, confirming that this particular neuronal cell population, which belongs to the sensory population, does not carry this CXCL12 receptor (Fig. 3.13, 3.17). In conclusion, CXCR4 showed an axonal expression in mouse and rat neurons, which was confirmed by the co-localization staining with the axonal markers PAM311-NP, PAM312-P, and Tuj1. CXCR4 seems to be expressed also in a subtype of neurons, such as motoneurons but not in CGRP-positive neurons in the mouse and rat spinal cord.

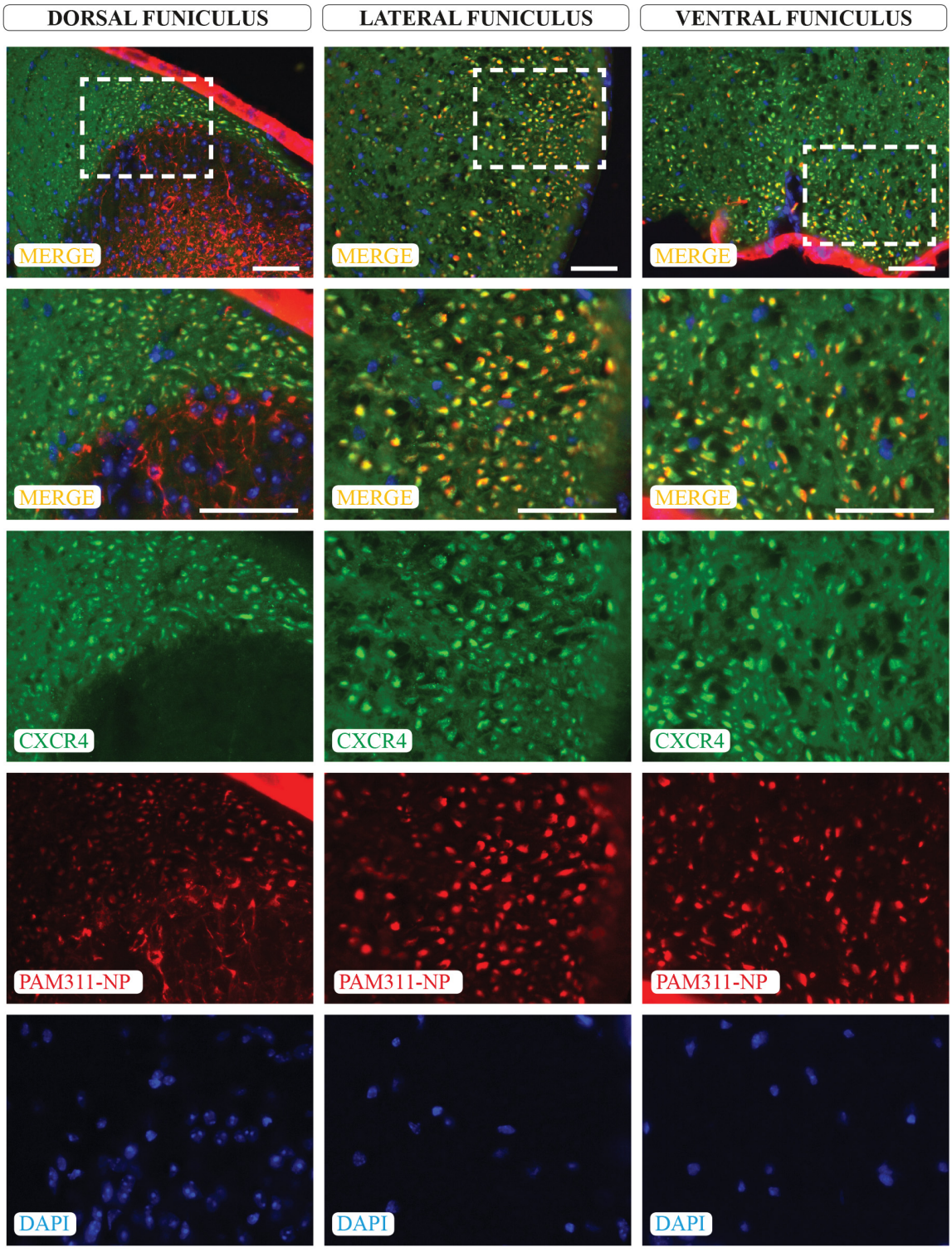

Fig. 3.10: Immunofluorescence staining of CXCR4 with the neuronal marker PAM311-NP on mouse spinal cord sections.
Dorsal funiculus (left pannel), lateral funiculus (middle pannel) and ventral funiculus (right pannel) of a transverse mouse spinal cord section stained for CXCR4 (green), the neuronal marker PAM311-NP (red), which recognizes non-phosphorylated neurofilaments and nuclear staining with DAPI (blue). Images in the first row are overviews. Dashed rectangle indicates higher magnification for the following images. Scale bar: 50 µm.

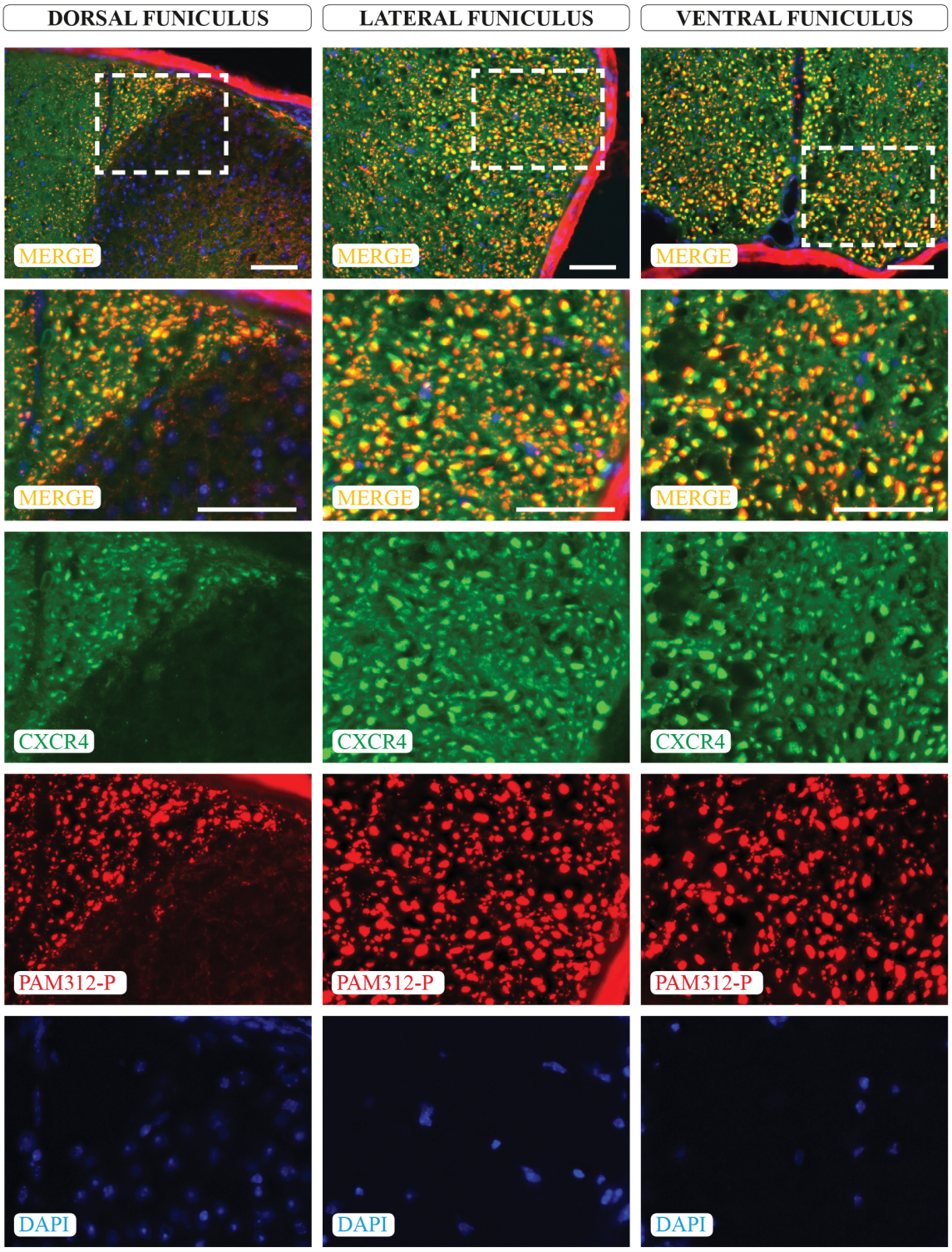

Fig. 3.11: Immunofluorescence staining of CXCR4 with the neuronal marker PAM312-P on mouse spinal cord sections.
Dorsal funiculus (left pannel), lateral funiculus (middle pannel) and ventral funiculus (right pannel) of a transverse mouse spinal cord section stained for CXCR4 (green), the neuronal marker PAM312-P (red), which recognizes phosphorylated neurofilaments and nuclear staining with DAPI (blue). Images in the first row are overviews. Dashed rectangle indicates higher magnification for the following images. Scale bar: 50 µm.

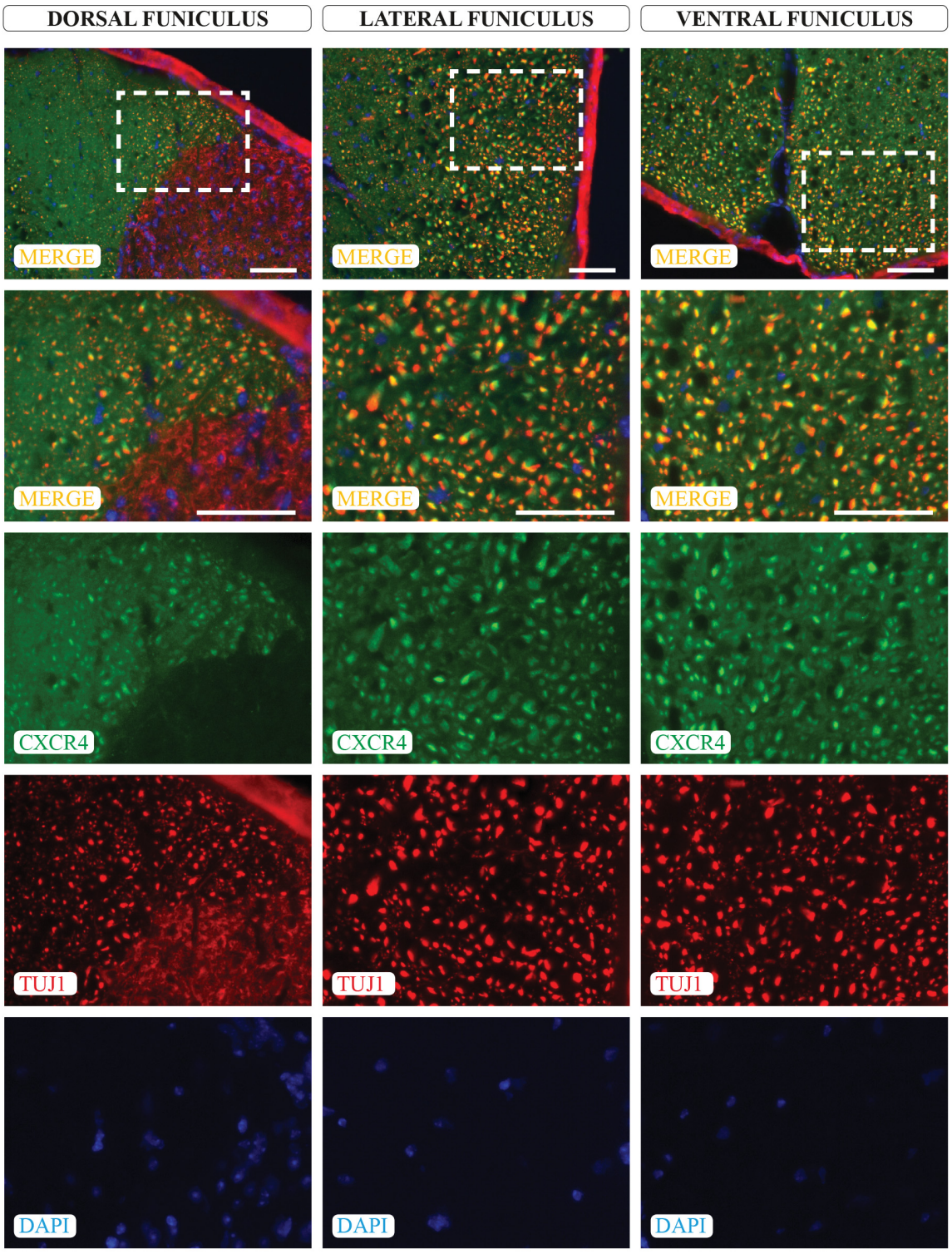

Fig. 3.12: Immunofluorescence staining of CXCR4 with the neuronal marker Tuj1 on mouse spinal cord sections.
Dorsal funiculus (left pannel), lateral funiculus (middle pannel) and ventral funiculus (right pannel) of a transverse mouse spinal cord section stained for CXCR4 (green), the neuronal marker Tuj1 (red) and nuclear staining with DAPI (blue). Images in the first row are overviews. Dashed rectangle indicates higher magnification for the following images. Scale bar: 50 µm.

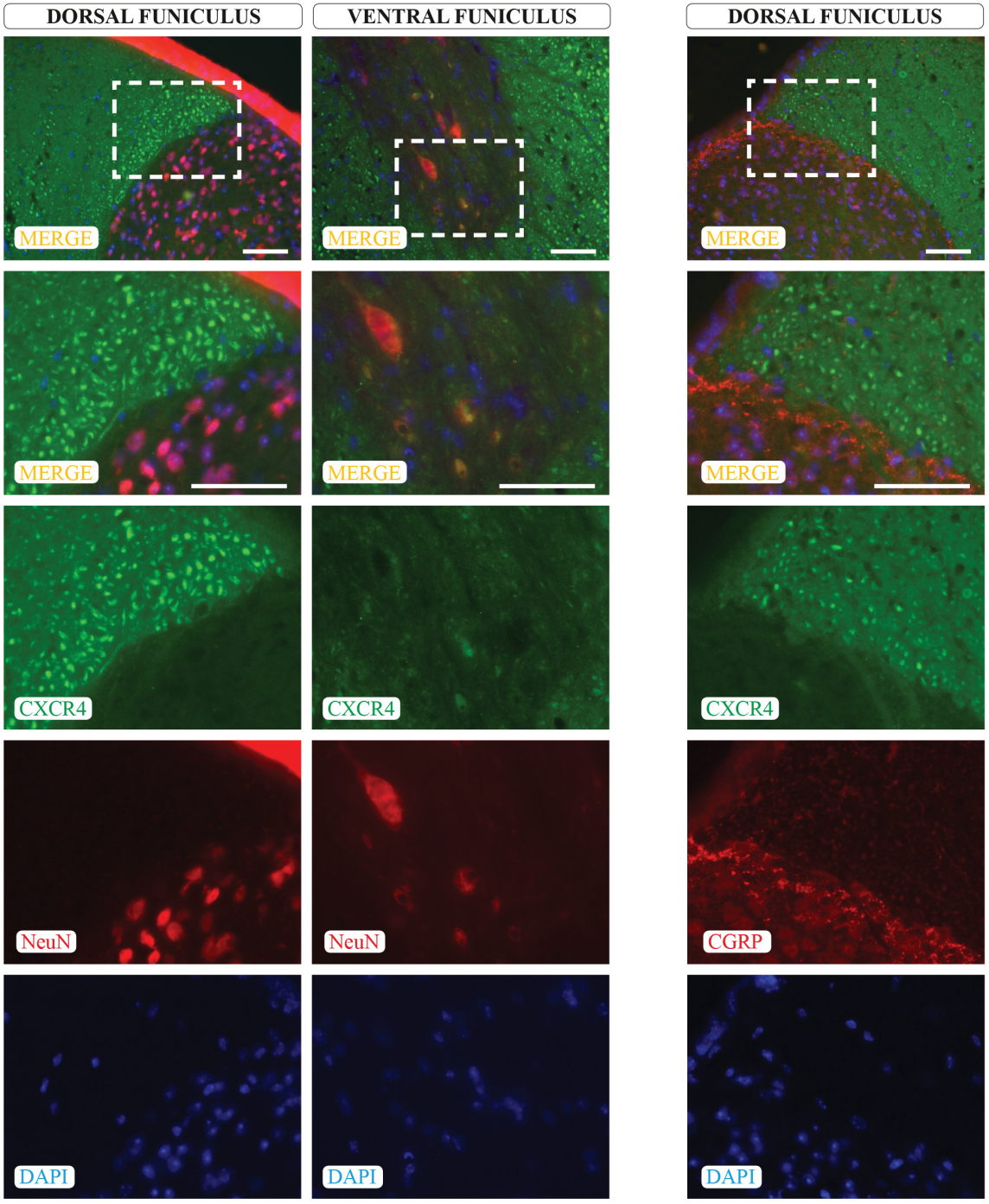

Fig. 3.13: Immunofluorescence staining of CXCR4 with the neuronal marker NeuN and CGRP on mouse spinal cord sections.
Dorsal funiculus (left and right pannel) and ventral funiculus (middle pannel) of a transverse mouse spinal cord section stained for CXCR4 (green), either with the neuronal marker NeuN or CGRP (red) and nuclear staining with DAPI (blue). Images in the first row are overviews. Dashed rectangle indicates higher magnification for the following images. Scale bar: 50 µm.

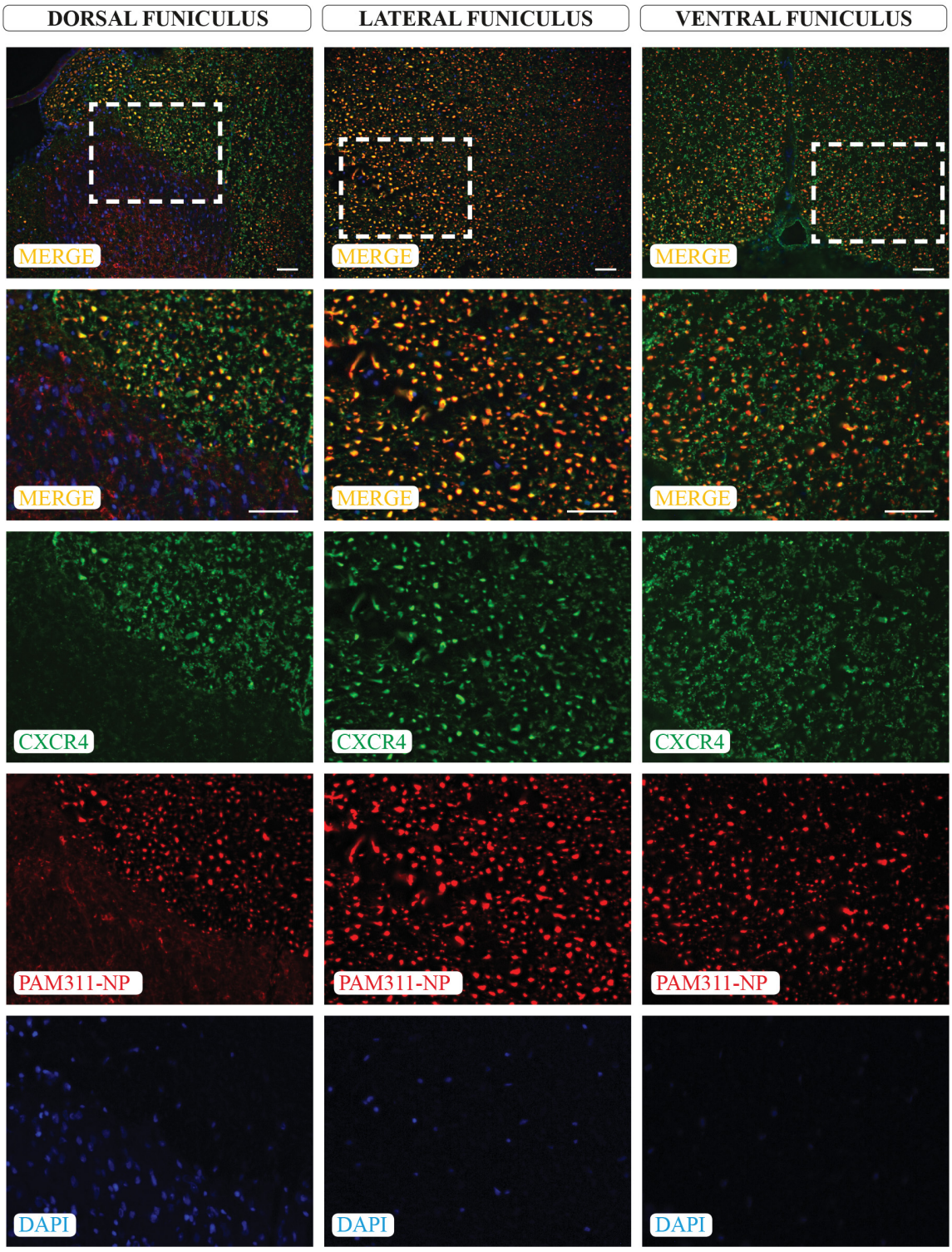

Fig. 3.14: Immunofluorescence staining of CXCR4 with the neuronal marker PAM311-NP on rat spinal cord sections.
Dorsal funiculus (left pannel), lateral funiculus (middle pannel) and ventral funiculus (right pannel) of a transverse rat spinal cord section stained for CXCR4 (green), the neuronal marker PAM311-NP (red), which recognizes non-phosphorylated neurofilaments and nuclear staining with DAPI (blue). Images in the first row are overviews. Dashed rectangle indicates higher magnification for the following images. Scale bar: 50 µm.

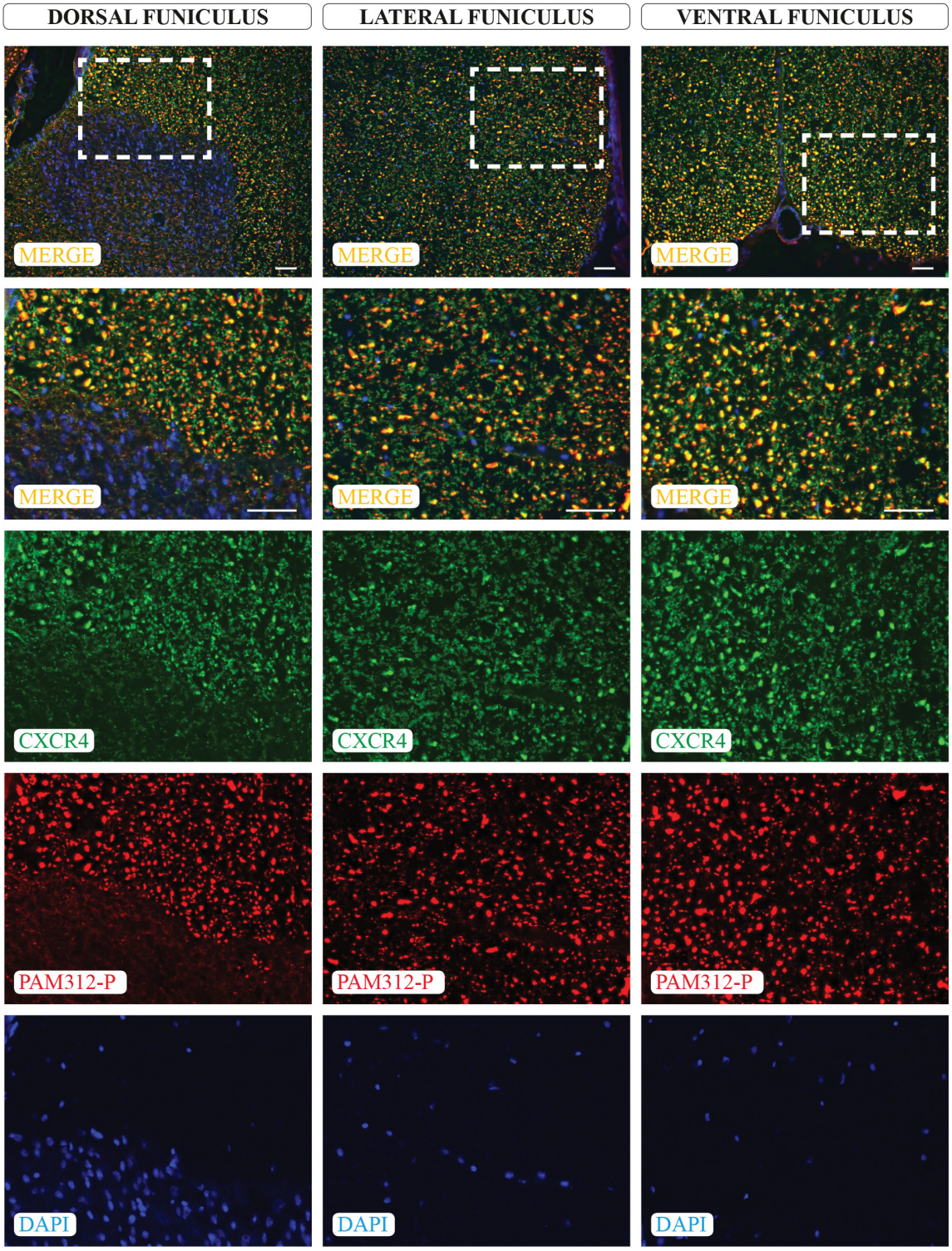

Fig. 3.15: Immunofluorescence staining of CXCR4 with the neuronal marker PAM312-P on rat spinal cord sections.
Dorsal funiculus (left pannel), lateral funiculus (middle pannel) and ventral funiculus (right pannel) of a transverse rat spinal cord section stained for CXCR4 (green), the neuronal marker PAM312-P (red), which recognizes phosphorylated neurofilaments and nuclear staining with DAPI (blue). Images in the first row are overviews. Dashed rectangle indicates higher magnification for the following images. Scale bar: 50 µm.

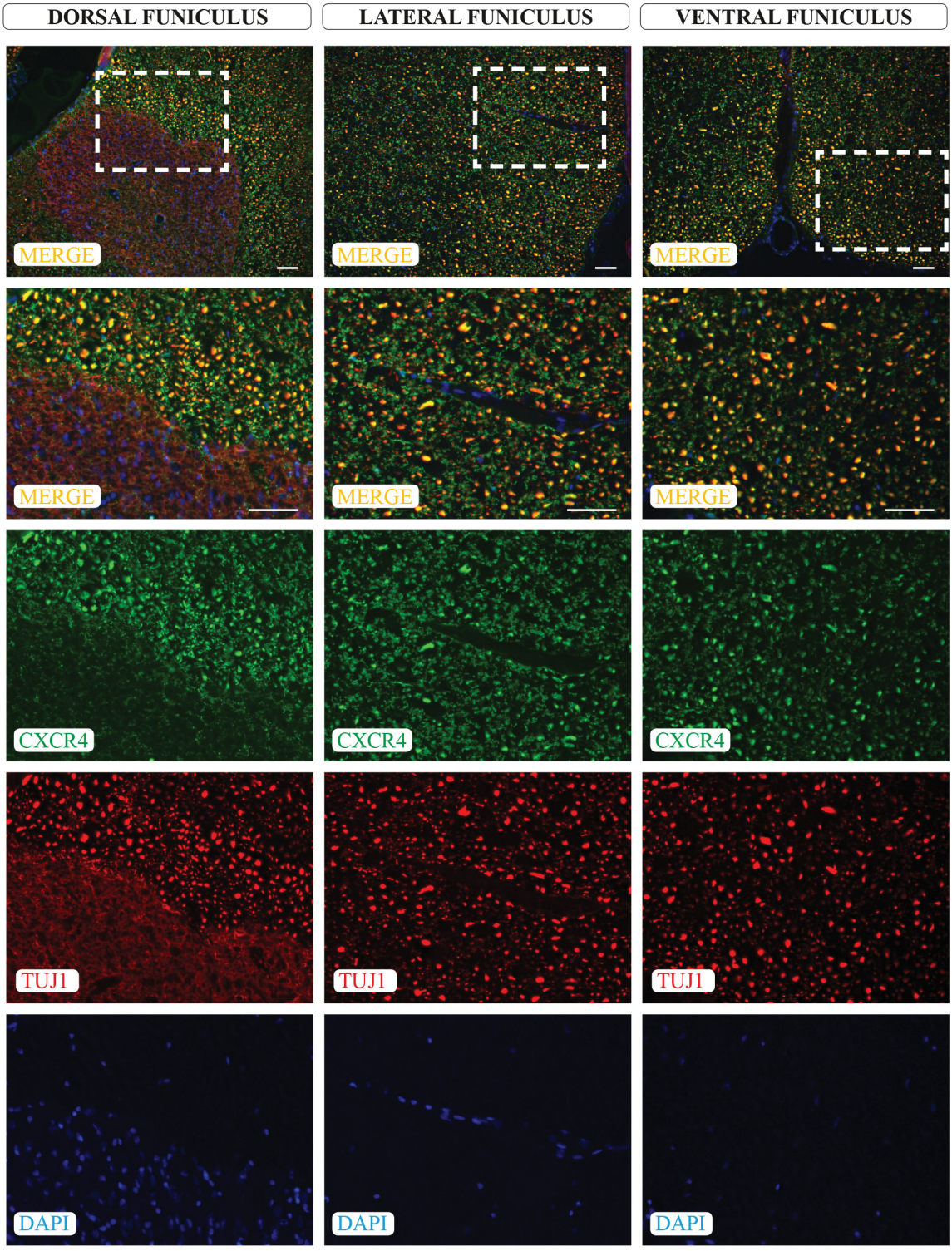

Fig. 3.16: Immunofluorescence staining of CXCR4 with the neuronal marker Tuj1 on rat spinal cord sections.

Dorsal funiculus (left pannel), lateral funiculus (middle pannel) and ventral funiculus (right pannel) of a transverse rat spinal cord section stained for CXCR4 (green), the neuronal marker Tuj1 (red) and nuclear staining with DAPI (blue). Images in the first row are overviews. Dashed rectangle indicates higher magnification for the following images. Scale bar: 50 µm.

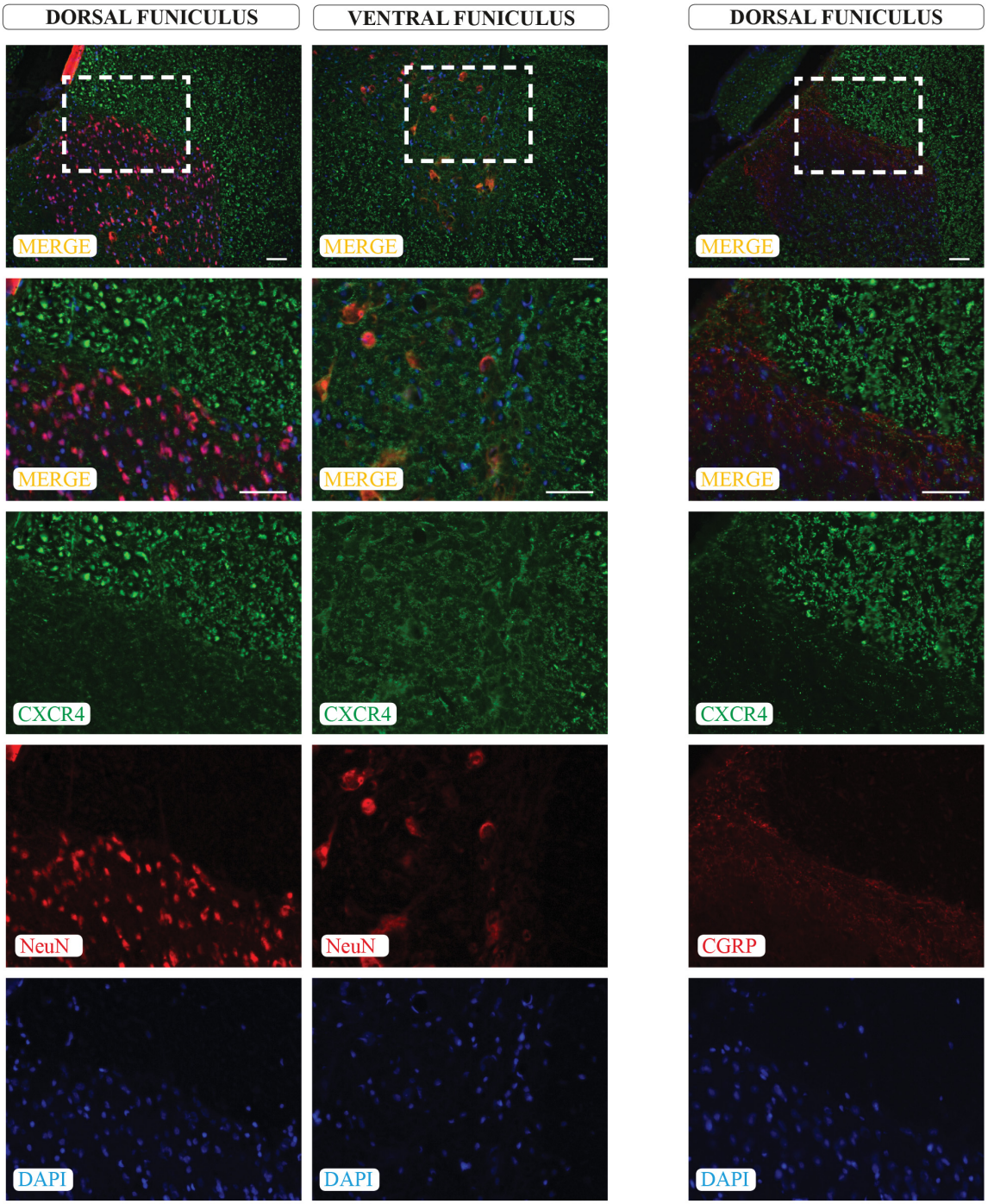

Fig. 3.17: Immunofluorescence staining of CXCR4 with the neuronal marker NeuN and CGRP on spinal cord sections.
Dorsal funiculus (left and right pannel) and ventral funiculus (middle pannel) of a transverse rat spinal cord section stained for CXCR4 (green), either with the neuronal marker NeuN or CGRP (red) and nuclear staining with DAPI (blue). Images in the first row are overviews. Dashed rectangle indicates higher magnification for the following images. Scale bar: 50 µm.

3.3.3 CXCR4 is expressed in mature oligodendrocytes and not in astrocytes

In order to analyze if CXCR4 is expressed by glial cells, such as astrocytes and mature oligodendrocytes, a double staining with glial markers was done. Both, in the mouse and in the rat spinal cord, GFAP (Glial fibrillary acidic protein), the most widely used marker for astroglial cells, which stains intermediate filaments in astrocytes, recognized morphologically different cells compared to the CXCR4 staining (Fig. 3.18, 3.20). The vast majority of the dot-like CXCR4 positive structures did not or only slightly co-localize with the long-shaped GFAP positively stained astrocytes (Fig. 3.18, 3.20). In contrast, the marker for developing and mature oligodendrocytes MBP (Myelin basic protein), which is the major structural component of myelin, co-localized with the CXCR4 staining (Fig. 3.19, 3.21). The signal only overlapped at the edges of the CXCR4 dot-like structures, where it seemed to strongly co-localize with MBP, emphasizing that apart from neurons, also other cells in the nervous system may carry the CXCL12 receptor CXCR4.

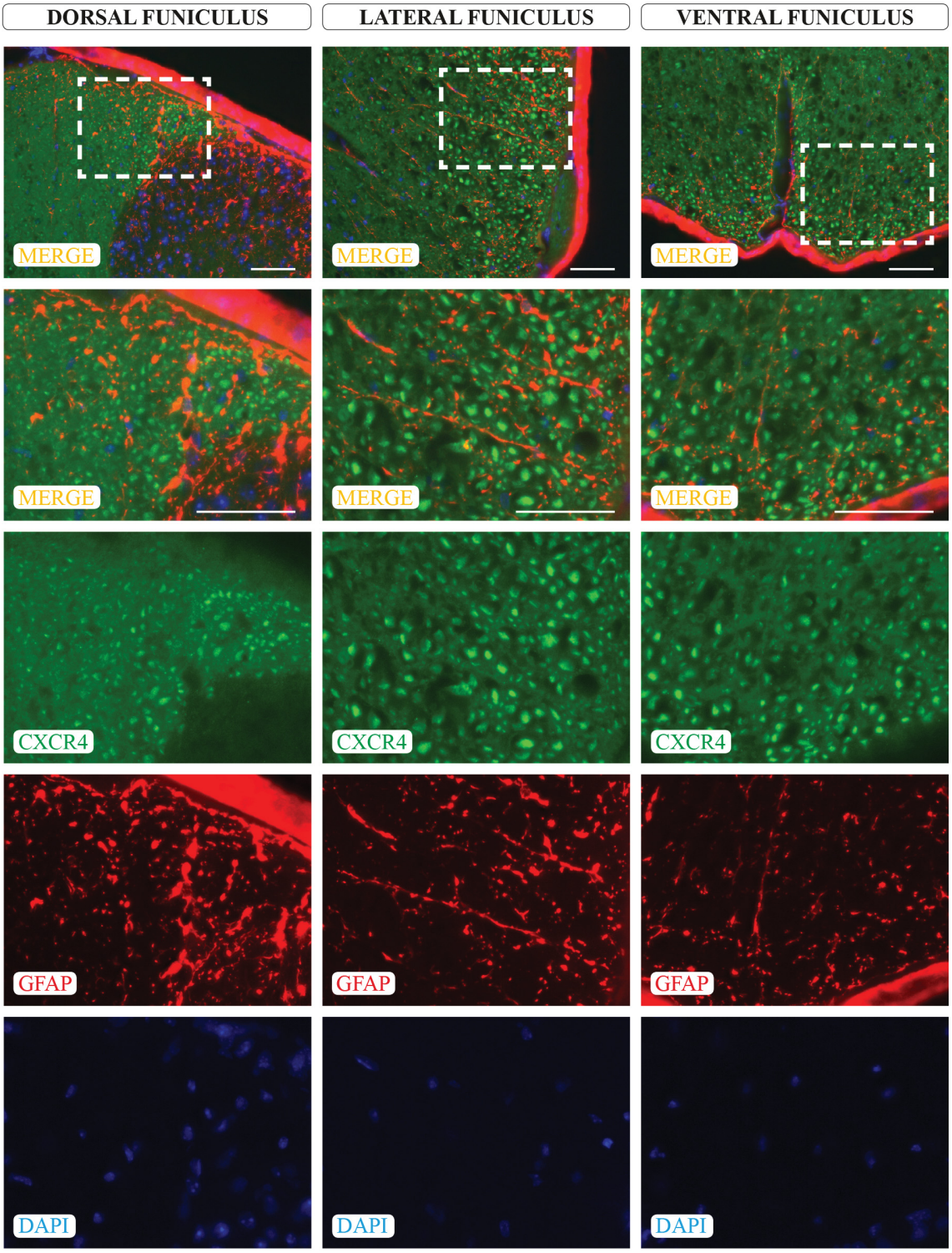

Fig. 3.18: Immunofluorescence staining of CXCR4 with the astrocytic marker GFAP on mouse spinal cord sections.
Dorsal funiculus (left pannel), lateral funiculus (middle pannel) and ventral funiculus (right pannel) of a transverse mouse spinal cord section stained for CXCR4 (green), the astrocytic marker GFAP (red) and nuclear staining with DAPI (blue). Images in the first row are overviews. Dashed rectangle indicates higher magnification for the following images. Scale bar: 50 µm.

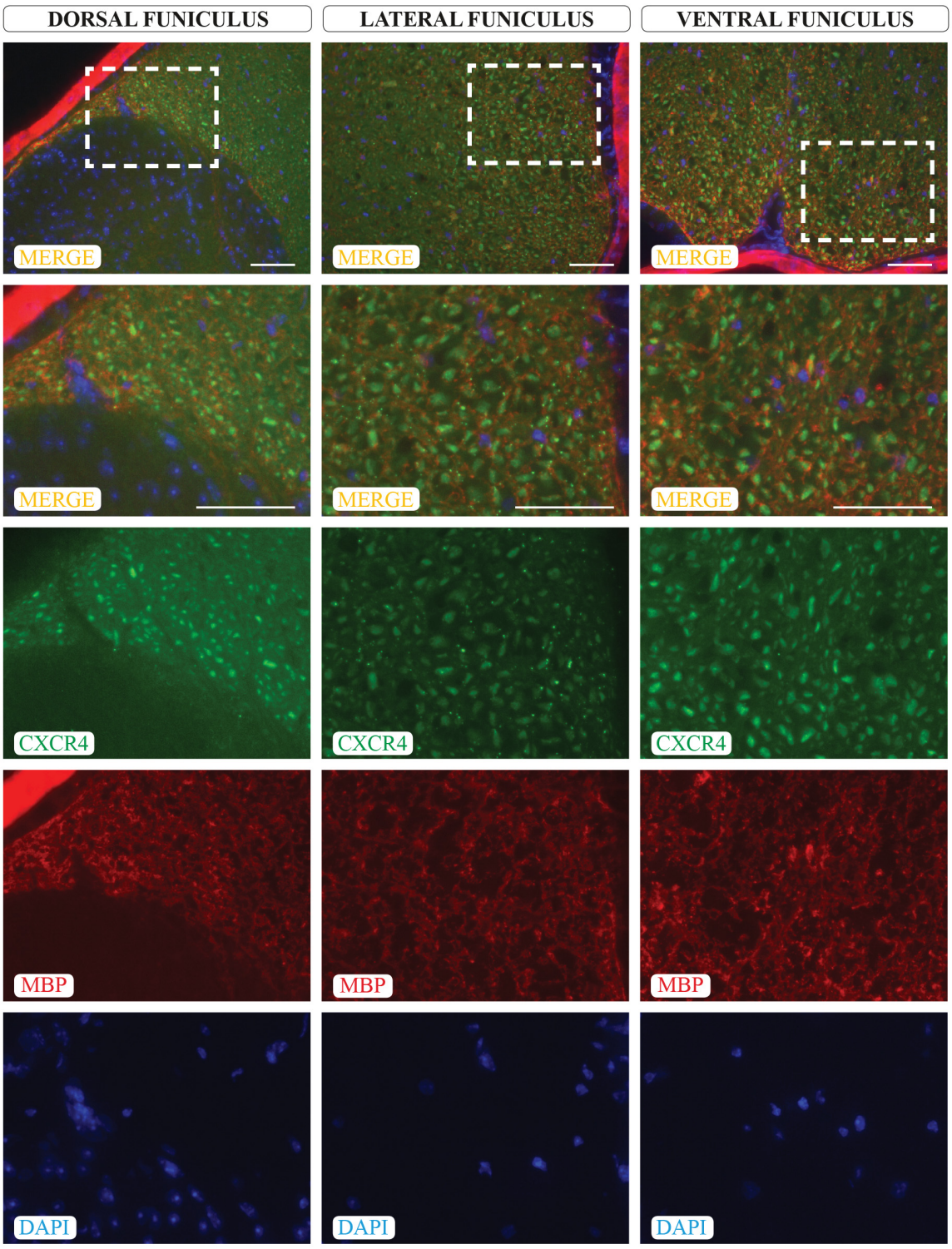

Fig. 3.19: Immunofluorescence staining of CXCR4 with the adult oligodendrocytic marker MBP on mouse spinal cord sections.
Dorsal funiculus (left pannel), lateral funiculus (middle pannel) and ventral funiculus (right pannel) of a transverse mouse spinal cord section stained for CXCR4 (green), the adult oligodendrocytic marker MBP (red) and nuclear staining with DAPI (blue). Images in the first row are overviews. Dashed rectangle indicates higher magnification for the following images. Scale bar: 50 µm.

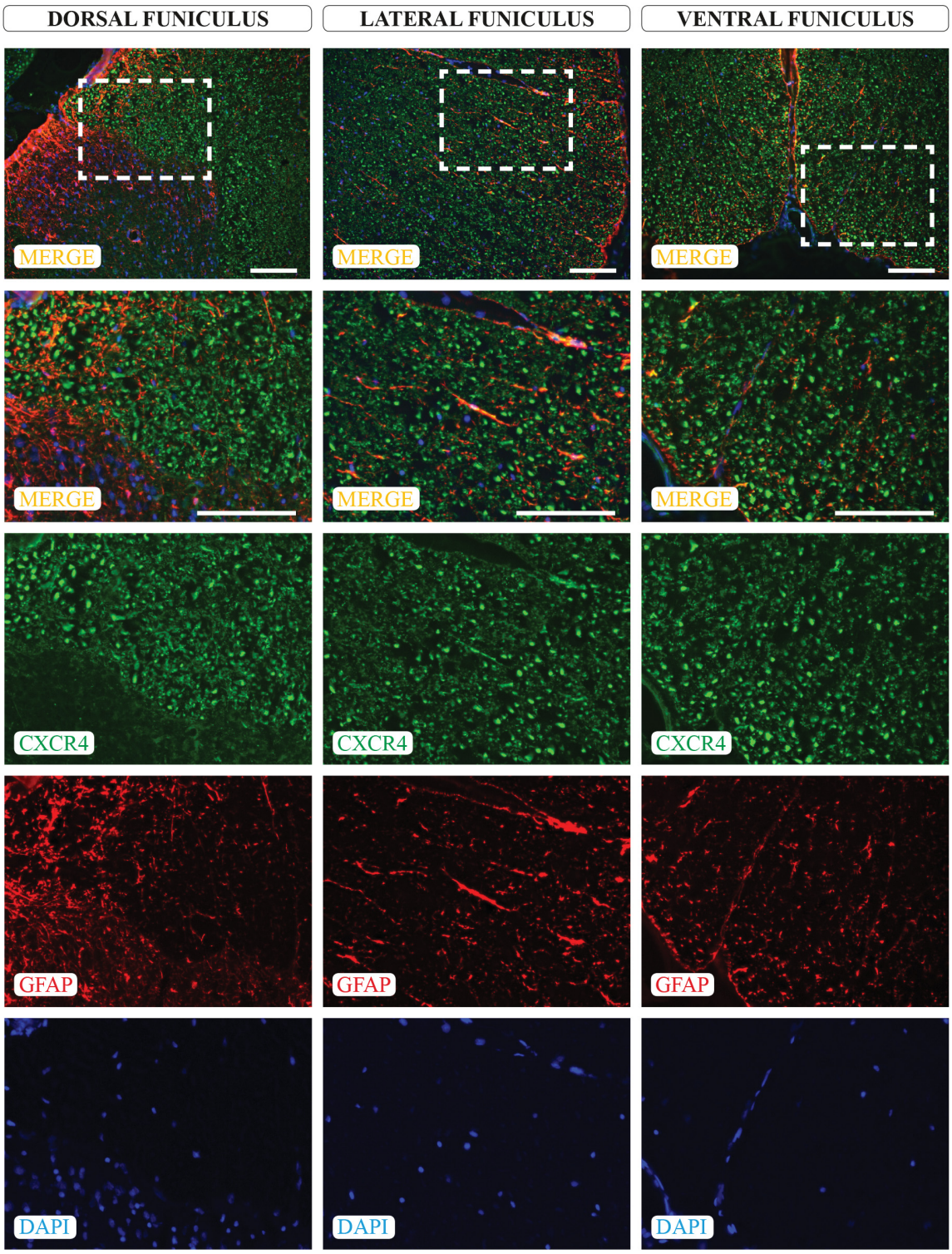

Fig. 3.20: Immunofluorescence staining of CXCR4 with the astrocytic marker GFAP on rat spinal cord sections.
Dorsal funiculus (left pannel), lateral funiculus (middle pannel) and ventral funiculus (right pannel) of a transverse rat spinal cord section stained for CXCR4 (green), the astrocytic marker GFAP (red) and nuclear staining with DAPI (blue). Images in the first row are overviews. Dashed rectangle indicates higher magnification for the following images. Scale bar: 50 µm.

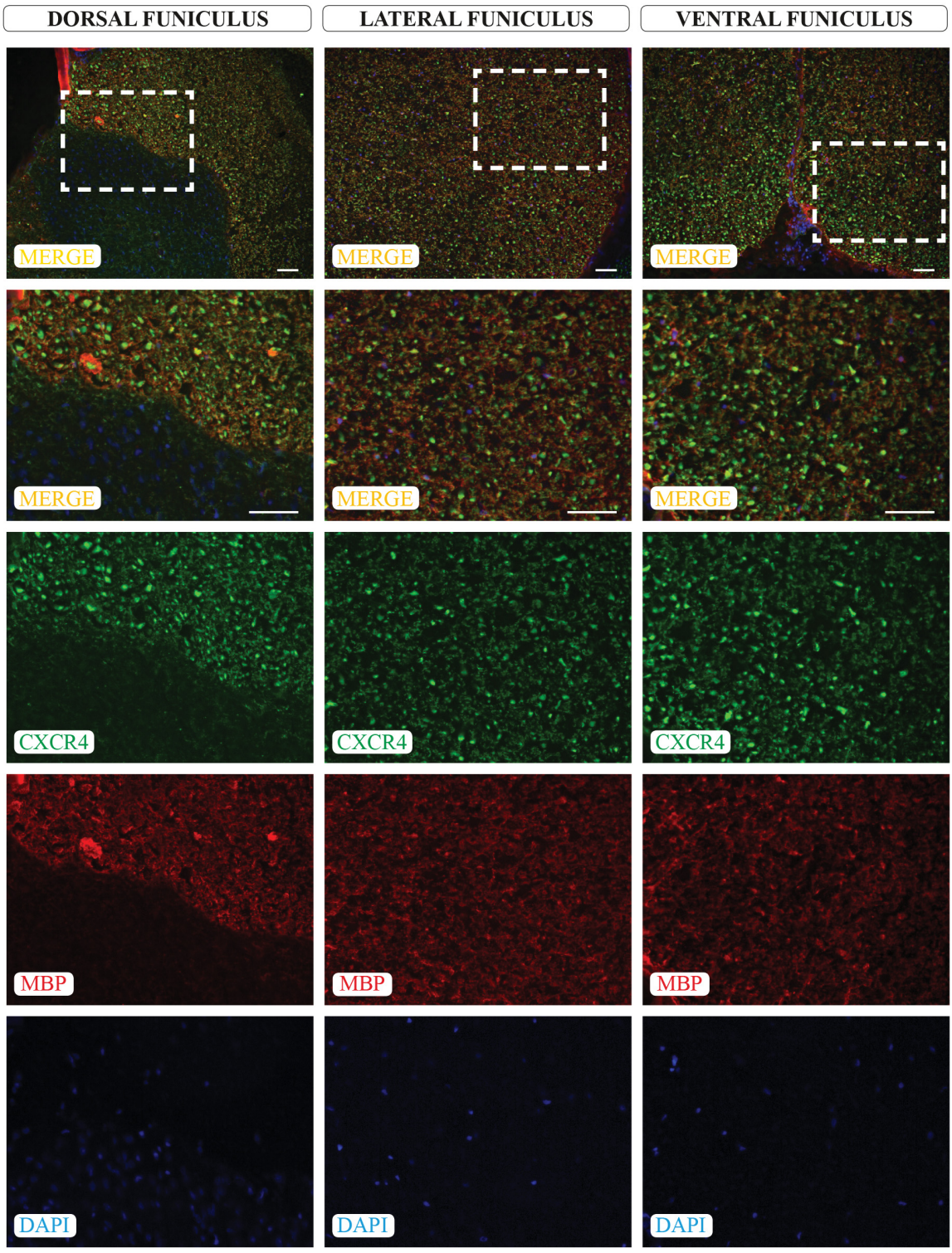

Fig. 3.21: Immunofluorescence staining of CXCR4 with the adult oligodendrocytic marker MBP on rat spinal cord sections.
Dorsal funiculus (left pannel), lateral funiculus (middle pannel) and ventral funiculus (right pannel) of a transverse rat spinal cord section stained for CXCR4 (green), the adult oligodendrocytic marker MBP (red) and nuclear staining with DAPI (blue). Images in the first row are overviews. Dashed rectangle indicates higher magnification for the following images. Scale bar: 50 µm.

3.3.4 Immunofluorescence staining of CXCR4 in spinal cord sections and specifically in the dCST is not increased after spinal cord injury

The cell-recruiting via CXCL12/CXCR4 signaling is an important element in regulating spinal cord responses to injury (Sanchez-Martín et al., 2011; Tysseling et al., 2011). CXCL12 was reported to be upregulated upon CNS injury mainly by reactive astrocytes (Hill et al., 2004; Miller et al., 2005), however, the role of the CXCL12/CXCR4 axis following spinal cord injury still remains unclear. In order to investigate if CXCR4 is involved in the regulation of spinal cord responses to injury and if CXCR4 expression in the spinal cord, specifically in the dCST, is increased after injury, the CXCR4 expression in injured mice was quantified. The intensity of the CXCR4 staining in the entire transverse section as well as in the dCST alone was measured (Fig. 3.22). There was no increase in CXCR4 expression neither in the dorsal, in the lateral or in the ventral funiculi nor in the dCST of injured animals as compared to controls. This confirms the complete absence of the CXCR4 receptor in the dCST in both control and in injured mice. Furthermore, rostral to the injury site the observed expression of the CXCR4 receptor was not enhanced in transverse spinal cord sections, and therefore no additional cells expressing CXCR4 were recruited in this specific region. The same observation was found for CXCR4 expression in control *vs.* injured rats (data not shown).

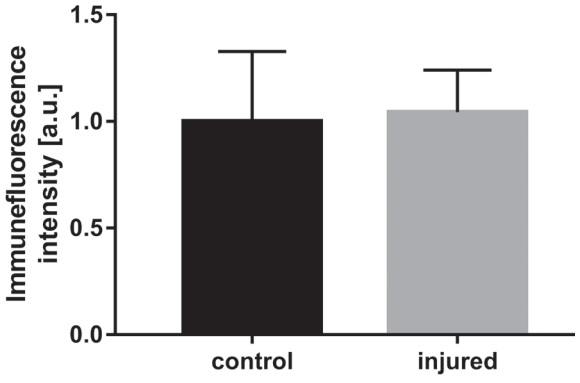

Fig. 3.22: CXCR4 protein expression in the dCST is not induced by a spinal cord injury. Quantification of the immunofluorescence intensity of CXCR4 expression in the dCST of uninjured control (black bar) *vs.* injured (gray bar) mice. Values were normalized to the control group. Data are presented as the mean ± SEM. N = four control, unlesioned and 11 injured animals. The non-parametric Mann-Whitney-U-test was applied to compare the two unpaired groups for significant difference in the parameter of interest.

3.3.5 CXCR4 mRNA is not expressed in layer V neurons of the cerebral cortex of adult mouse and rat brain sections

During development, the CXCR4 expression is exposed to variations. In the embryonic stage CXCR4 is highly expressed in the nervous system and decreases progressively till adulthood (Schonemeier et al., 2008a; Tissir et al., 2004). However, the chemokine receptor is still detectable in subpopulations of mature neurons, such as interneurons in the cerebral cortex, and in brain regions that are associated with adult neurogenesis, such as the olfactory bulb, throughout the ventricular system and within the subgranular zone of the dentate gyrus in the hippocampus (Lu et al., 2002; Stumm et al., 2002; Stumm et al., 2003; Tissir et al., 2004). In order to confirm the absence of the CXCR4 receptor in the pyramidal corticospinal neurons in layer V of the sensorimotor cortex an *in situ* hybridization in mouse and rat brain sections was performed (Fig. 2.1). Furthermore, also the mRNA expression of the second chemokine receptor CXCR7 and the respective ligand CXCL12 were analyzed. The lack of CXCR4 expression on the

protein level in the dCST observed in immunofluorescence staining was consistent with the *in situ* hybridization. The absence of CXCR4 mRNA expression in the pyramidal neurons of layer V, which project their axons into the dCST, was observed in mouse (Fig. 3.23, 3.25) as well as in rat brains (Fig. 3.24, 3.26). The complete hind limb region of the primary sensorimotor cortex was negative for CXCR4 mRNA expression. Only some few cells in the layer II/III and VI were positively stained for CXCR4, most likely interneurons. The subventricular zone of the lateral ventricle and the hippocampus served as positive control areas to confirm the experimental success (data not shown). In contrast to CXCR4, the *in situ* hybridization results of both CXCL12 as well as the CXCR7 receptor clearly demonstrated mRNA expression in the layer V neurons of mouse and rat cerebral cortex (Fig. 3.24-3.26). Here, the stratum moleculare of the dentate gyrus was used as a positive control area (data not shown). In conclusion, CXCR4 gene expression was not detectable in the cerebral cortex of mouse and rat brains, while CXCL12 and CXCR7 mRNA expression was present in the pyramidal corticospinal neurons in laxer V of the sensorimotor cortex.

3.3.6 CXCR4 mRNA expression is not altered in adult mouse and rat brain sections upon spinal cord injury

In the cerebral cortex the pyramidal neurons, which project their axons into the dCST to the spinal cord do not express the CXCR4 receptor in mouse and rat brains. To investigate a possible alteration in expression upon injury, an *in situ* hybridization of brain sections of control animals versus injured animals was performed (Fig. 3.23-3.26). No striking changes in gene expression for CXCL12 and its receptors CXCR4 and CXCR7 were observed after spinal cord injury in both species (Fig. 3.23, 3.24). The more detailed microscopic images also revealed no alteration in gene expression in injured animals compared to control animals (Fig. 3.25, 3.26). The expression of the chemokine and its receptors is not changed in both, the early (3 days after SCI) and the late time point after injury (5 weeks after SCI).

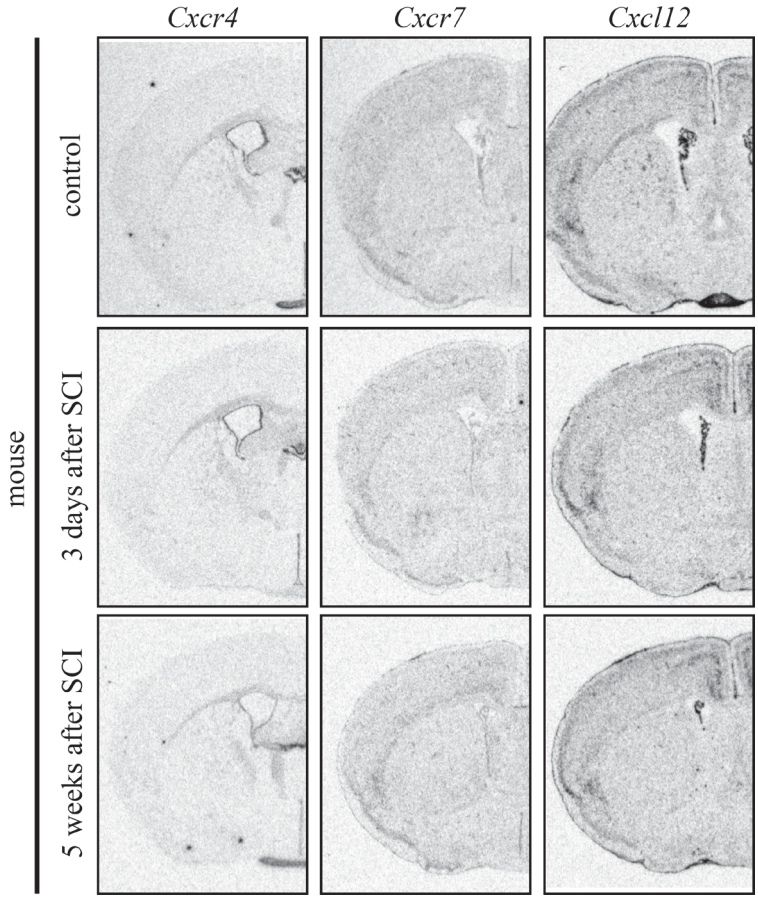

Fig. 3.23 CXCL12, CXCR4 and CXCR7 *in situ* hybridization of control and injured mouse brain sections.
The mRNA expression of the chemokine receptors CXCR4 (left column) and CXCR7 (middle column) as well as the chemokine CXCL12 (right column) was analyzed via *in situ* hybridization in the hind limb region of the primary sensorimotor cortex in brains of control mice (first row) and mice that got a spinal cord injury (SCI). Two time points after SCI were analyzed: 3 days after SCI (middle row) and 5 weeks after SCI (last row).

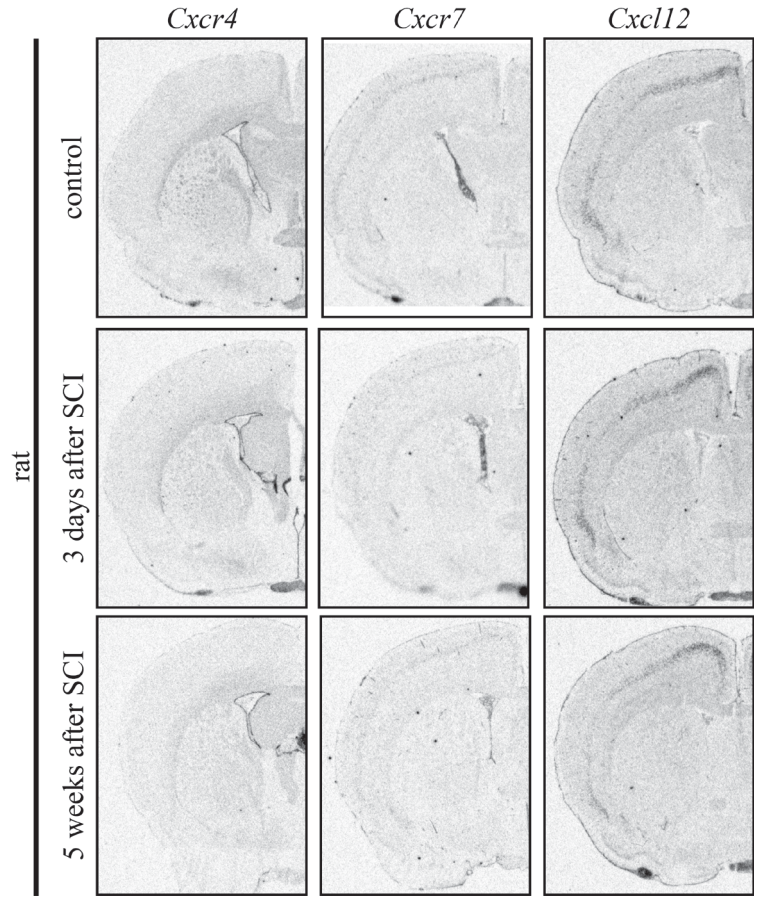

Fig. 3.24 CXCL12, CXCR4 and CXCR7 *in situ* hybridization of control and injured rat brain sections.
The mRNA expression of the chemokine receptors CXCR4 (left column) and CXCR7 (middle column) as well as the chemokine CXCL12 (right column) was analyzed via *in situ* hybridization in the hind limb region of the primary sensorimotor cortex in brains of control rats (first row) and rats that got a spinal cord injury (SCI). Two time points after SCI were analyzed: 3 days after SCI (middle row) and 5 weeks after SCI (last row).

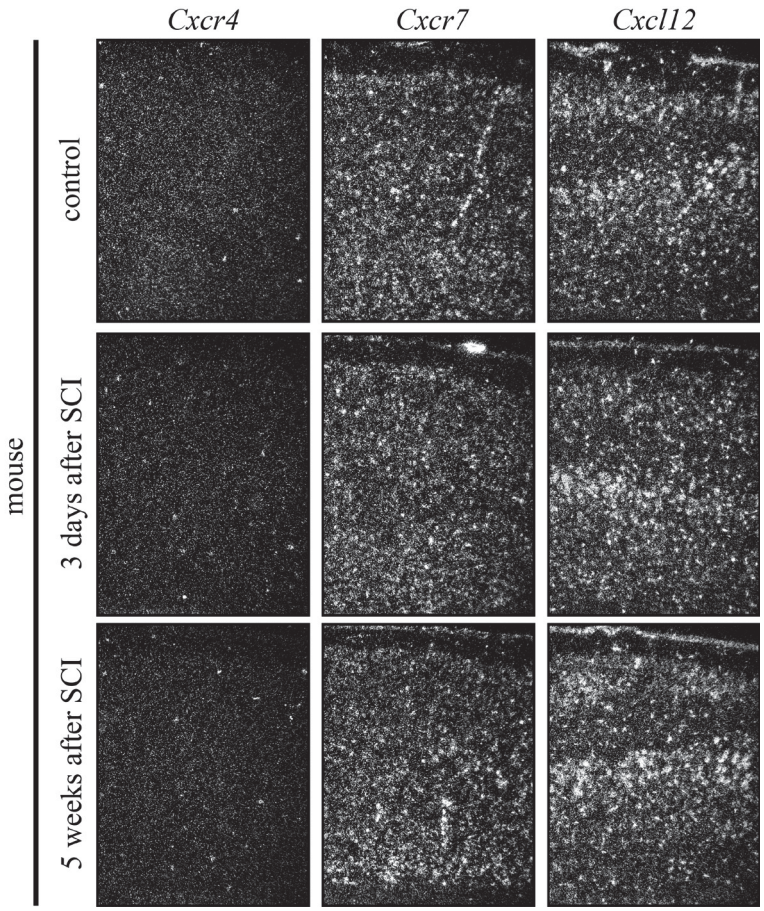

Fig. 3.25: Microscopic images of CXCL12, CXCR4 and CXCR7 *in situ* hybridization of control and injured mice brain sections.
Microscopic images of the mRNA expression of the chemokine receptors CXCR4 (left column) and CXCR7 (middle column) as well as the chemokine CXCL12 (right column) that was analyzed via *in situ* hybridization in the hind limb region of the primary sensorimotor cortex in brains of control (first row) and injured mice. Two time points after spinal cord injury (SCI) were analyzed: 3 days after SCI (middle row) and 5 weeks after SCI (last row).

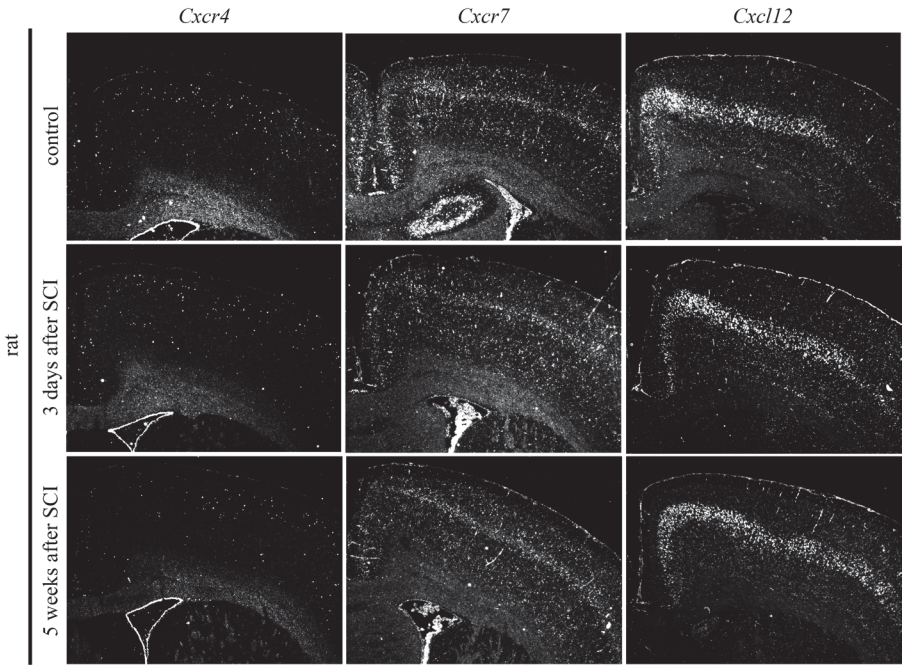

Fig. 3.26: Microscopic images of CXCL12, CXCR4 and CXCR7 *in situ* hybridization of control and injured rat brain sections.
Microscopic images of the mRNA expression of the chemokine receptors CXCR4 (left column) and CXCR7 (middle column) as well as the chemokine CXCL12 (right column) that was analyzed via *in situ* hybridization in the hind limb region of the primary sensorimotor cortex in brains of control (first row) and injured rats. Two time points after spinal cord injury (SCI) were analyzed: 3 days after SCI (middle row) and 5 weeks after SCI (last row).

4. DISCUSSION

4.1 CXCL12 desensitizes adult DRG neurons toward CNS myelin by exerting disinhibitory effects and mediates neurite outgrowth via the chemokine receptor CXCR4

A vast number of different factors impair the regeneration of injured CNS neurons. One major impediment is the oligodendrocyte derived myelin-associated inhibitors in the CNS, which form an inhibitory environment for axon growth. In fact, *in vitro* neurite outgrowth is inhibited when mammalian neurons are cultured in presence of myelin (Bähr and Przyrembel, 1995; Benson et al., 2005; Chen et al., 2000; McKerracher et al., 1994; Moreau-Fauvarque et al., 2003; Wang et al., 2002). While outgrowth inhibition is restricted to post-embryonic developmental stages of the CNS, neurons in the embryonic stage are not sensitive to myelin during CNS development and axonal pathfinding. These "embryonic intracellular settings" need to be restored in adult damaged CNS neurons, since the events that neurons normally undergo during development resemble the events required for the structural and functional recovery of injured axons. The chemokine CXCL12, a constitutively secreted and ubiquitously expressed chemokine has a crucial role in developmental processes, including hematopoiesis, cardiogenesis, vascular formation and neurogenesis (Aiuti et al., 1997; Nagasawa et al., 1996b; Sugiyama et al., 2006; Tachibana et al., 1998; Zou et al., 1998). In this thesis, several aspects of CXCL12 and its receptor CXCR4 were investigated in relation to axonal outgrowth. Previous studies demonstrated that CXCL12 stimulates axonal elongation of cultured cerebellar granule cells, branching of hippocampal neurons and neurite growth of adult dissociated RGCs on the growth-permissive substrate laminin (Arakawa et al., 2003; Heskamp et al., 2013; Pujol et al., 2005). In order to investigate the effect of CXCL12 on neurite outgrowth of adult mouse DRGs, neurons were dissociated, plated on laminin coated plates and incubated with CXCL12 or control solution, e.g., BSA, respectively. Controversial to the previous data and to the analyzed cell types, CXCL12 did not stimulate axonal outgrowth of adult DRG neurons plated on laminin although the cells were exposed to the highest chemokine concentration tested for adult RGC, which yielded the strongest neurite outgrowth (Fig. 3.2 A, C-D). One explanation could be that DRG neurons need a higher CXCL12 concentration to initiate neurite outgrowth on a permissive substrate. The short half-life of the recombinant CXCL12 ligand in culture could also play an important role here. On the other hand, since the CXCL12 concentration is already relatively high one could assume that there are no free available receptors anymore on the surface

of the neuron and that the recycling of the receptor is the limiting factor. It could be that the internalization of the CXCR4 receptor after ligand binding is slower in DRG neurons than in the other cell types and that the receptor molecules present on the surface are already saturated with CXCL12.

In early nervous system development, neurons migrate in response to chemotactic cues. For normal axon pathfinding, it is crucial that the axonal growth cones are chemoattracted or chemorepelled on their way by axonal guidance molecules. CXCL12 was shown not to exhibit chemoattracting or repelling effects, but it reduced the responsiveness of growth cones to multiple repellents, hence suggesting an important role of CXCL12 as a modulator of effectivness of repellent cues during development (Chalasani et al., 2003; Chalasani et al., 2007). Additionally, CXCL12 was described to exert disinhibitory effects by reducing the sensitivity of axonal growth cones of postnatal rat DRG neurons as well as mature rat RGCs towards CNS myelin, stimulating neurite outgrowth (Heskamp et al., 2013; Opatz et al., 2009). While adult mouse DRG neurons displayed excellent outgrowth on laminin-coated plates, the neurite outgrowth of the DRG neurons was impaired on CNS myelin-coated plates, although the comparison of total cell number of neurons growing on laminin and myelin, respectively, was unchanged (Fig 3.2 A, C-D). The impairment of neurite outgrowth was therefore not due to impaired adherence of the DRG neurons on the myelin substrate, but it was dependent on the inhibitory environment for axon growth. This result was expected, since adult DRG neurons, which already experienced the intrinsic neuronal switch leading to myelin-sensitivity and not embryonic DRG neurons, which have still the capacity to regenerate, were used for this experiment. Consistently with the previous studies in adult rodent RGCs and postnatal rat DRGs, the addition of the chemokine CXCL12 to the adult mouse DRG culture grown on inhibitory myelin was sufficient to overcome the myelin-induced outgrowth inhibition and to stimulate axon outgrowth (Fig. 3.2 A, C). Heskamp and colleagues analyzed the signaling pathway responsible for the desensitization of mature RGCs towards inhibitory myelin and they could show that this effect depends on the CXCR4/PI3K/AKT/mTOR-signaling cascade (Heskamp et al., 2013). Also in earlier studies, when CXCR4 was the only known CXCL12 receptor, the CXCL12 induced axon growth was demonstrated to be CXCR4-dependent, as blocking this receptor resulted in a decreased neuronal tolerance of growth inhibitors (Chalasani et al., 2003). By a pharmacological approach and in accordance to these studies it was shown in this thesis, that also in this case the chemokine receptor CXCR4 is responsible for the CXCL12 mediated axonal outgrowth of adult mouse DRG neurons on an inhibitory substrate (Fig. 3.2 B, E-F). The positive neurite growth promoting effects of CXCL12 were abrogated by a pharmacological approach using the specific CXCR4-antagonist AMD3100 (Hatsea et al., 2002). This antagonist is a potent inhibitor of the binding and function of CXCL12 with high affinity and potency. The simultaneous treatment with both the antagonist and the recombinant CXCL12 ligand resulted in a slight increase of DRG axon outgrowth on inhibitory myelin. This effect could be due to the exaggerated concentration of the CXCL12 ligand used in cell culture, which in turn increased the proportion of receptors occupied by the ligand mediating axon growth. The antagonist competes with the ligand CXCL12 for the same binding site at the CXCR4 receptor. To overcome the high concentration of the ligand, one could assume that a higher concentration of the AMD3100 antagonist would be required to obtain the same degree of binding site occupancy, and to be able to completely abrogate the DRG axon growth in the simultaneous treatment. Furthermore, in this thesis, due to the small sample size, it was not possible to check normality of volume parameter and therefore non-parametric tests were applied. Although the results showed a decrease of 50 %,

the statistical difference is not significant, since the application of the non-parametric test is stricter than the application of a parametric test. Therefore, to confirm the trend seen in the *in vitro* experiments of this thesis, further experiments with larger sample size would be required. The ability of CXCL12 to affect axon growth in DRG neurons grown on myelin and the fact that these positive effects can be abrogated by a CXCR4-antagonist suggest that this receptor is expressed on DRG neurons. The presence of the CXCR4 receptor was assessed via immunocytochemistry. Indeed, the soma, the neurites and growth cones of adult mouse DRG neurons expressed the chemokine receptor suggesting a CXCR4-dependent effect of CXCL12 (Fig.3.3). Actually, CXCL12 acts through two different seven-transmembrane receptors, CXCR4 and CXCR7. Previous studies also indicated that these receptors are able to homo- and heterodimerize (Levoye et al., 2009; Luker et al., 2009). However, whether CXCL12 mediates its effects through CXCR7 is still under debate. The initial aim of this thesis was to reveal the receptor responsible for the CXCL12 mediated effect. The availability of validated antibodies that was raised against CXCR4 or CXCR7 is therefore essential. A number of studies showed controversial data in this regard, since the specificity of the antibodies used was not validated at prior, leading to incorrect interpretation of the data and conclusions (Berahovich et al., 2010; Fischer et al., 2008). Therefore, in this thesis, the most commonly used knockout validated rabbit monoclonal anti-CXCR4 antibody clone UMB-2, was used. The UMB-2 antibody recognizes its epitope located in the intracellular C-Terminal sequence of the CXCR4 receptor (Fig. 1.3 A). The binding of the chemokine CXCL12 to its receptor CXCR4 leads to phosphorylation of the serine cluster 346-347 and this epitope cannot be longer recognized by the antibody. The UMB-2 antibody recognizes therefore only the receptor in its unphosphorylated and inactive state. Upon ligand binding the CXCR4 receptor is internalized and then either degraded or recycled back to the plasma membrane (Marchese et al., 2003). Sustained stimulation of the CXCR4 receptor with CXCL12 causes lysosomal degradation of the receptor (Marchese and Benovic, 2001). In order to validate the specificity of this antibody, this simple proof of principle was utilized. Cultured embryonal mouse cortical neurons were subjected to recombinant human CXCL12 and the immunoreactivity of CXCR4 was measured. Upon ligand binding, the immunoreactivity of the CXCR4 receptor disappeared, confirming both the specificity of the UMB-2 antibody and the functional interaction between the human CXCL12 with mouse CXCR4 (Fig. 3.1 C). However, immunohistochemical and fluorescence staining using commercially available antibodies against CXCR7 did not show any specific signal (data not shown). Therefore, the question whether CXCR7 is also involved in CXCL12 mediated signaling in adult mouse DRG neurons still needs to be addressed in future studies. In fact, the slight increase in DRG axon growth during the simultaneous incubation of CXCL12 and the specific CXCR4-antagonist AMD3100 (Fig. 3.2 B, E) could also be due to the activation of the CXCR7 receptor. Thus, the involvement of CXCR7 to some degree in DRG axon growth cannot be completely excluded.

Pharmacological approaches can involve several limitations since the compound can affect all cell types in the culture. Therefore, it is recommended to expand the study from a pharmacological approach to a genetic one. This is also the reason for choosing the DRG neurons in place of a primary cerebral cortex culture. Initially, to be in line with the *in vivo* part of the spinal cord injury project, where axons of the central nervous were injured, cerebral cortex neurons were prepared for the cell culture experiments. After several technical limitations in culturing adult cerebral cortex neurons, which are generally difficult to culture and also resistant to genetic manipulation, the neurite outgrowth assay was performed with adult DRG neurons of CXCR4 floxed mice.

In these experiments, the deletion of the CXCR4 receptor via Lipofection methods and viral gene delivery systems, such as recombinant lentivirus did not achieve high transfection rates in these primary adult neurons. Recently, a novel highly efficient transduction method of primary adult PNS and CNS neurons using VSV-G pseudo-typed, recombinant baculovirus has been developed by a colleague in Prof. Fischer Laboratory (Levin et al., 2016). This novel genetic approach needs to be tested in future studies. As already shown for adult mouse RGCs, the deletion of CXCR4 abolished completely the positive effects mediated by CXCL12 on both laminin and myelin, strongly suggesting a CXCR4-dependency (Heskamp, 2015). One could assume that the same mechanism works also in adult DRG neurons but further experiments are needed to elucidate this and whether CXCR7 is also involved in CXCL12 mediated signaling in adult DRG neurons.

4.2 Effect of CXCL12 in an *in vivo* mouse model of spinal cord injury and functional recovery after chemokine application

The generation of conditional knockout mutants for both receptors, CXCR4 and CXCR7, as well as viable receptor-deficient double mutants would definitely be useful to determine the individual functional roles of the chemokine receptors. To corroborate our *in vitro* observations, on the neurite growth supporting function of CXCL12 on inhibitory myelin substrate in adult mouse DRG neurons, an *in vivo* model of traumatic spinal cord injury in the mouse was established. The excellent expertise of Prof. Müllers working group on rat spinal cord injuries was fundamental. The principal idea of this work was to analyze the sprouting effect of the lesioned dCST axons of conditional CXCR4 and CXCR7 knockout mice. The deletion of the gene of interest occurs only in dCST when floxed receptor mice are backcrossed with a ROSA reporter mouse, which carries a floxed stop-sequence in the ROSA26 locus that inhibits the transcription of the red fluorescent protein tdTomato ($CXCR4_{fl/fl}/ROSA_{fl/wt}$) (Fig. 2.2 A). By stereotactic injections of the adeno-associated virus serotype 2, which expresses the HA-tagged Cre-Recombinase, into the pyramidal cells of layer V of the hind limb sensorimotor cortex, the excision of the floxed stop sequence occurs, leading to a visualization of the transduced neurons that are also depleted of the gene of interest. However, the procedure was first tested in CXCR4 wild type and ROSA floxed mice as control mice ($CXCR4_{wt/wt}/ROSA_{fl/wt}$) using the viral injection for anterograde labeling of dCST, to investigate the expression of CXCR4 and the sprouting effect of dCST neurons after CXCL12 treatment in WT mice prior to investigating the conditional knockout mice.

4.2.1 Local intrathecal infusion in a mouse spinal cord injury model

The advantages of intrathecal infusion are numerous. For long-term drug delivery into the subarachnoid space, this method is optimal and commonly used. Drug level fluctuations and repetitive injections, which subsequently results in more surgical complications and physical stress, are avoided by this method (Taiwo et al., 2005). Intrathecal infusions are used not only in the clinic for the administration of e.g., analgesics or anti-spasticity drugs in human patients after traumatic injury (Burchiel and Hsu, 2001; Saval and Chiodo, 2010), but also in experimental approaches in animal models to develop spinal cord therapies (Kojima and Tator, 2002). There are several published studies of intrathecal spinal cord catheterization methods in rats that lead to

an improved outcome after spinal cord injury. In contrast, due to the small size of mice, lumbar punctures or spinal cord microinjections are mostly performed, and rare information is available about thoracic intrathecal infusions (Hylden and Wilcox, 1980; Njoo et al., 2014; Taiwo et al., 2005). In fact, there are also studies that describe catheter-induced negative side effects in rats, as compression, scarring and damage of the spinal cord (Jones and Tuszynski, 2001; Sakura et al., 1996; Zhang et al., 2010). Most probably, the pressure of the intrathecally placed catheter onto the spinal cord and the activation of the immune response against the tubing material, cause compression and extensive scarring of the spinal cord. One of the main reasons for these negative side effects is the very narrow subdural and subarachnoid space compared with the diameter of the smallest possible intrathecal tubing (Haines et al., 1993; Reina et al., 2002). Therefore, intrathecal catheter infusions in rodents are rarely used and, instead, systemic delivery routes (e.g., intraperitoneal, oral etc.) are preferred as first-line delivery system unless intrathecal drug application is required (Njoo et al., 2014). However, for the correct interpretation of the data of spinal cord injury experiments, a reliable local intrathecal infusion method is indispensable where no further damage is induced to the spinal cord with the infusion device. In the current study, based on a newly developed optimized catheterization method for spinal cord injured rats conceived by a colleague of the Prof. Müller Laboratory (König, 2014), a novel catheterization method designed for mice was introduced (Fig. 3.4 A-B). The most critical points in promoting damage and scarring in the spinal cord found during the optimization of the rat catheterization model were catheter diameter, catheter material, length of catheter tubing inside the subarachnoid space and catheter bending at the area of initial contact with the spinal cord (T11). In a rat spinal cord study it was demonstrated that in contrast to polyethylene, the catheter material polyurethane, did not induce spinal tissue damage (Sakura et al., 1996). Therefore, an Alzet 32G (0.23 mm OD x 0.09 mm ID) polyurethane mouse intrathecal catheter was applied in this study. This was the catheter with the smallest diameter available. Another key point to avoid scarring and compression is the intrathecal tubing distance that should be kept as short as possible. In the rat catheterization protocol the catheter is mostly running epidurally before insertion into the subarachnoid space above the spinal lesion near by the dura suture. Differently, the catheter in the mouse catheterization protocol is running completely epidurally lacking supporting hold through the dura mater (Fig. 3.4 A). In fact, a dura suture is impossible in mice since through the opening of the dura mater the latter retracts beneath the vertebrae. Therefore, an appropriate and strong catheter fixation was fundamental to avoid catheter retraction and compression. Indeed, the attachment of the epidural mouse catheter to the base of vertebra T10 with a surgical thread resulted in a stable catheter fixation method (Fig. 3.4 A, B3). The tip of the catheter was lifted and placed directly above the lesion site. Through the removing of the spinous process of T10 the shifting of the catheter either to one or to the other side could be avoided. To minimize catheter bending, as in rats, a total laminectomy of T11 was performed. Furthermore, to minimize also compression of the spinal cord, the exposed spinal cord was covered with a cushion of autologous fat tissue and another one, used to fix the surgical thread, stabilized the catheter additionally (Fig. 3.4 A, B3-4). In conclusion, the new mouse catheterization method presented here, demonstrated a stable intrathecal catheter fixation and local intrathecal drug infusion over seven days, avoiding compression of spinal cord tissue and therefore allowing correct interpretation of the experimental data (Fig. 3.4 C-E).

4.2.2 Excessive CXCL12 does neither promote sprouting of lesioned corticospinal tract axons nor improve the functional behavior in a mouse model of spinal cord injury

The neurite growth promoting effects of CXCL12 on inhibitory substrate *in vitro* were described in several studies for adult rat RGC cells and postnatal rat DRG neurons and were further confirmed in this thesis for adult mouse DRG neurons (Fig. 3.2). Furthermore, in previous *in vivo* studies, local intrathecal infusion of CXCL12 into a rat spinal cord dorsal hemisection model promoted sprouting of the lesioned corticospinal tract (Opatz et al., 2009) and improved neuronal recovery after spinal cord contusion in rats (Zendedel et al., 2012). In order to confirm the CXCL12 mediated neurite outgrowth and the locomotor recovery in a mouse *in vivo* model of traumatic spinal cord injury, CXCL12 was intrathecally infused in the lesioned spinal cord using the technique described above. Since the chemokine CXCL12 needs BSA as a carrier protein, a BSA/PBS group was included in this study as individual control group. To exclude the beneficial effects of BSA, previously seen in a study of our lab (König, 2014), also a PBS control group lacking addition of BSA was included. In contrast to the rat data published by Opatz et al. (2009), the infusion of CXCL12 into the mouse spinal cord did not promote rostral sprouting of lesioned CST fibers compared to both control groups (Fig. 3.7). Although there was a slight trend in the CXCL12 treatment group in increased sprouting, this was, however, not significant. These results are in line with the locomotor data, which do not show any improvement in functional behavior after CXCL12 infusion compared to the control group (Fig. 3.8). The BMS scores of the CXCL12 treated animals were always higher starting from the 7th to the 35th day post injury, and a slight tendency into a faster recovery was observed within the CXCL12 treated group after the shock phase, but no statistically significant differences were observed in comparison to the control group. Indeed, starting from the 7th till the 35th day post injury, CXCL12 treated animals recovered faster in relation to day 1 post injury than control animals. This was not the case in the PBS control group.

Comparing several studies previously performed, where CXCL12 was intrathecally infused into lesioned spinal cords of rats, a crucial variable issue was the concentration used for the reagents CXCL12 and BSA. Indeed, the lyophilized CXCL12 used in some studies contained already 50µg BSA per 1 µg CXCL12, which must be considered in the calculation of the vehicle control (Opatz et al., 2009; (König, 2014). Opatz et al., (2009) observed an increase in the sprouting of lesioned CST fibers after local intrathecal CXCL12 infusion. However, the vehicle control did not include the same amount of BSA as the treatment group, but contained 50 times less BSA, which, therefore, cannot be considered an appropriate control. In addition, even though an increase in rostral sprouting was described by Opatz et al., (2009), there was no functional improvement in the locomotor open field test BBB (Schiwy, 2010). Furthermore, a PBS only control group was missing in the respective study. In a further study (König, 2014), the CXCL12 sprouting treatment was combined with deferoxamine mesylate (DFO), an anti-scarring treatment in lesioned rats. Also in this case, the outcome of the locomotor open field test was not statistically different from the CXCL12-only treated group and no improvement was observed. The CXCL12 promoting effects on sprouting were not analysed here, however an optimal vehicle control and a PBS-only control group were used. The most surprising finding in Brigitte König`s study (2014) was, that, compared to the PBS control group, the local intrathecal infusion of BSA alone induced significant functional recovery using two locomotor tests, the horizontal ladder walking test and the CatWalk gait analysis test.

A beneficial effect of BSA in spinal cord injury was first described by Cain et al. (2007) and then by Avila-Martin et al. (2011), who both described locomotor improvement and neuroprotective properties of albumin. This phenomenon was not seen in the present study although the double concentration of BSA was used here as compared to the concentration used previously (König, 2014). To avoid degradation or loss of a certain protein due to binding to the storage tube, it is a common practice to add a carrier protein, such as BSA to 0.1-0.5 % (50 µg BSA per 1 µg CXCL12 as recommended on the datasheet) to the protein solution. In this study, the CXCL12 was dissolved in 1 % BSA. The probability that some of the chemokine substance might adhere to the wall of the osmotic minipump and of the intrathecal catheter was also taken into account here and, therefore, a higher carrier/chemokine ratio was chosen. Zendedel et al. (2012) also dissolved the CXCL12 in a 1 % BSA solution. By evaluating behavioral scores and histopathological changes, they could demonstrate that CXCL12 improves neural recovery after spinal cord contusion in rats, which is contradictory to the findings observed in this work. They observed that the functional recovery in the BBB open field test was less distinct in a high CXCL12 concentration (1000 ng/ml) group compared to an intermediate CXCL12 concentration (500 ng/ml) group. The authors explained the impaired functional recovery by an increased astrocytosis in CXCL12 high dose treated animals compared to CXCL12 intermediate dose treated animals, speculating that high CXCL12 concentrations may boost anti-regenerative effects of astrocytes. Furthermore, they assumed that receptor desensitization could also play a mechanistic role. In this thesis, and in earlier studies in our lab (Opatz et al., 2009; (König, 2014), an 80 times higher CXCL12 concentration was used compared to the highest one used in the Zendedel et al. study. Although, Zendedel and colleagues investigated the functional recovery after CXCL12 infusion in spinal cord injured rats and described significant histopathological changes in the spinal cord in presence and absence of CXCL12, they did not correlate the behavioral scores and the other outcomes to collateral sprouting events. In fact, the impact of CXCL12 on functional recovery was described in their work as a reduction of apoptosis, boosting of astroglia and microglia response and induced angiogenesis upon CXCL12 treatment (Zendedel et al., 2012). In a subsequent publication, the group of Zendedel additionally showed that after SCI the inflammasome is activated at the injury site and that CXCL12 mediated neuroprotection could depend on the attenuation of the inflammasome complex (Zendedel et al., 2016).

Recently, another combinatorial approach was applied, where ChABC, an enzyme that degrades inhibitory components of the glial scar, was combined with CXCL12 to recruit endogenous neural precursor cells to the injury site and to improve their survival and distribution within the tissue (Pakulska et al., 2017). However, the effects seen in tissue and the functional repair were attributed to ChABC treatment. CXCL12 alone did not improve behavioral recovery after SCI. In fact, they claimed, that the clinically relevant compression injury model they used was not appropriate and that a different SCI model may be required to elucidate the effect of CXCL12 on nerve regeneration. Furthermore, they used an alternative strategy to deliver the chemokine to the injury site, which was based on affinity and electrostatic interactions. Polymeric nanoparticles embedded in a crosslinked methylcellulose hydrogel delivered the CXCL12 at the injury site. However, although the delivery system was minimally invasive, localized and controlled, the authors recommend an optimization of the delivery of the chemokine, implicating that changes in the CXCL12 concentration could have a different impact on the results. This study elucidates the importance of the fine settings for each planned experiment. Nevertheless, it is not possible to compare the amount of CXCL12 used by Pakulska et al. with the amount used in this study. Since

Zendedel used a lower CXCL12 concentration and additionally a very low administration rate of the chemokine at the lesion site with a flow rate of only 0.25 µl/h, an optimization of CXCL12 concentration and a longer chemokine incubation period of 28 days should be also taken into account for further investigations.

4.2.3 CXCR4 is not expressed in the dorsal corticospinal tract of mice and rats, hence other mechanisms rather than direct ligand-receptor interactions are responsible for neurite sprouting in the rat CNS.

In contrast to the previous *in vivo* study published by Opatz and colleagues (2009), where CXCL12 promoted sprouting of the dCST in rats but no improvement in locomotor function was shown (Schiwy, 2010) in the present study CXCL12 did not promote sprouting of the lesioned mouse dCST (Fig. 3.7) and comparably no improvement in locomotor function was assessed (Fig 3.8). As mentioned above and according to the hypothesis of Zendedel, the high CXCL12 concentration used in the experiments rather impaired than promoted beneficial effects. Due to the described presence of the CXCR4 and CXCR7 receptors on the dCST axons of rat spinal cords in the paper of Opatz et al. (2009), a direct interaction of CXCL12 with its neuronal receptors was suggested to be responsible for the axonal sprouting. Therefore, possible differences between the rat and mouse species in the expression of the chemokine receptor CXCR4 on the spinal cord were investigated. Since the CXCR4 antibody used previously (Opatz et al., 2009) was reported to bind less specifically (Fischer et al., 2008), a knockout validated CXCR4 antibody (UMB-2) was used in the present study. In mouse spinal cord, CXCR4 specific signal was absent in the dCST tract where the motor descending tract is located (Fig. 3.9). In contrast to Opatz et al., 2009, a similar result was also observed in the rat spinal cord, suggesting that the sprouting seen after CXCL12 infusion in rats, if mediated by CXCL12 and not through excess BSA, is activated by indirect axon-growth promoting mechanism of neuronal or non-neuronal cells rather than by a direct interaction with axonal CXCR4. In the paper of Tysseling et al. (2011) CXCL12-EGFP and CXCR4-EGFP transgenic reporter mice were used to examine the expression and function of CXCL12 and its receptor in the spinal cord of adult mice (Tysseling et al., 2011). They showed that the ligand itself, CXCL12 was expressed throughout the dCST and in the meninges, whereas in accordance to our finding, the CXCR4 receptor was absent in the dCST and was only found in the ependymal cells surrounding the central canal. These findings are in line with previous reports showing CXCL12 expression in several neuronal populations, importantly, in the layer V neurons of the cortex, the meninges and in endothelial but not glial cells (Schonemeier et al., 2008a; Stumm et al., 2007; Stumm et al., 2002; Tham et al., 2001). Also in the *in situ* study described in the present thesis, CXCL12 mRNA was found to be expressed in the pyramidal neurons of layer V of rats and mouse brains consistent with the previously published data (Fig. 3.23-3.26). CXCR4, on the other hand, was expressed in the ependymal cell layer, which was also in accordance to previous studies (Fig. 3.9) (Tysseling et al., 2011). These cells, which constitute the endogenous stem cell pool, are of great importance, since they give rise to all neuronal and macroglial cells (astroglia and oligodendroglia) in the spinal cord (Saker et al., 2016). CXCL12 is known as the major effector of endogenous neural precursor cell migration after SCI and these cells could play a significant role in spinal cord repair after SCI (Jaerve et al., 2012). Furthermore, CXCR4 mRNA was described to be present in GABAergic interneurons and absent in glutamatergic pyramidal neurons both in rats and in mice (Stumm et al., 2007; Stumm et al., 2003; Tiveron et al., 2006).

These finding are also in line with the immunofluorescence results of this thesis, as the absence of CXCR4 protein expression in the dCST, which contains the axonal projections of the pyramidal layer V neurons of the sensorimotor cortex was observed (Fig. 3.9). Additionally, these results were comparable with the *in situ* hybridization findings. Here, the pyramidal neurons in layer V of the hind limb region in the sensorimotor cortex did not express the chemokine receptor CXCR4 (Fig. 3.23-3.26). Only a few cells, most likely interneurons, in layers II/III and VI were positively stained for CXCR4. Indeed, in the present study only a subset (25 %) of the embryonic mouse cerebral cortical neurons plated on dishes for the *in vitro* validation of the CXCR4-UMB2 antibody were shown to express the chemokine receptor CXCR4. This result fits with the estimation that cortical neurons consist of approximately 80 % glutamatergic principal neurons and 20 % GABAergic interneurons (Abe et al., 2015; Parnavelas, 2000) and confirms the absence of the CXCR4 receptor in pyramidal neurons. Although CXCR4 was not expressed in the dCST of the mouse and rat spinal cord, CXCR4 immunofluorescence staining co-labeled with neuronal markers such as Tuj1, PAM311-NP and PAM312-P in the dorsal, lateral and ventral funiculus of the mouse and rat spinal cord (Fig. 3.10 – 3.12 and Fig.3.14 – 3.3.16). Furthermore, CXCR4 was expressed in a subtype of neurons, such as spinal motoneurons, but not in CGRP-positive sensory neurons (Fig. 3.13 and Fig. 3.17). CXCR4 was also expressed in glial cells including oligodendrocytes but not in astrocytes (Fig. 3.18 – 3.21). These latter findings are in accordance to previous studies (Lieberam et al., 2005; Opatz et al., 2009; Stumm et al., 2002; Tysseling et al., 2011). Therefore, in contradiction to the assumption of Opatz et al. (2009), it is postulated here that sprouting of the dCST in rats after CXCL12 infusion is not promoted by a direct interaction of CXCL12 with CXCR4, but is rather an indirect axon-growth promoting effect mediated by neuronal and/or non-neuronal cells. Moreover, the CXCL12 receptor CXCR4 is highly expressed in brain regions that are associated with adult neurogenesis, but during development the CXCR4 expression decreases progressively (Schonemeier et al., 2008a; Tissir et al., 2004). Due to the large number of unspecific antibodies and/or *in situ* probes that were developed during the last decades, in the literature controversial interpretations are common regarding where and by which cell types the CXCL12 chemokine receptor is expressed. The carefully determined expression pattern of CXCR4 in the present thesis are in accordance with the previous report, where the same knockout validated antibody and the same *in situ* probes were used (Stumm et al.) as well as in accordance with a previous study, where CXCL12 and chemokine receptor transgenic reporter mice were used (Tysseling et al., 2011).

Another important issue, which is often discussed in several reports, is the involvement of CXCL12 and its receptors after injury. The cell-recruitment via CXCL12/CXCR4 signaling is an important element in regulating spinal cord responses to injury (Sanchez-Martín et al., 2011; Tysseling et al., 2011). To investigate if CXCR4 expression is increased after SCI specifically either in the dCST or in the layer V of the cerebral cortex of adult mouse and rat brains, the expression of CXCR4 was semi-quantified on the protein level using immunofluorescence stainings, and on mRNA level using the *in situ* hybridization, respectively. CXCR4 protein expression was not increased after spinal cord injury in the dCST (Fig. 3.22) and CXCR4 mRNA was also not altered in the brain sections (Fig. 3.23-3.26). The CXCL12 and CXCR7 mRNA expression was also not increased in brain sections upon spinal cord injury (Fig. 3.23-3.26). These results are consistent with a previous study performed in our group, where cortical gene expression in sham operated animals and injured animals revealed no increase in CXCL12 or CXCR4 gene expression (Kruse et al., 2011). In the present thesis, the immunofluorescence analysis was performed on rostrally

harvested spinal cord samples five weeks after SCI. The same was done in the paper of Tysseling et al., where the author described no changes in the expression pattern of CXCL12 rostral to the lesion, but, in contrast, found a dramatical change in CXCR4 expression after SCI, mainly due to infiltrating macrophages (Tysseling et al., 2011). In the present thesis, the increase of CXCR4 expression in the spinal cord was not observed, but it could be that the rostral position of investigation in the study of Tysseling et al. (2011) was not identical but far more rostral to the lesion site. However, the lesion in the spinal cord did not increase the mRNA expression of CXCL12, CXCR4 or CXCR7 in the pyramidal neurons of the hind limb region of the sensorimotor cortex of mice and rats. In contrast, CXCL12 was reported to be upregulated in the brain in response to cerebral ischemia in the penumbra of the lesion site and to be associated with blood vessels (Hill et al., 2004; Miller et al., 2005; Schonemeier et al., 2008b; Stumm et al., 2002). CXCR4 mRNA upregulation was observed in the border zone and in the ischemic core associated with peripheral blood cells, including macrophages, which are positive for CXCR4 in contrast to resident CXCR4-negative microglial cells (Stumm et al., 2002) and bone-marrow-derived cells.
The role of the CXCL12/CXCR4 axis following spinal cord injury remains unclear but CXCL12 seems to play an important role in cell recruitment to injured tissue and, as such, the chemokine can be used to find novel therapeutic strategies to enhance repair of injured nerves. In fact, a recent publication observed neural recovery after intrathecal CXCL12 infusion in a rat spinal cord injury model. The authors suggested that the functional recovery after spinal cord contusion in rats correlates with a reduction of apoptosis, boosting of astroglia and microglia response, induced angiogenesis and attenuation of the inflammasome complex (Zendedel et al., 2016; Zendedel et al., 2012). Furthermore, the authors explain that an extensive CXCL12 concentration may boost anti-regenerative effects and therefore impair functional recovery. Unfortunately, the authors did not correlate the functional recovery to collateral sprouting events and in their study the histopathological aspect is missing to be able to compare both studies. However, it is worth taking into consideration that the site of analysis is very important for the data interpretation, and additionally slight variations in lesion site, sex, age, species, methodology etc. could change the whole outcome of the experiment. Furthermore, the presence of the second CXCL12 receptor, CXCR7 cannot be excluded. In contrast to CXCR4, CXCR7 mRNA is upregulated during postnatal development. It is expressed in cortical layer V neurons, in cortical interneurons and in the hippocampus, in astrocytes, meningeal cells and endothelial cells of brain blood vessels, resembling the expression pattern of CXCL12 (Schonemeier et al., 2008a; Shimizu et al., 2011; Tissir et al., 2004). The presence of the receptor in the cortical layer V neurons was also confirmed by the *in situ* analysis in the present study (Fig. 3.23-3.26). At present, there are no specific antibodies commercially available, which can be reliably used for CXCR7 receptor expression and function analysis. Therefore, due to lack of information regarding CXCR7 expression, the ambiguity remains, whether CXCR7 is involved in CXCL12 signaling and required for the widespread effects of CXCL12 (Schonemeier et al., 2008b).
In conclusion, according to the present findings observed in mice, the generation of a dCST receptor conditional knockout mouse was not considered to be reasonable any more. The CXCR4 receptor is not expressed in the dCST of control animals and its expression is not increased after spinal cord injury. However, the CXCR7 receptor was found to be expressed in the layer V neurons of the sensorimotor cortex and further analyses will reveal the importance of this chemokine receptor.

5. CONCLUSION AND FURTHER CONSIDERATION

In contrast to the PNS where spontaneous axonal regeneration occurs following injury, axons of the CNS do not regenerate easily and the axons stop growing when they reach the lesion site. This results in the failure of CNS neurons to re-innervate their original targets. The lack of regeneration of CNS neurons is attributed to, *inter alia*, the suppression of axonal outgrowth by inhibitory molecules present in the environment, such as inhibitory factors associated with the myelin in CNS, and inhibitory factors of the glial scar at the injury site. Moreover, the insufficient intrinsic neuronal capacity to start a regeneration program after lesion is another important limiting factor for CNS regeneration *in vivo*. Furthermore, barriers for axonal regeneration are the lack of growth support as well as an increase in apoptotic cell death. The chemotactic cytokine CXCL12 was shown to fulfill a therapeutic aim of researchers: the stimulation of the regenerative axon growth of lesioned spinal cord axons. In the present thesis the molecular mechanisms underlying the failure of axonal regeneration in the CNS and particularly the functional role of the chemokine CXCL12 and its receptors in axonal regeneration after spinal cord injury was characterized. It was found that DRG neurons displayed a reduced outgrowth performance on a surface coated with CNS myelin. This effect was reverted and growth was restored following application of the chemokine CXCL12. Thus, CXCL12 exerts disinhibitory effects by reducing the sensitivity of axonal growth cones towards CNS myelin. The inhibition of the CXCR4 receptor with an antagonist led to a partial albeit not complete abrogation of CXCL12 mediated neurite outgrowth promotion. Although CXCR4 receptor expression on adult DRG neurons was confirmed, the involvement of an additional signal transduction pathway activated by CXCL12, e.g., through the second CXCL12 receptor CXCR7, cannot be completely excluded. Due to the lack of commercially available, functional antibodies against CXCR7, the involvement of CXCR7 was not further investigated. Furthermore, both the rather small sample size and the high CXCL12 concentration used in the cell culture experiments could also have influenced the results. To test the CXCL12 mediated disinhibitory effects *in vivo* a novel spinal intrathecal catheterization method for mouse spinal cord injury models, which allows unrestricted local drug infusion and avoids catheter induced spinal cord compression for reliable conclusions about the treatment efficacy, was established. Furthermore, an experimental mouse spinal cord injury model as well as the anterograde labeling of the dCST using an AAV2-Cre transduction method were established. It was found that the intrathecally infused CXCL12 did not stimulate rostral neurite outgrowth of the injured dCST

of wildtype mice. Consistent with these results the locomotor function was not improved after SCI and local intrathecal infusion of CXCL12. However, the recovery rate was slightly faster in CXCL12 treated mice in comparison to the control mice. In the case of the *in vivo* experiments, the sample size should also be increased in further experiments to strengthen the results. Due to these results, the generation of CXCL12 receptor conditional knockout mice was no longer required. Immunofluorescence analysis of spinal cord sections with highly specific antibody UMB-2 revealed that the CXCR4 receptor was not expressed in the mouse and rat dCST, hence suggesting that other mechanisms, rather than direct interactions, are responsible for neurite sprouting in the rat spinal cord. Additionally, *in situ* hybridization studies confirmed the absence of the CXCR4 receptor transcript in the pyramidal corticospinal neurons in layer V of the sensorimotor cortex in control and in injured mice and rats. In contrast, *in situ* hybridization of the CXCR7 receptor was expressed in layer V cortical neurons, resembling the expression pattern of CXCL12. However, the uncertainty remains whether CXCR7 is involved in CXCL12 signaling and required for a least some of the widespread effects of CXCL12. Dispersed cell culture generally destroys the cyto-architecture of the associated neuronal circuits whereas *in vivo* studies preserve the integrity of the glial and neuronal counterparts. Therefore, it could be plausible that CXCL12 may promote neurite outgrowth and act disinhibitory in *in vitro* cultures grown on myelin coated plates, while *in vivo* it does not. For future studies, an appropriate CXCL12 concentration combined with a dorsal spinal cord hemisection, a mouse intrathecal-catheterization method for CXCL12 infusion and a higher number of animals to improve the power should be considered for histopathological analysis, functional recovery and sprouting events. In conclusion, with respect to the diversity of molecular and functional properties of CXCL12, CXCR4 and CXCR7, targeting this system could serve as a possible means of therapeutic intervention, although – according to the results presented here - it does not seem to act via direct interaction, but rather seems to be based on indirect neuroprotection effects.

ABBREVIATIONS

5-HT	serotonin (5-hydroxytryptamine)
AAV2	adeno-associated virus of serotype 2
ACKR3	atypical chemokine receptor 3
ACM	astrocytes conditioned medium
aq. bidest.	aqua bidestillata
AMD3100	Octahydrochloride hydrate
ANOVA	analysis of variance
ASIA	American Spinal Injury Association
BBB	open filed Basso, Beattie and Bresnahan locomotor test
BDNF	brain-derived neurotrophic factor
BMS	Basso Mouse Scale
BPY-DCA	2,2`-bipyridine-5,5`-dicarboxylic acid
BSA	Bovine Serum Albumin
Ca^{2+}	calcium
cAMP	cyclic adenoside monophosphate
cc	central canal
cAMP	Cyclic adenosine monophosphate
cDNA	complementary deoxyribonucleic acid
CGRP	Calcitonin gene-related peptide
ChABC	chondroitinase ABC
CMV	Human cytomegalovirus promotor
CNS	central nervous system
CO_2	Carbon dioxide
Cre	Cre-Recombinase
CSF	cerebrospinal fluid
CSPG	chondroitin sulfate proteoglycan
CST	corticospinal tract
C-terminus	Carboxy terminus
Ctip2/Bcl11b	B-Cell CLL/Lymphoma 11B, transcription factor
CXCR4	C-X-C chemokine receptor type 4
CXCR7	C-X-C chemokine receptor type 7
CXCL12	C-X-C chemokine ligand 12
DAG	Diacylclycerol
DAPI	4‘,6-Diamidino-2-phenylindole
DFO	Deferoxamine mesylate
dk	donkey
DMEM	Dulbecco’s modified eagle medium
DNA	Deoxyribonucleic acid
DPX	xylol-containing mounting fluid

DRG	dorsal root ganglion
DS	donkey serum
ECM	extracellular matrix
EDTA	Ethylenediaminetetraacetic acid
ERK	Extracellular-signal regulated kinases
EtOH	ethanol
FBS	Fetal bovine serum
FCS	fetal calf serum
Fezf2	forebrain embryonic zinc finger protein, transcription factor
fl	floxed
GDNF	glial cell-derived neurotrophic factor
GDP	Guanosine diphosphate
GFAP	glial fibrillary acidic protein, astrocyte marker
GPCR	G-protein-coupled receptor
GRK	GPCR kinase
gt	goat
GTP	Guanosine-5‘-triphosphate
HA	Hemagglutinin
HCl	hydrochloric acid
HIV	human immunodeficiency virus
IP3	Inositol 1, 4, 5 triphosphate
LANUV	state office of environmental and consumer protection
LESTR	Leukocyte-expressed seven transmembrane-domain receptor
MAG, NOGO, OMgp, Sema4D	myelin-associated inhibitors
MAPK	Mitogen-activated protein kinases
MBP	myelin basic protein
MCS	multiple cloning site
MeOH	methanol
mRNA	Messenger Ribonucleic acid
ms	mouse
Na2HPO4	di-sodium hydrogen phosphate anhydrous
NaCl	sodium chloride
NaH2PO4 x H20	sodium di-hydrogen phosphate monohydrate
NaOH	sodium hydroxide solution
NGS	Normal goat serum
NT	neurotrophin
N-terminus	amino terminus
NO_2	nitrous oxide
NRW	North-Rhine Westfalia
O_2	oxygen
PB	phosphate buffer
PBS	phosphate buffered saline
PE	polyethylene
PFA	paraformaldehyde
PI3K	Phosphatidylinositol-4,5-bisphosphate 3-kinase
PIP2	Phosphatidylinositol 4,5-biphosphate
PKC	Protein kinase C
PLC	Phospholipase C
PNS	peripheral nervous system
PCR	polymerase chain reaction
PU	polyurethane
RAG	regeneration-associated gene
rb	rabbit
ReST	reticulospinal tract

RGC	retinal ganglion cell
rpm	revolutions per minute
RST	rubrospinal tract
RT	room temperature
SCI	spinal cord Injury
Sox5	transcription factor
SDF-1α	stromal cell-derived growth factor-1 alpha
SEM	standard error of the mean
s.c.	subcutan
TH	tyrosine hydroxylase
v	ventral
VeST	vestibulospinal tract
vs.	versus
v/v	volume per volume
Wt	wildtype
ZETT	Zentrale Einrichtung für Tierversuche und Tierschutzaufgaben

UNITS

%	percent
°C	degree Celsius
cm	centimeter
g	gram
h	hour
kDa	kilodalton
kg	kilogram
M	molar
min	minute
µl	microliter
µm	micrometer
mg	milligram
ml	milliliter
mm	millimeter
mM	millimolar
sec	second

BIBLIOGRAPHY

Abe, P., Molnar, Z., Tzeng, Y.S., Lai, D.M., Arnold, S.J., and Stumm, R. (2015). Intermediate Progenitors Facilitate Intracortical Progression of Thalamocortical Axons and Interneurons through CXCL12 Chemokine Signaling. J Neurosci 35, 13053-13063.

Aguayo, A.J., David, S., and Bray, G.M. (1981). Influences of the glial environment on the elongation of axons after injury: transplantation studies in adult rodents. J Exp Biol 95.

Ahmed, Z., Mazibrada, G., Seabright, R.J., Dent, R.G., Berry, M., and Logan, A. (2006). TACE-induced cleavage of NgR and p75NTR in dorsal root ganglion cultures disinhibits outgrowth and promotes branching of neurites in the presence of inhibitory CNS myelin. FASEB journal : official publication of the Federation of American Societies for Experimental Biology 20, 1939-1941.

Aiuti, A., Webb, I.J., Bleul, C., Springer, T., and Gutierrez-Ramos, J.C. (1997). The chemokine SDF-1 is a chemoattractant for human CD34+ hematopoietic progenitor cells and provides a new mechanism to explain the mobilization of CD34+ progenitors to peripheral blood. The Journal of experimental medicine 185, 111-120.

Alstermark, B., Ogawa, J., and Isa, T. (2004). Lack of monosynaptic corticomotoneuronal EPSPs in rats: disynaptic EPSPs mediated via reticulospinal neurons and polysynaptic EPSPs via segmental interneurons. J Neurophysiol 91, 1832-1839.

Arakawa, Y., Bito, H., Furuyashiki, T., Tsuji, T., Takemoto-Kimura, S., Kimura, K., Nozaki, K., Hashimoto, N., and Narumiya, S. (2003). Control of axon elongation via an SDF-1alpha/Rho/mDia pathway in cultured cerebellar granule neurons. J Cell Biol 161, 381-391.

Arimont, M., Sun, S., Leurs, R., Smit, M., De Esch, I.J., and de Graaf, C. (2017). Structural Analysis of Chemokine Receptor-Ligand Interactions. J Med Chem.

Arlotta, P., Molyneaux, B.J., Chen, J., Inoue, J., Kominami, R., and Macklis, J.D. (2005). Neuronal subtype-specific genes that control corticospinal motor neuron development in vivo. Neuron 45, 207-221.

Asher, R.A., Morgenstern, D.A., Fidler, P.S., Adcock, K.H., Oohira, A., Braistead, J.E., Levine, J.M., Margolis, R.U., Rogers, J.H., and Fawcett, J.W. (2000). Neurocan is upregulated in injured brain and in cytokine-treated astrocytes. J Neurosci 20, 2427–2438.

Avila-Martin, G., Galan-Arriero, I., Gomez-Soriano, J., and Taylor, J. (2011). Treatment of rat spinal cord injury with the neurotrophic factor albumin-oleic acid: translational application for paralysis, spasticity and pain. PLoS One 6, e26107.

Bachelerie, F., Ben-Baruch, A., Burkhardt, A.M., Combadiere, C., Farber, J.M., Graham, G.J., Horuk, R., Sparre-Ulrich, A.H., Locati, M., Luster, A.D., et al. (2014). International Union of Basic and Clinical Pharmacology. [corrected]. LXXXIX. Update on the extended family of chemokine receptors and introducing a new nomenclature for atypical chemokine receptors. Pharmacol Rev 66, 1-79.

Baek, R.C., Broekman, M.L., Leroy, S.G., Tierney, L.A., Sandberg, M.A., d'Azzo, A., Seyfried, T.N., and Sena-Esteves, M. (2010). AAV-mediated gene delivery in adult GM1-gangliosidosis mice corrects lysosomal storage in CNS and improves survival. PLoS One 5, e13468.

Baggiolini, M., Dewald, B., and Moser, B. (1997). Human chemokines: an update. Annu Rev Immunol 15, 675-705.

Bähr, M., and Przyrembel, C. (1995). Myelin from peripheral and central nervous system is a nonpermissive substrate for retinal ganglion cell axons. Exp Neurol 134, 87-93.

Bajetto, A., Bonavia, R., Barbero, S., and Schettini, G. (2002). Characterization of chemokines and their receptors in the central nervous system: physiopathological implications. J Neurochem 82, 1311-1329.

Balabanian, K., Lagane, B., Infantino, S., Chow, K.Y., Harriague, J., Moepps, B., Arenzana-Seisdedos, F., Thelen, M., and Bachelerie, F. (2005). The chemokine SDF-1/CXCL12 binds to and signals through the orphan receptor RDC1 in T lymphocytes. J Biol Chem 280, 35760-35766.

Bancroft, J.D., Stevens, A., and Turner, D.R. (1996). „Theory and practice of histological techniques.“ 4 ed ed Churchill Livingstone, New York [ua].

Banisadr, G., Fontanges, P., Haour, F., Kitabgi, P., Rostene, W., and Melik Parsadaniantz, S. (2002). Neuroanatomical distribution of CXCR4 in adult rat brain and its localization in cholinergic and dopaminergic neurons. European Journal of Neuroscience 16, 1661-1671.

Bareyre, F.M., Kerschensteiner, M., Raineteau, O., Mettenleiter, T.C., Weinmann, O., and Schwab, M.E. (2004). The injured spinal cord spontaneously forms a new intraspinal circuit in adult rats. Nat Neurosci 7, 269-277.

Bareyre, F.M., and Schwab, M.E. (2003). Inflammation, degeneration and regeneration in the injured spinal cord: insights from DNA microarrays. Trends in neurosciences 26, 555-563.

Barritt, A.W., Davies, M., Marchand, F., Hartley, R., Grist, J., Yip, P., McMahon, S.B., and Bradbury, E.J. (2006). Chondroitinase ABC promotes sprouting of intact and injured spinal systems after spinal cord injury. J Neurosci 26, 10856-10867.

Basso, D.M., Beattie, M.S., and Bresnahan, J.C. (1995). A Sensitive and Reliable Locomotor Rating Scale for Open Field Testing in Rats. Journal of Neurotrauma 12, 1-21.

Basso, D.M., Fisher, L.C., Anderson, A.J., Jakeman, L.B., McTigue, D.M., and Popovich, P.G. (2006). Basso Mouse Scale for Locomotion Detects Differences in Recovery after Spinal Cord Injury in Five Common Mouse Strains. Journal of Neurotrauma 23, 635-659.

Benfey, M., and Aguayo, A.J. (1982). Extensive elongation of axons from rat brain into peripheral nerve grafts. Nature 1982, 150-152.

Benson, M.D., Romero, M.I., Lush, M.E., Lu, Q.R., Henkemeyer, M., and Parada, L.F. (2005). Ephrin-B3 is a myelin-based inhibitor of neurite outgrowth. Proceedings of the National Academy of Sciences of the United States of America 102, 10694-10699.

Berahovich, R.D., Penfold, M.E., and Schall, T.J. (2010). Nonspecific CXCR7 antibodies. Immunol Lett 133, 112-114.

Bernhagen, J., Krohn, R., Lue, H., Gregory, J.L., Zernecke, A., Koenen, R.R., Dewor, M., Georgiev, I., Schober, A., Leng, L., et al. (2007). MIF is a noncognate ligand of CXC chemokine receptors in inflammatory and atherogenic cell recruitment. Nat Med 13, 587-596.

Bickenbach, J., Bodine, C., Brown, D., Burns, A., Campbell, R., Cardenas, D., Charlifue, S., Chen, Y., Gray, D., Li, L., et al. (2013). International Perspectives on Spinal Cord Injury. World Health Organization (WHO) and the International Spinal Cord Society (ISCoS).

Blesch, A., and Tuszynski, M.H. (2003). Cellular GDNF delivery promotes growth of motor and dorsal column sensory axons after partial and complete spinal cord transections and induces remyelination. The Journal of comparative neurology 467, 403-417.

Bleul, C.C., Farzan, M., Choe, H., Parolin, C., Clark-Lewis, I., Sodroski, J., and Springer, T.A. (1996). The lymphocyte chemoattractant SDF-1 is a ligand for LESTR/fusin and blocks HIV-1 entry. Nature 382, 829-833.

Blight, A.R. (1983). Cellular morphology of chronic spinal cord injury in the cat: analysis of myelinated axons by line-sampling. Neuroscience 10, 521–543.

Bomze, H.M., Bulsara, K.R., Iskandar, B.J., Caroni, P., and Skene, J.H. (2001). Spinal axon regeneration evoked by replacing two growth cone proteins in adult neurons. Nat Neurosci 4, 38-43.

Borgens, R.B., Blight, A.R., and McGinnis, M.E. (1987). Behavioral recovery induced by applied electric fields after spinal cord hemisection in guinea pig. Science 238, 366-369.

Borgens, R.B., and Bohnert, D.M. (1997). The responses of mammalian spinal axons to an applied DC voltage gradient. Exp Neurol 145, 376-389.

Bosse, F. (2012). Extrinsic cellular and molecular mediators of peripheral axonal regeneration. Cell and tissue research 349, 5-14.

Bradbury, E.J., and McMahon, S.B. (2006). Spinal cord repair strategies: why do they work? Nature reviews Neuroscience 7, 644-653.

Bradbury, E.J., Moon, L.D., Popat, R.J., King, V.R., Bennett, G.S., Patel, P.N., Fawcett, J.W., and McMahon, S.B. (2002). Chondroitinase ABC promotes functional recovery after spinal cord injury. Nature 416, 636-640.

Brazda, N., Estrada, V., Voss, C., Seide, K., Trieu, H.K., and Muller, H.W. (2016). Experimental Strategies to Bridge Large Tissue Gaps in the Injured Spinal Cord after Acute and Chronic Lesion. Journal of visualized experiments : JoVE, e53331.

Brazda, N., and Müller, H.W. (2009). Pharmacological modification of the extracellular matrix to promote regeneration of the injured brain and spinal cord. Prog Brain Res 175, 269-281.

Brazda, N., Voss, C., Estrada, V., Lodin, H., Weinrich, N., Seide, K., Muller, J., and Muller, H.W. (2013). A mechanical microconnector system for restoration of tissue continuity and long-term drug application into the injured spinal cord. Biomaterials 34, 10056-10064.

Brelot, A., Heveker, N., Montes, M., and Alizon, M. (2000). Identification of residues of CXCR4 critical for human immunodeficiency virus coreceptor and chemokine receptor activities. J Biol Chem 275, 23736-23744.

Buchli, A.D., and Schwab, M.E. (2005). Inhibition of Nogo: a key strategy to increase regeneration, plasticity and functional recovery of the lesioned central nervous system. Annals of medicine 37, 556-567.

Bunge, M.B. (2001). Bridging areas of injury in the spinal cord. Neuroscientist 7, 325-339.

Büngner, O.v. (1891). Über die Degenerations- und Regenerationsvorgänge am Nerven nach Verletzungen. Beitr Pathol Anat 10, 321-387.

Burchiel, K.J., and Hsu, F.P.K. (2001). Pain and Spasticity After Spinal Cord Injury: Mechanisms and Treatment. Spine (Phila Pa 1976) 26 (24 Suppl), 146-160.

Burns, J.M., Summers, B.C., Wang, Y., Melikian, A., Berahovich, R., Miao, Z., Penfold, M.E., Sunshine, M.J., Littman, D.R., Kuo, C.J., et al. (2006). A novel chemokine receptor for SDF-1 and I-TAC involved in cell survival, cell adhesion, and tumor development. J Exp Med 203, 2201-2213.

Busch, S.A., and Silver, J. (2007). The role of extracellular matrix in CNS regeneration. Current opinion in neurobiology 17, 120-127.

Busillo, J.M., Armando, S., Sengupta, R., Meucci, O., Bouvier, M., and Benovic, J.L. (2010). Site-specific phosphorylation of CXCR4 is dynamically regulated by multiple kinases and results in differential modulation of CXCR4 signaling. J Biol Chem 285, 7805-7817.

Busillo, J.M., and Benovic, J.L. (2007). Regulation of CXCR4 signaling. Biochim Biophys Acta 1768, 952-963.

Cai, D., Deng, K., Mellado, W., Lee, J., Ratan, R.R., and Filbin, M.T. (2002). Arginase I and Polyamines Act Downstream from Cyclic AMP in Overcoming Inhibition of Axonal Growth MAG and Myelin In Vitro. Neuron 35, 711-719.

Cai, D., Qiu, J., Cao, Z., McAtee, M., Bregman, B.S., and Filbin, M.T. (2001). Neuronal Cyclic AMP Controls the Developmental Loss in Ability of Axons to Regenerate. The Journal of Neuroscience 21, 4731–4739.

Cai, S.H., Tan, Y., Ren, X.D., Li, X.H., Cai, S.X., and Du, J. (2004). Loss of C-terminal α-helix decreased SDF-1α-mediated signaling and chemotaxis without influencing CXCR4 internalization. Acta Pharmacol Sin 25, 152-160.

Cain, L.D., Nie, L., Hughes, M.G., Johnson, K., Echetebu, C., Xu, G.Y., Hulsebosch, C.E., and McAdoo, D.J. (2007). Serum albumin improves recovery from spinal cord injury. Journal of neuroscience research 85, 1558-1567.

Campbell, S.J., Perry, V.H., Pitossi, F.J., Butchart, A.G., Chertoff, M., Waters, S., Dempster, R., and Anthony, D.C. (2005). Central Nervous System Injury Triggers Hepatic CC and CXC Chemokine Expression that Is Associated with Leukocyte Mobilization and Recruitment to Both the Central Nervous System and the Liver. The American Journal of Pathology 166, 1487-1497.

Capogrosso, M., Milekovic, T., Borton, D., Wagner, F., Moraud, E.M., Mignardot, J.B., Buse, N., Gandar, J., Barraud, Q., Xing, D., et al. (2016). A brain-spine interface alleviating gait deficits after spinal cord injury in primates. Nature 539, 284-288.

Caroni, P., and Schwab, M.E. (1988). Two membrane protein fractions from rat central myelin with inhibitory properties for neurite growth and fibroblast spreading. J Cell Biol 106, 1281-1288.

Caruz, A., Samsom, M., Alonso, J.M., Alcami, J., Baleux, F., Virelizier, J.L., Parmentier, M., and Arenzana-Seisdedos, F. (1998). Genomic organization and promoter characterization of human CXCR4 gene1. FEBS Letters 426, 271-278.

Chalasani, S.H., Sabelko, K.A., Sunshine, M.J., Littman, D.R., and J.A., R. (2003). A Chemokine, SDF-1, Reduces the Effectiveness of Multiple Axonal Repellents and Is Required for Normal Axon Pathfinding. The Journal of Neuroscience 23, 1360-1371.

Chalasani, S.H., Sabol, A., Xu, H., Gyda, M.A., Rasband, K., Granato, M., Chien, C.B., and Raper, J.A. (2007). Stromal cell-derived factor-1 antagonizes slit/robo signaling in vivo. J Neurosci 27, 973-980.

Chen, M.S., Huber, A.B., van der Haar, M.E., Frank, M., Schnell, L., Spillmann, A.A., Christ, F., and Schwab, M.E. (2000). Nogo-A is a myelin-associated neurite outgrowth inhibitor and an antigen for monoclonal antibody IN-1. Nature 403, 434-439.

Chu, P., Saito, H., and Abe, K. (1995). Polyamines promote regeneration of injured axons of cultured rat hippocampal neurons. Brain Research 673, 233-241.

Cohen, A.H., Mackler, S.A., and Selzer, M.E. (1988). Behavioral recovery following spinal transection, functional regeneration in the lamprey CNS. TINS 11, 227-231.

Conta, A.C., and Stelzner, D.J. (2009). The propriospinal system. In The Spinal Cord - A Christopher and Dana Reeve Foundation Text and Atlas, C. Watson, G. Paxinos, and G. Kayalioglu, eds. (London: Academic Press - Elsevier), pp. 180-190.

Cook, J.S., Wolsing, D.H., Lamehb, J., Olson, C.A., Correa, P.E., Sadeeb, W., Blumenthal, E.M., and Rosenbaum, J.S. (1992). Characterization of the RDC1 gene which encodes the canine homolog of a proposed human VIP receptor. Expression does not correlate with an increase in VIP binding sites. FEBS Lett 300, 149-152.

Daniel, D., Rossel, M., Seki, T., and Konig, N. (2005). Stromal cell-derived factor-1 (SDF-1) expression in embryonic mouse cerebral cortex starts in the intermediate zone close to the pallial-subpallial boundary and extends progressively towards the cortical hem. Gene expression patterns : GEP 5, 317-322.

David, S., and Aguayo, A.J. (1981). Axonal elongation into peripheral nervous system “bridges” after central nervous system injury in adult rats Science 214, 931–933.

De La Luz Sierra, M., Yang, F., Narazaki, M., Salvucci, O., Davis, D., Yarchoan, R., Zhang, H.H., Fales, H., and Tosato, G. (2004). Differential processing of stromal-derived factor-1alpha and stromal-derived factor-1beta explains functional diversity. Blood 103, 2452-2459.

Deng, X., Xu, J., He, G., Tao, Y., Yang, T., Peng, X., and Cao, Y. (2014). Posttranslational Modifications of CXCR4: Implications in Cancer Metastasis. Receptors & Clinical Investigation.

DeVries, M.E., Kelvin, A.A., Xu, L., Ran, L., Robinson, J., and Kelvin, D.J. (2005). Defining the Origins and Evolution of the Chemokine/Chemokine Receptor System. The Journal of Immunology 176, 401-415.
Dou, C.L., and Levine, J.M. (1994). Inhibition of neurite growth by the NG2 chondroitin sulfate proteoglycan.
J Neurosci 14, 7616–7628.

Ebadi, M., Bashir, R.M., Heidrick, M.L., Hamada, F.M., Refaey, H.E., Hamed, A., Helal, G., Baxi, M.D., Cerutis, D.R., and Lassi, N.K. (1997). Neurotrophins and their receptors in nerve injury and repair. Neurochemistry international 30, 347-374.

Estrada, V., Brazda, N., Schmitz, C., Heller, S., Blazyca, H., Martini, R., and Muller, H.W. (2014). Long-lasting significant functional improvement in chronic severe spinal cord injury following scar resection and polyethylene glycol implantation. Neurobiol Dis 67, 165-179.

Faulkner, J.R., Herrmann, J.E., Woo, M.J., Tansey, K.E., Doan, N.B., and Sofroniew, M.V. (2004). Reactive astrocytes protect tissue and preserve function after spinal cord injury. J Neurosci 24, 2143-2155.

Fawcett, J.W., and Asher, R.A. (1999). The glial scar and central nervous system repair. Brain Res Bull 49, 377-391.

Fehlings, M.G., and Tator, C.H. (1995). The relationships among the severity of spinal cord injury, residual neurological function, axon counts, and counts of retrogradely labeled neurons after experimental spinal cord injury. Exp Neurol 132, 220-228.

Feng, Y., Broder, C.C., Kennedy, P.E., and Berger, E.A. (1996). HIV-1 Entry Cofactor: Functional cDNA Cloning of a Seven-Transmembrane, G Protein-Coupled Receptor. Science 272, 872-877.

Fischer, T., Nagel, F., Jacobs, S., Stumm, R., and Schulz, S. (2008). Reassessment of CXCR4 chemokine receptor expression in human normal and neoplastic tissues using the novel rabbit monoclonal antibody UMB-2. PLoS One 3, e4069.

Fouad, K., Dietz, V., and Schwab, M.E. (2001). Improving axonal growth and functional recovery after experimental spinal cord injury by neutralizing myelin associated inhibitors. Brain Res Brain Res Rev 36, 204-212.

Fouad, K., Schnell, L., Bunge, M.B., Schwab, M.E., Liebscher, T., and Pearse, D.D. (2005). Combining Schwann cell bridges and olfactory-ensheathing glia grafts with chondroitinase promotes locomotor recovery after complete transection of the spinal cord. J Neurosci 25, 1169-1178.

Fournier, A.E., Takizawa, B.T., and Strittmatter, S.M. (2003). Rho kinase inhibition enhances axonal regeneration in the injured CNS. J Neurosci 23, 1416-1423.

Garcia-Alias, G., Lin, R., Akrimi, S.F., Story, D., Bradbury, E.J., and Fawcett, J.W. (2008). Therapeutic time window for the application of chondroitinase ABC after spinal cord injury. Experimental neurology 210, 331-338.

Gerard, C., and Rollins, B.J. (2001). Chemokines and disease. Nat Immunol 2.

Gerrits, H., van Ingen Schenau, D.S., Bakker, N.E., van Disseldorp, A.J., Strik, A., Hermens, L.S., Koenen, T.B., Krajnc-Franken, M.A., and Gossen, J.A. (2008). Early postnatal lethality and cardiovascular defects in CXCR7-deficient mice. Genesis 46, 235-245.

Gleichmann, M., Gillen, C., Czardybon, M., Bosse, F., Greiner-Petter, R., Auer, J., and Müller, H.W. (2000). Cloning and characterization of SDF-1γ, a novel SDF-1 chemokine transcript with developmentally regulated expression in the nervous system. Eur J Neurosci 12, 1857-1866.

Gobrecht, P., Leibinger, M., Andreadaki, A., and Fischer, D. (2014). Sustained GSK3 activity markedly facilitates nerve regeneration. Nature communications 5, 4561.

Graham, G.J., Locati, M., Mantovani, A., Rot, A., and Thelen, M. (2012). The biochemistry and biology of the atypical chemokine receptors. Immunol Lett 145, 30-38.

Haines, D., Harkey, H.L., and Al-Mefty, O. (1993). The „Subdural“ Space: A New Look at an Outdated Concept. Neurosurgery 32, 111-120.

Harrison, M., O‘Brien, A., Adams, L., Cowin, G., Ruitenberg, M.J., Sengul, G., and Watson, C. (2013). Vertebral landmarks for the identification of spinal cord segments in the mouse. Neuroimage 68, 22-29.

Hatsea, S., Princena, K., Bridgerb, G., De Clercqa, E., and Scholsa, D. (2002). Chemokine receptor inhibition by AMD3100 is strictly confined to CXCR4. FEBS Letters, 255-262.

Hejcl, A., Lesny, P., Pradny, M., Michalek, J., Jendelova, P., Stulik, J., and Sykova, E. (2008). Biocompatible hydrogels in spinal cord injury repair. Physiol Res 57, 121-132.

Hermanns, S., Klapka, N., and Müller, H.W. (2001). The collagenous lesion scar-an obstacle for axonal regeneration in brain and spinal cord injury. Restor Neurol Neurosci 19, 139-148.

Heskamp, A. (2015). Role of CXCL12 and CXCR4 in axonal regeneration of mature retinal ganglion cells. In Experimentelle Neurologie der Neurologischen Klinik (Heinrich-Heine-Universität), pp. 117.

Heskamp, A., Leibinger, M., Andreadaki, A., Gobrecht, P., Diekmann, H., and Fischer, D. (2013). CXCL12/SDF-1 facilitates optic nerve regeneration. Neurobiol Dis 55, 76-86.

Hiebert, G.W., Dyer, J.K., Tetzlaff, W., and Steeves, J.D. (2000). Immunological myelin disruption does not alter expression of regeneration-associated genes in intact or axotomized rubrospinal neurons. Experimental neurology 163, 149-156.

Hill, W.D., Hess, D.C., Martin-Studdard, A., Carothers, J.J., Zheng, J., Hale, D., Maeda, M., Fagan, S.C., Carroll, J.E., and Conway, S.J. (2004). SDF-1 (CXCL12) Is Upregulated in the Ischemic Penumbra Following Stroke: Association with Bone Marrow Cell Homing to Injury. Journal of Neuropathology and Experimental Neurology 63, 84-96.

Hoffmann, F., Muller, W., Schutz, D., Penfold, M.E., Wong, Y.H., Schulz, S., and Stumm, R. (2012). Rapid uptake and degradation of CXCL12 depend on CXCR7 carboxyl-terminal serine/threonine residues. J Biol Chem 287, 28362-28377.

Huebner, E.A., and Strittmatter, S.M. (2009). Axon regeneration in the peripheral and central nervous systems. Results and problems in cell differentiation 48, 339-351.

Hylden, J.L.K., and Wilcox, G.L. (1980). Intrathecal morphine in mice: a new technique. European Journal of Pharmacology 67, 313-316.

Imai, T., Hieshima, K., Haskell, C., Baba, M., Nagira, M., Nishimura, M., Kakizaki, M., Takagi, S., Nomiyama, H., Schall, T.J., et al. (1997). Identification and molecular characterization of fraktalkine receptor CX3CR1, which mediates both leukocyte migration and adhesion. Cell 91, 521-530.

Inatani, M., Honjo, M., Otori, Y., Oohira, A., Kido, N., Tano, Y., Honda, Y., and Tanihara, H. (2001). Inhibitory effects of neurocan and phosphacan on neurite outgrowth from retinal ganglion cells in culture. Invest Ophthalmol Vis Sci 42, 1930–1938.

Jaerve, A., and Muller, H.W. (2012). Chemokines in CNS injury and repair. Cell and tissue research 349, 229-248.

Jaerve, A., Schira, J., and Muller, H.W. (2012). Concise review: the potential of stromal cell-derived factor 1 and its receptors to promote stem cell functions in spinal cord repair. Stem Cells Transl Med 1, 732-739.

Jaerve, A., Schiwy, N., Schmitz, C., and Mueller, H.W. (2011). Differential effect of aging on axon sprouting and regenerative growth in spinal cord injury. Experimental neurology 231, 284-294.

Jara, J.H., Villa, S.R., Khan, N.A., Bohn, M.C., and Ozdinler, P.H. (2012). AAV2 mediated retrograde transduction of corticospinal motor neurons reveals initial and selective apical dendrite degeneration in ALS. Neurobiol Dis 47, 174-183.

Jones, L., and Tuszynski, M.H. (2001). Chronic Intrathecal Infusions After Spinal Cord Injury Cause Scarring and Compression. Microscopy research and technique 54, 317-324.

Joosten, E.A.J., Schuitman, R.L., Vermelis, M.E.J., and Dederen, P.J.W.C. (1992). Postnatal development of the ipsilateral corticospinal component in rat spinal cord: A light and electron microscopic anterograde HRP study. Journal of Comparative Neurology 326, 133-146.

Kawano, H., Kimura-Kuroda, J., Komuta, Y., Yoshioka, N., Li, H.P., Kawamura, K., Li, Y., and Raisman, G. (2012). Role of the lesion scar in the response to damage and repair of the central nervous system. Cell and tissue research 349, 169-180.

Kayalioglu, G. (2009a). Projections from the spinal cord to the brain. In The Spinal Cord - A Christopher and Dana Reeve Foundation Text and Atlas, C. Watson, G. Paxinos, and G. Kayalioglu, eds. (London: Academic Press - Elsevier), pp. 148-167.

Kayalioglu, G. (2009b). The spinal nerves. In The Spinal Cord - A Christopher and Dana Reeve Foundation Text and Atlas, C. Watson, G. Paxinos, and G. Kayalioglu, eds. (London: Academic Press - Elsevier), pp. 37-56.

Kelner, G.S., Kennedy, J., Bacon, K.B., Kleyensteuber, S., Largaespada, D.A., Jenkins, N.A., Copeland, N.G., Bazan, J.F., Moore, K.W., Schall, T.J., et al. (1994). Lymphotactin: a cytokine that represents a new class of chemokine. Science 266, 1395-1399.

Kim, D., Zai, L., Liang, P., Schaffling, C., Ahlborn, D., and Benowitz, L.I. (2013). Inosine enhances axon sprouting and motor recovery after spinal cord injury. PLoS One 8, e81948.

Kim, K.K., Adelstein, R.S., and Kawamoto, S. (2009). Identification of neuronal nuclei (NeuN) as Fox-3, a new member of the Fox-1 gene family of splicing factors. J Biol Chem 284, 31052-31061.

Kirshblum, S.C., Burns, S.P., Biering-Sorensen, F., Donovan, W., Graves, D.E., Jha, A., Johansen, M., Jones, L., Krassioukov, A., Mulcahey, M.J., et al. (2011). International standards for neurological classification of spinal cord injury (revised 2011). The journal of spinal cord medicine 34, 535-546.

Klapka, N., Hermanns, S., Straten, G., Masanneck, C., Duis, S., Hamers, F.P., Muller, D., Zuschratter, W., and Muller, H.W. (2005). Suppression of fibrous scarring in spinal cord injury of rat promotes long-distance regeneration of corticospinal tract axons, rescue of primary motoneurons in somatosensory cortex and significant functional recovery. Eur J Neurosci 22, 3047-3058.

Klapka, N., and Müller, H.W. (2006). Collagen matrix in spinal cord injury. J Neurotrauma 23, 422-435.

Koda, M., Hashimoto, M., Murakami, M., Shirasawa, H., Sakao, S., Ino, H., Yoshinaga, K., Ikeda, O., Yamazaki, M., Koshizuka, S., et al. (2004). Adenovirus vector-mediated in vivo gene transfer of brain- derived neurotrophic factor (BDNF) promotes rubrospinal axonal regeneration and functional recovery after complete transection of the adult rat spinal cord J Neurotrauma 21, 329–337.

Kojima, A., and Tator, C.H. (2002). Intrathecal Administration of Epidermal Growth Factor and Fibroblast Growth Factor 2 Promotes Ependymal Proliferation and Functional Recovery after Spinal Cord Injury in Adult Rats. Journal of Neurotrauma 19, 223-238.

König, B. (2014). Biochemical and pharmacological modulation of scarring, axon regeneration and long-term functional improvement after spinal cord injury in rat. In Labor für Molekulare Neurobiologie der Neurologischen Klinik (Heinrich-Heine-Universität), pp. 119.

Krupnick, J.G., and Benovic, J.L. (1998). The role of receptor kinases and arrestins in G protein-coupled receptor regulation. Annu Rev Pharmacol Toxicol 38, 289-319.

Kruse, F., Bosse, F., Vogelaar, C.F., Brazda, N., Kury, P., Gasis, M., and Muller, H.W. (2011). Cortical gene expression in spinal cord injury and repair: insight into the functional complexity of the neural regeneration program. Front Mol Neurosci 4, 26.

Küchler, M., Fouad, K., Weinmann, O., Schwab, M.E., and Raineteau, O. (2002). Red nucleus projections to distinct motor neuron pools in the rat spinal cord. The Journal of comparative neurology 448, 349-359.

Lee, B.B., Cripps, R.A., Fitzharris, M., and Wing, P.C. (2014). The global map for traumatic spinal cord injury epidemiology: update 2011, global incidence rate. Spinal cord 52, 110-116.

Lee, S.K., and Wolfe, S.W. (2000). Peripheral nerve injury and repair. JAmAcadOrthopSurg 8, 243-252.

Levin, E., Diekmann, H., and Fischer, D. (2016). Highly efficient transduction of primary adult CNS and PNS neurons. Sci Rep 6, 38928.

Levoye, A., Balabanian, K., Baleux, F., Bachelerie, F., and Lagane, B. (2009). CXCR7 heterodimerizes with CXCR4 and regulates CXCL12-mediated G protein signaling. Blood 113, 6085-6093.

Li, J., and Lepski, G. (2013). Cell transplantation for spinal cord injury: a systematic review. BioMed research international 2013, 786475.

Li, Q., Shirabe, K., Thisse, C., Thisse, B., Okamoto, H., Masai, I., and Kuwada, J.Y. (2005). Chemokine signaling guides axons within the retina in zebrafish. J Neurosci 25, 1711-1717.

Libert, F., Parmentier, M., Lefort, A., Dumont, J.E., and Vassart, G. (1990). Complete nucleotide sequence of a putative G protein coupled receptor: RDC1. Nucleic Acids Res 18, 1917.

Lieberam, I., Agalliu, D., Nagasawa, T., Ericson, J., and Jessell, T.M. (2005). A Cxcl12-CXCR4 chemokine signaling pathway defines the initial trajectory of mammalian motor axons. Neuron 47, 667-679.

Lipfert, J., Odemis, V., Wagner, D.C., Boltze, J., and Engele, J. (2013). CXCR4 and CXCR7 form a functional receptor unit for SDF-1/CXCL12 in primary rodent microglia. Neuropathology and applied neurobiology 39, 667-680.

Liu, K., Lu, Y., Lee, J.K., Samara, R., Willenberg, R., Sears-Kraxberger, I., Tedeschi, A., Park, K.K., Jin, D., Cai, B., et al. (2010). PTEN deletion enhances the regenerative ability of adult corticospinal neurons. Nat Neurosci 13, 1075-1081.

Liu, K., Tedeschi, A., Park, K.K., and He, Z. (2011). Neuronal intrinsic mechanisms of axon regeneration. Annual review of neuroscience 34, 131-152.

Loetscher, M., Geiser, T., O'Reilly, T., Zwahlen, R., Baggiolini, M., and Moser, B. (1994). Cloning of a human seven-transmembrane domain receptor, LESTR, that is highly expressed in leukocytes. The Journal of biological chemistry 269, 232-237.

Lopez-Bendito, G., Sanchez-Alcaniz, J.A., Pla, R., Borrell, V., Pico, E., Valdeolmillos, M., and Marin, O. (2008). Chemokine signaling controls intracortical migration and final distribution of GABAergic interneurons. J Neurosci 28, 1613-1624.

Lu, M., Grove, E.A., and Miller, R.J. (2002). Abnormal development of the hippocampal dentate gyrus in mice lacking the CXCR4 chemokine receptor. Proceedings of the National Academy of Sciences of the United States of America 99, 7090-7095.

Lu, P., and Tuszynski, M.H. (2008). Growth factors and combinatorial therapies for CNS regeneration. Experimental neurology 209, 313-320.

Luker, K.E., Gupta, M., and Luker, G.D. (2009). Imaging chemokine receptor dimerization with firefly luciferase complementation. FASEB journal : official publication of the Federation of American Societies for Experimental Biology 23, 823-834.

Ma, Q., Jones, D., Borghesani, P.R., Segal, R.A., Nagasawa, T., Kishimoto, T., Bronson, R.T., and Springer, T.A. (1998). Impaired B-lymphopoiesis, myelopoiesis, and derailed cerebellar neuron migration in CXCR4- and SDF-1-deficient mice. Proceedings of the National Academy of Sciences of the United States of America 95, 9448-9453.

Mahabaleshwar, H., Tarbashevich, K., Nowak, M., Brand, M., and Raz, E. (2012). beta-arrestin control of late endosomal sorting facilitates decoy receptor function and chemokine gradient formation. Development 139, 2897-2902.

Maier, I.C., and Schwab, M.E. (2006). Sprouting, regeneration and circuit formation in the injured spinal cord: factors and activity. Philosophical transactions of the Royal Society of London Series B, Biological sciences 361, 1611-1634.

Mann, C.M., and Kwon, B.K. (2007). An Update on the Pathophysiology of Acute Spinal Cord Injury. Seminars in Spine Surgery 19, 272-279.

Marchese, A., and Benovic, J.L. (2001). Agonist-promoted ubiquitination of the G protein-coupled receptor CXCR4 mediates lysosomal sorting. J Biol Chem 276, 45509-45512.

Marchese, A., Chen, C., Kim, Y.-M., and Benovic, J.L. (2003). The ins and outs of G protein-coupled receptor trafficking. Trends in Biochemical Sciences 28, 369-376.

McGrath, E.K., Koniski, A.D., Maltby, K.M., McGann, J.K., and Palis, J. (1999). Embryonic Expression and Function of the Chemokine SDF-1 and Its Receptor, CXCR4. Developmental Biology 213, 442-456.

McKerracher, L., David, S., Jackson, D.L., Kottis, V., Dunn, R.J., and Braun, P.E. (1994). Identification of myelin-associated glycoprotein as a major myelin-derived inhibitor of neurite growth. Neuron 13, 805-811.

McKerracher, L., and Higuchi, H. (2006). Targeting Rho to stimulate repair after spinal cord injury. J Neurotrauma 23, 309-317.

Memi, F., Abe, P., Cariboni, A., MacKay, F., Parnavelas, J.G., and Stumm, R. (2013). CXC chemokine receptor 7 (CXCR7) affects the migration of GnRH neurons by regulating CXCL12 availability. J Neurosci 33, 17527-17537.

Miller, J.T., Bartley, J.H., Wimborne, H.J., Walker, A.L., Hess, D.C., Hill, W.D., and Carroll, J.E. (2005). The neuroblast and angioblast chemotaxic factor SDF-1 (CXCL12) expression is briefly up regulated by reactive astrocytes in brain following neonatal hypoxic-ischemic injury. BMC neuroscience 6, 63.

Miyasaka, N., Knaut, H., and Yoshihara, Y. (2007). Cxcl12/Cxcr4 chemokine signaling is required for placode assembly and sensory axon pathfinding in the zebrafish olfactory system. Development 134, 2459-2468.

Molyneaux, B.J., Goff, L.A., Brettler, A.C., Chen, H.H., Brown, J.R., Hrvatin, S., Rinn, J.L., and Arlotta, P. (2015). DeCoN: genome-wide analysis of in vivo transcriptional dynamics during pyramidal neuron fate selection in neocortex. Neuron 85, 275-288.

Moore, D.L., Blackmore, M.G., Hu, Y., Kaestner, K.H., Bixby, J.L., Lemmon, V.P., and Goldberg, J.L. (2009). KLF Family Members Regulate Intrinsic Axon Regeneration Ability. Science 9, 298-301.

Moore, D.L., and Goldberg, J.L. (2011). Multiple transcription factor families regulate axon growth and regeneration. Developmental neurobiology 71, 1186-1211.

Moreau-Fauvarque, C., Kumanogoh, A., Camand, E., Jaillard, C., Barbin, G., Boquet, I., Love, C., Jones, E.Y., Kikutani, H., Lubetzki, C., et al. (2003). The transmembrane semaphorin Sema4D/CD100, an inhibitor of axonal growth, is expressed on oligodendrocytes and upregulated after CNS lesion. J Neurosci 23, 9229-9239.

Moser, B., and Loetscher, P. (2001). Lymphocyte traffic control by chemokines. Nat Immunol 2, 123-128.

Moser, B., Wolf, M., Walz, A., and Loetscher, P. (2004). Chemokines: multiple levels of leukocyte migration control. Trends Immunol 25, 75-84.

Mothe, A.J., and Tator, C.H. (2013). Review of transplantation of neural stem/progenitor cells for spinal cord injury. Int J Dev Neurosci 31, 701-713.

Mueller, W., Schutz, D., Nagel, F., Schulz, S., and Stumm, R. (2013). Hierarchical organization of multi-site phosphorylation at the CXCR4 C terminus. PLoS One 8, e64975.

Mukhopadhyay, G., Doherty, P., Walsh, F.S., Crocker, P.R., and Filbin, M.T. (1994). A novel role for myelin-associated glycoprotein as an inhibitor of axonal regeneration. Neuron 13, 757-767.
Mullen, R.J., Buck, C.R., and Smith, A.M. (1992). NeuN, a neuronal specific nuclear protein in vertebrates. Development 116, 201-211.

Müller, A., Homey, B., Soto, H., Ge, N., Catron, D., Buchanan, M.E., McClanahan, T., Murphy, E., Yuan, W., Wagners, S.N., et al. (2001). Involvement of chemokine receptors in breast cancer metastasis. Nature 410, 50-56.

Murdoch, C., and Finn, A. (2000). Chemokine receptors and their role in inflammation and infectious diseases. Blood 95, 3032-3043.

Murphy, P.M., Baggiolini, M., Charo, I.F., Hébert, C.A., Horuk, R., Matsushima, K., Miller, L.H., Oppenheim, J.J., and Power, C.A. (2000). International union of pharmacology. XXII. Nomenclature for chemokine receptors. Pharmacol Rev 52, 145-176.

Nagasawa, T., Hirota, S., Tachibana, K., Takakura, N., Nishikawa, S., Kitamura, Y., Yoshida, N., Kikutani, H., and Kishimoto, T. (1996a). Defects of B-cell lymphopoiesis and bone marrow myelopoiesis in mice lacking the CXC chemokine PBSF/SDF-1. Nature 382, 635-638.

Nagasawa, T., Kikutani, H., and Kishimoto, T. (1994). Molecular cloning and structure of a pre-B-cell growth-stimulating factor. Proceedings of the National Academy of Sciences of the United States of America 91, 2305-2309.

Nagasawa, T., Nakajima, T., Tachibana, K., Ilzasa, H., Bleuli, C.C., Yoshie, O., Matsushima, K., YoshidaA, N., Springeri, T.A., and Kishimoto, T. (1996b). Molecular cloning and characterization of a murine pre-B-cell growth-stimulating factorystromal cell-derived factor 1 receptor, a murine homolog of the human immunodeficiency virus 1 entry coreceptor fusin. Proceedings of the National Academy of Sciences of the United States of America 93, 14726-14729.

Nagata, S., Ishihara, T., Robberecht, P., Libert, F., Parmentier, M., Christophe, J., and Vassart, G. (1992). RDC1 may not be VIP receptor. Trends Pharmacol Sci 13, 102-103.

Naumann, U., Cameroni, E., Pruenster, M., Mahabaleshwar, H., Raz, E., Zerwes, H.G., Rot, A., and Thelen, M. (2010). CXCR7 functions as a scavenger for CXCL12 and CXCL11. PLoS One 5, e9175.

Neumann, S., Bradke, F., Tessier-Lavigne, M., and Basbaum, A.I. (2002). Regeneration of Sensory Axons within the Injured Spinal Cord Induced by Intraganglionic cAMP Elevation. Neuron 34, 885-893.

Njoo, C., Heinl, C., and Kuner, R. (2014). In vivo SiRNA transfection and gene knockdown in spinal cord via rapid noninvasive lumbar intrathecal injections in mice. Journal of visualized experiments : JoVE.

Nomiyama, H., Osada, N., and Yoshie, O. (2011). A family tree of vertebrate chemokine receptors for a unified nomenclature. Dev Comp Immunol 35, 705-715.

Nomura, H., Tator, C.H., and Shoichet, M.S. (2006). Bioengineered strategies for spinal cord repair. JNeurotrauma 23, 496-507.

O'Hayre, M., Salanga, C.L., Handel, T.M., and Allen, S.J. (2008). Chemokines and cancer: migration, intracellular signalling and intercellular communication in the microenvironment. Biochem J 409, 635-649.

Oberlin, E., Amara, A., Bachelerie, F., Bessia, C., Virelizier, J.L., Arenzana-Seisdedos, F., Schwartz, O., Heard, J.M., Clark-Lewis, I., Legler, D.F., et al. (1996). The CXC chemokine SDF-1 is the ligand for LESTR/fusin and prevents infection by T-cell-lineadapted HIV-1 Nature 382, 833-835.

Odemis, V., Lamp, E., Pezeshki, G., Moepps, B., Schilling, K., Gierschik, P., Littman, D.R., and Engele, J. (2005). Mice deficient in the chemokine receptor CXCR4 exhibit impaired limb innervation and myogenesis. Molecular and cellular neurosciences 30, 494-505.

Opatz, J., Kury, P., Schiwy, N., Jarve, A., Estrada, V., Brazda, N., Bosse, F., and Muller, H.W. (2009). SDF-1 stimulates neurite growth on inhibitory CNS myelin. Molecular and cellular neurosciences 40, 293-300.

Pakulska, M.M., Tator, C.H., and Shoichet, M.S. (2017). Local delivery of chondroitinase ABC with or without stromal cell-derived factor 1alpha promotes functional repair in the injured rat spinal cord. Biomaterials 134, 13-21.

Park, K.K., Liu, K., Hu, Y., Smith, P.D., Wang, C., Cai, B., Xu, B., Connolly, L., Kramvis, I., Sahin, M., et al. (2008). Promoting Axon Regeneration in the Adult CNS by Modulation of the PTEN/mTOR Pathway. Science 322, 963-966.

Parnavelas, J.G. (2000). The origin and migration of cortical neurones: new vistas. Trends in neurosciences 23, 126 -131.

Patel, N., and Poo, M. (1982). Orientation of neurite growth by extracellular electric felds. J Neurosci 2, 483-496.

Paxinos, G., and Franklin, K.B.J. (2001). The mouse brain in stereotaxic coordinates (second edition).

Pearse, D.D., and Bunge, M.B. (2006). Designing cell- and gene-based regeneration strategies to repair the injured spinal cord. JNeurotrauma 23, 438-452.

Pekny, M., and Nilsson, M. (2005). Astrocyte activation and reactive gliosis. Glia 50, 427-434.

Plunet, W., Kwon, B.K., and Tetzlaff, W. (2002). Promoting axonal regeneration in the central nervous system by enhancing the cell body response to axotomy. Journal of neuroscience research 68, 1-6.

Proudfoot, A.E. (2002). Chemokine receptors: multifaceted therapeutic targets. Nat Rev Immunol 2, 106-115.

Pujol, F., Kitabgi, P., and Boudin, H. (2005). The chemokine SDF-1 differentially regulates axonal elongation and branching in hippocampal neurons. Journal of Cell Science 118, 1071-1080.

Qiu, J., Cai, D., Dai, H., McAtee, M., Hoffman, P.N., Bregman, B.S., and Filbin, M.T. (2002). Spinal Axon Regeneration Induced by Elevation of Cyclic AMP. Neuron 34, 895-903,.

Raivich, G., Bohatschek, M., Da Costa, C., Iwata, O., Galiano, M., Hristova, M., Nateri, A.S., Makwana, M., Riera-Sans, L., Wolfer, D.P., et al. (2004). The AP-1 transcription factor c-Jun is required for efficient axonal regeneration. Neuron 43, 57-67.

Ramón y Cajal, S. (1928). Degeneration and regeneration of the nervous system Oxford University Press [ua], London.

Reina, M.A., Casasola, O.L., Lopez, A., De Andrés, J.A., Mora, M., and Fernandez, A. (2002). The Origin of the Spinal Subdural Space: Ultrastructure Findings. Anesth Analg 94, 991-995.

Rempel, S.A., Dudas, S., Ge, S., and Gutierrez, J.A. (2000). Identification and localization of the cytokine SDF-1 and its receptor, CXC chemokine receptor 4, to regions of necrosis and angiogenesis in human glioblastoma. Clin Cancer Res 6, 102-111.

Richardson, P.M., McGuinness, U.M., and Aguayo, A.J. (1980). Axons from CNS neurons regenerate into PNS grafts. Nature 284, 264-265.

Rollins, B.J. (1997). Chemokines. Blood 90, 909-928.

Rolls, A., Shechter, R., and Schwartz, M. (2009). The bright side of the glial scar in CNS repair. Nature reviews Neuroscience 10, 235-241.

Rossi, D., and Zlotnik, A. (2000). The biology of chemokines and their receptors Annual review of immunology 18, 217-242.

Saini, V., Marchese, A., Tang, W.J., and Majetschak, M. (2011). Structural determinants of ubiquitin-CXC chemokine receptor 4 interaction. J Biol Chem 286, 44145-44152.

Saker, E., Henry, B.M., Tomaszewski, K.A., Loukas, M., Iwanaga, J., Oskouian, R.J., and Tubbs, R.S. (2016). The Human Central Canal of the Spinal Cord: A Comprehensive Review of its Anatomy, Embryology, Molecular Development, Variants, and Pathology. Cureus 8, e927.

Sakla, F.B. (1969). Quantitative Studies on the Postnatal Growth of the Spinal Cord and the Vertebral Column of the Albino Mouse. J Comp Neurol 136, 237-247.

Sakura, S., Hashimoto, K., Bollen, A.W., Ciriales, R., and Drasner, K. (1996). Intrathecal catheterization in the rat. Improved technique for morphologic analysis of drug-induced injury. . Anesthesiology 85, 1184-1189.

Salanga, C.L., O'Hayre, M., and Handel, T. (2009). Modulation of chemokine receptor activity through dimerization and crosstalk. Cell Mol Life Sci 66, 1370-1386.

Sanchez-Alcaniz, J.A., Haege, S., Mueller, W., Pla, R., Mackay, F., Schulz, S., Lopez-Bendito, G., Stumm, R., and Marin, O. (2011). Cxcr7 controls neuronal migration by regulating chemokine responsiveness. Neuron 69, 77-90.

Sanchez-Martín, L., Estecha, A., Samaniego, R., Sanchez-Ramon, S., Vega, M.A., and Sanchez-Mateos, P. (2011). The chemokine CXCL12 regulates monocyte-macrophage differentiation and RUNX3 expression. 117.

Sapede, D., Rossel, M., Dambly-Chaudiere, C., and Ghysen, A. (2005). Role of SDF1 chemokine in the development of lateral line efferent and facial motor neurons. Proceedings of the National Academy of Sciences of the United States of America 102, 1714-1718.

Saval, A., and Chiodo, A.E. (2010). Intrathecal Baclofen for Spasticity Management: A Comparative Analysis of Spasticity of Spinal vs Cortical Origin. J Spinal Cord Med 33, 16-21.

Schiwy, N., Brazda, N., and Muller, H.W. (2009). Enhanced regenerative axon growth of multiple fibre populations in traumatic spinal cord injury following scar-suppressing treatment. Eur J Neurosci 30, 1544-1553.

Schiwy, N.E. (2010). Axonale Regeneration und Plastizität unterschiedlicher Fasersysteme nach Rückenmarksverletzungen und verschiedenen Behandlungsansätzen in der adulten Ratte. In Labor für Molekulare Neurobiologie der Neurologischen Klinik (Heinrich-Heine-Universität), pp. 117.

Schonemeier, B., Kolodziej, A., Schulz, S., Jacobs, S., Hoellt, V., and Stumm, R. (2008a). Regional and cellular localization of the CXCl12/SDF-1 chemokine receptor CXCR7 in the developing and adult rat brain. The Journal of comparative neurology 510, 207-220.

Schonemeier, B., Schulz, S., Hoellt, V., and Stumm, R. (2008b). Enhanced expression of the CXCl12/SDF-1 chemokine receptor CXCR7 after cerebral ischemia in the rat brain. J Neuroimmunol 198, 39-45.

Schwab, M.E., and Caroni, P. (1988). Oligodendrocytes and CNS myelin are nonpermissive substrates for neurite growth and fibroblast spreading in vitro. J Neurosci 8, 2381-2393.

Scott, B.S. (1977). Adult Mouse Dorsal Root Ganglia Neurons in Cell Culture. Journal of neurobiology 8, 417-427.

Seijffers, R., Allchorne, A.J., and Woolf, C.J. (2006). The transcription factor ATF-3 promotes neurite outgrowth. Molecular and cellular neurosciences 32, 143-154.

Sengottuvel, V., Leibinger, M., Pfreimer, M., Andreadaki, A., and Fischer, D. (2011). Taxol facilitates axon regeneration in the mature CNS. J Neurosci 31, 2688-2699.

Sharma, S.C., Jadhao, A.G., and Prasada, R.P.D. (1993). Regeneration of supraspinal projection neurons in the adult goldfish. . Brain Res 620, 221-228.

Shen, Y.J., DeBellard, M.E., Salzer, J.L., Roder, J., and Filbin, M.T. (1998). Myelin-associated glycoprotein in myelin and expressed by Schwann cells inhibits axonal regeneration and branching. . Mol Cell Neurosci 12, 79-91.

Shimizu, S., Brown, M., Sengupta, R., Penfold, M.E., and Meucci, O. (2011). CXCR7 protein expression in human adult brain and differentiated neurons. PLoS One 6, e20680.

Shirozu, M., Nakano, T., Inazawa, J., Tashiro, K., Tada, H., Shinohara, T., and Honjo, T. (1995). Structure and chromosomal localization of the human stromal cell-derived factor 1 (SDF1) gene. Genomics 28, 495-500.

Sierro, F., Biben, C., Martinez-Munoz, L., Mellado, M., Ransohoff, R.M., Li, M., Woehl, B., Leung, H., Groom, J., Batten, M., et al. (2007). Disrupted cardiac development but normal hematopoiesis in mice deficient in the second CXCL12/SDF-1 receptor, CXCR7. Proceedings of the National Academy of Sciences of the United States of America 104, 14759-14764.

Sreedharan, S.P., Robichon, A., Peterson, K.E., and Goetzl, E.J. (1991). Cloning and expression of the human vasoactive intestinal peptide receptor. Proc Natl Acad Sci USA 88, 4986-4990.

Stichel, C.C., Hermanns, S., Luhmann, H.J., Lausberg, F., Niermann, H., D'Urso, D., Servos, G., Hartwig, H.G., and Müller, H.W. (1999). Inhibition of collagen IV deposition promotes regeneration of injured CNS axons. Eur J Neurosci 11, 632-646.

Stichel, C.C., and Müller, H.W. (1998). Experimental strategies to promote axonal regeneration after traumatic central nervous system injury. Progress in neurobiology 56, 119-148.

Strieter, R.M., Polverini, P.J., Arenberg, D.A., Walz, A., Opdenakker, G., Van Damme, J., and Kunkel, S.L. (1995). Role of C-X-C chemokines as regulators of angiogenesis in lung cancer. J Leukocyte Biol 57, 752-762.

Stumm, R., and Hollt, V. (2007). CXC chemokine receptor 4 regulates neuronal migration and axonal pathfinding in the developing nervous system: implications for neuronal regeneration in the adult brain. J Mol Endocrinol 38, 377-382.

Stumm, R., Kolodziej, A., Schulz, S., Kohtz, J.D., and Hollt, V. (2007). Patterns of SDF-1alpha and SDF-1gamma mRNAs, migration pathways, and phenotypes of CXCR4-expressing neurons in the developing rat telencephalon. The Journal of comparative neurology 502, 382-399.

Stumm, R.K., Rummel, J., Junker, V., Culmsee, C., Pfeiffer, M., Krieglstein, J., Hollt, V., and Schulz, S. (2002). A dual role for the SDF-1/CXCR4 chemokine receptor system in adult brain: isoform-selective regulation of SDF-1 expression modulates CXCR4-dependent neuronal plasticity and cerebral leukocyte recruitment after focal ischemia. Journal of Neuroscience 22, 5865-5878.

Stumm, R.K., Zhou, C., Ara, T., Lazarini, F., Dubois-Dalcq, M., Nagasawa, T., Hollt, V., and Schulz, S. (2003). CXCR4 regulates interneuron migration in the developing neocortex. Journal of Neuroscience 23, 5123-5130.

Sugiyama, T., Kohara, H., Noda, M., and Nagasawa, T. (2006). Maintenance of the hematopoietic stem cell pool by CXCL12-CXCR4 chemokine signaling in bone marrow stromal cell niches. Immunity 25, 977-988.

Szaro, B., Whitnall, M.H., and Gainer, H. (1990). Phosphorylation-Dependent Epitopes on Neurofilament Proteins and Neurofilament Densities Differ in Axons in the Corticospinal and Primary Sensory Dorsal ColumnTracts in the Rat Spinal Cord. The Journal of comparative neurology 302, 220-235.

Tachibana, K., Hirota, S., Iizasa, H., Yoshida, H., Kawabata, K., Kataoka, Y., Kitamura, Y., Matsushima, K., Yoshida, N., Nishikawa, S., et al. (1998). The chemokine receptor CXCR4 is essential for vascularization of the gastrointestinal tract. Nature 393, 591-594.

Taiwo, O.B., Kovacs, K.J., and Larson, A.A. (2005). Chronic daily intrathecal injections of a large volume of fluid increase mast cells in the thalamus of mice. Brain Res 1056, 76-84.

Talac, R., Friedman, J.A., Moore, M.J., Lu, L., Jabbari, E., Windebank, A.J., Currier, B.L., and Yaszemski, M.J. (2004). Animal models of spinal cord injury for evaluation of tissue engineering treatment strategies. Biomaterials 25, 1505-1510.

Tanaka, E., and Sabry, J. (1995). Making the Connection: Cytoskeletal Rearrangements during Growth Cone Guidance. Cell 83, 171-176.

Tashiro, K., Tada, H., Heilker, R., Shirozu, M., Nakano, T., and Honjo, T. (1993). Signal sequence trap: a cloning strategy for secreted proteins and type I membrane proteins. Science 261, 600-603.

Teicher, B.A., and Fricker, S.P. (2010). CXCL12 (SDF-1)/CXCR4 pathway in cancer. Clin Cancer Res 16, 2927-2931.

Tham, T.N., Lazarini, F., Franceschini, I.A., Lachapelle, F., Amara, A., and Dubois-Dalcq, M. (2001). Developmental pattern of expression of the alpha chemokine stromal cell-derived factor 1 in the rat central nervous system. European Journal of Neuroscience 13, 845±856.

Tissir, F., Wang, C.E., and Goffinet, A.M. (2004). Expression of the chemokine receptor Cxcr4 mRNA during mouse brain development. Brain research Developmental brain research 149, 63-71.

Tiveron, M.C., Rossel, M., Moepps, B., Zhang, Y.L., Seidenfaden, R., Favor, J., Konig, N., and Cremer, H. (2006). Molecular interaction between projection neuron precursors and invading interneurons via stromal-derived factor 1 (CXCL12)/CXCR4 signaling in the cortical subventricular zone/intermediate zone. J Neurosci 26, 13273-13278.

Tonge, D.A., Golding, J.P., Edbladh, M., Kroon, M., Ekstrom, P.E., and Edstrom, A. (1997). Effects of extracellular matrix components on axonal outgrowth from peripheral nerves of adult animals in vitro. Experimental neurology 146, 81-90.

Trecki, J., Brailoiu, G.C., and Unterwald, E.M. (2010). Localization of CXCR4 in the forebrain of the adult rat. Brain Res 1315, 53-62.

Tuszynski, M.H., Grill, R., Jones, L.L., Brant, A., Blesch, A., Löw, K., Lacroix, S., and Lu, P. (2003). NT-3 gene delivery elicits growth of chronically injured corticospinal axons and modestly improves functional deficits after chronic scar resection. Experimental neurology 181, 47-56.

Tuszynski, M.H., Peterson, D.A., Ray, J., Baird, A., Nakahara, Y., and Gage, F.H. (1994). Fibroblasts genetically modified to produce nerve growth factor induce robust neuritic ingrowth after grafting to the spinal cord. Exp Neurol 126, 1-14.

Twery, E.N., and Raper, J.A. (2011). SDF1-induced antagonism of axonal repulsion requires multiple G-protein coupled signaling components that work in parallel. PLoS One 6, e18896.

Tysseling, V.M., Mithal, D.S., Sahni, V., Birch, D., Jung, H., Belmadani, A., Miller, R.J., and Kessler, J.A. (2011). SDF1 in the dorsal corticospinal tract promotes CXCR4+ cell migration after spinal cord injury. Journal of Neuroinflammation 8.

Vargas, M.E., and Barres, B.A. (2007). Why is Wallerian degeneration in the CNS so slow? Annual review of neuroscience 30, 153-179.

Venkatesh, I., Mehra, V., Wang, Z., Califf, B., and Blackmore, M.G. (2018). Developmental chromatin restriction of pro-growth gene networks acts as an epigenetic barrier to axon regeneration in cortical neurons. Developmental neurobiology.

Vogelaar, C.F., and Estrada, V. (2016). Experimental Spinal Cord Injury Models in Rodents: Anatomical Correlations and Assessment of Motor Recovery.

Waller, A. (1850). Experiments on the Section of the Glossopharyngeal and Hypoglossal Nerves of the Frog, and Observations of the Alterations Produced Thereby in the Structure of Their Primitive Fibres. Philosophical Transactions of the Royal Society of London 140, 423-429.

Wang, K.C., Koprivica, V., Kim, J.A., Sivasankaran, R., Guo, Y., Neve, R.L., and He, Z. (2002). Oligodendrocyte-myelin glycoprotein is a Nogo receptor ligand that inhibits neurite outgrowth. Nature 417, 941-944.

Wang, Y., Li, G., Stanco, A., Long, J.E., Crawford, D., Potter, G.B., Pleasure, S.J., Behrens, T., and Rubenstein, J.L. (2011). CXCR4 and CXCR7 have distinct functions in regulating interneuron migration. Neuron 69, 61-76.

Watson, C., and Harvey, A.R. (2009). Projections from the brain to the spinal cord. In The Spinal Cord - A Christopher and Dana Reeve Foundation Text and Atlas, C. Watson, G. Paxinos, and G. Kayalioglu, eds. (London: Academic Press - Elsevier), pp. 168-179.

Watson, C., and Kayalioglu, G. (2009). The organization of the spinal cord. . In The Spinal Cord - A Christopher and Dana Reeve Foundation Text and Atlas, C. Watson, G. Paxinos, and G. Kayalioglu, eds. (London: Academic Press - Elsevier), pp. 1-7.

Xu, L., Li, Y., Sun, H., Li, D., and Hou, T. (2013). Structural basis of the interactions between CXCR4 and CXCL12/SDF-1 revealed by theoretical approaches. Mol Biosyst 9, 2107-2117.

Yiu, G., and He, Z. (2006). Glial inhibition of CNS axon regeneration. Nature reviews Neuroscience 7, 617-627.

Yu, L., Cecil, J., Peng, S.B., Schrementi, J., Kovacevic, S., Paul, D., Su, E.W., and Wang, J. (2006). Identification and expression of novel isoforms of human stromal cell-derived factor 1. Gene 374, 174-179.

Yu, S., Crawford, D., Tsuchihashi, T., Behrens, T.W., and Srivastava, D. (2011). The chemokine receptor CXCR7 functions to regulate cardiac valve remodeling. Dev Dyn 240, 384-393.

Yurchenco, P.D., and Schittny, J.C. (1990). Molecular architecture of basement membranes. FASEB J 4, 1577-1590.

Zendedel, A., Johann, S., Mehrabi, S., Joghataei, M.T., Hassanzadeh, G., Kipp, M., and Beyer, C. (2016). Activation and Regulation of NLRP3 Inflammasome by Intrathecal Application of SDF-1a in a Spinal Cord Injury Model. Mol Neurobiol 53, 3063-3075.

Zendedel, A., Nobakht, M., Bakhtiyari, M., Beyer, C., Kipp, M., Baazm, M., and Joghataie, M.T. (2012). Stromal cell-derived factor-1 alpha (SDF-1alpha) improves neural recovery after spinal cord contusion in rats. Brain Res 1473, 214-226.

Zhang, S.X., Huang, F., Gates, M., White, J., and Holmberg, E.G. (2010). Extensive scarring induced by chronic intrathecal tubing augmented cord tissue damage and worsened functional recovery after rat spinal cord injury. J Neurosci Methods 191, 201-207.

Zheng, B., Ho, C., Li, S., Keirstead, H., Steward, O., and Tessier-Lavigne, M. (2003). Lack of enhanced spinal regeneration in Nogo-deficient mice. Neuron 38, 213-224.

Zhu, L., Zhao, Q., and Wu, B. (2013). Structure-based studies of chemokine receptors. Curr Opin Struct Biol 23, 539-546.

Zhu, Y., Matsumoto, T., Mikami, S., Nagasawa, T., and Murakami, F. (2009). SDF1/CXCR4 signalling regulates two distinct processes of precerebellar neuronal migration and its depletion leads to abnormal pontine nuclei formation. Development 136, 1919-1928.

Zhu, Y., and Murakami, F. (2012). Chemokine CXCL12 and its receptors in the developing central nervous system: emerging themes and future perspectives. Developmental neurobiology 72, 1349-1362.

Zlotnik, A., Yoshie, O., and Nomiyama, H. (2006). The chemokine and chemokine receptor superfamilies and their molecular evolution. Genome Biol 7.

Zolotukhin, S., Byrne, B.J., Mason, E., Zolotukhin, I., Potter, M., Chesnut, K., Summerford, C., Samulski, R.J., and Muzyczka, N. (1999). Recombinant adeno-associated virus purification using novel methods improves infectious titer and yield. Gene Therapy 6, 973–985.

Zou, Y.R., Kottmann, A.H., Kuroda, M., Taniuchi, I., and Littman, D.R. (1998). Function of the chemokine receptor CXCR4 in haematopoiesis and in cerebellar development. Nature 93, 595-599.

EIDESSTATTLICHE ERKLÄRUNG

Ich, Frau M.Sc. Federica Tundo-Lavalle versichere an Eides statt, dass die vorliegende Dissertation von mir selbständig und ohne unzulässige fremde Hilfe unter Beachtung der „Grundsätze zur Sicherung guter wissenschaftlicher Praxis an der Heinrich-Heine-Universität Düsseldorf“ erstellt worden ist. Diese Dissertation hat in gleicher oder ähnlicher Form noch keiner anderen Prüfungsbehörde vorgelegen. Ich habe bisher keine erfolglosen Promotionsversuche unternommen.

Düsseldorf, den 25. Februar 2019

_____

Unterschrift

ACKNOWLEDGEMENT

This thesis has greatly benefited from the support of many people I would like to thank here. Foremost, I want to thank the Interdisciplinary Graduate School for Brain Research and Translational Neuroscience (iBrain) for the financial support and for having given me the opportunity to work in an interdisciplinary environment and to get to know so many researcher that at the end of this journey became more than that. Thank you for having given me the chance to present my research data at international conferences, to discuss my results with international researcher and to find new collaboration partners. I want to thank iBrain and iGRAD (Interdisciplinary Graduate and Research Academy Düsseldorf) for the first-class research training and qualification program.

I want to express my sincere gratitude to my supervisors, Prof. Dr. Hans Werner Müller, Prof. Dr. Dietmar Fischer and Prof. Dr. Charlotte von Gall, who supported me throughout my doctoral study with their patience and knowledge.

Thank you, Hans Werner for having given me the opportunity to work in your laboratory on such an interesting project. This thesis would not have been possible without your help, advices and guidance.

I would also like to extend special thanks to Prof. Fischer for his valuables ideas and suggestions and for his support.

I also am thankful to Prof. von Gall for her invaluable support. She always believed in me and gave me the opportunity to write the thesis in her laboratory and to complete this chapter of my life.

Furthermore, I kindly thank Prof. Dr. Hermann Aberle for critical reading and taking the time to evaluate this thesis.

Special thanks go to my collaboration partner Prof. Dr. Ralf Stumm and his postdoctoral student Dr. Philipp Abe. Thank you for constant support and for scientific discussion, advice and for showing continuously willingness to help me.

My sincere thanks go also to the animal facility, zentrale Einrichtung für Tierforschung und wissenschaftliche Tierschutzaufgaben (ZETT), to Prof. Dr. Martin Sager, Dr. Eva Engelhardt, Ms. Eckert, Ms. Boldt, Ms. Gougoula, Ms. Niketta and all animal caretaker for helping me with the animal proposal, the breeding and for being there for me in all kinds of situations.

Many thanks go also to Daniela Keller for the statistical consulting. Thank you for the very friendly and uncomplicated way to explain statistic to me and for your professional and precise answers.

Thank you Ilenia Tundo for your help with the arrangement of the figures, for designing the figures and schemes and for developing the layout of this doctoral thesis. You were always there whenever I needed you, putting my needs in front of yours. Thank you very much!

I am grateful to my supervisor Dr. Veronica Estrada for her endless support for her encouragement and her accurate comments, which were of critical importance during this work. Your support and friendship have been invaluable not only on an academic, but also on a personal level, for which I am extremely grateful. You believed in me and supported me during my research work as well as during the writing of this thesis.

Many thanks also to my colleagues from the experimental neurology laboratory, Anastasia Andreadaki, Marcel Kohlhaas, Dr. Heike Diekmann, Dr. Philipp Gobrecht, Dr. Marco Leibinger, Dr. Annemarie Heskamp, Dr. Evgeny Levin and Alexander Hilla.

And of course, by the same occasion, I cannot forget to express my sincere thanks to my colleagues of the molecular neurobiology Laboratory, Dr. Frank Bosse, Marion Hendricks, Jennifer Illgen, Dr. Nicole Brazda, Julia Krebbers, Nadine Hamacher, Dr. Brigitte König, Marcia Gasis, Nicole Schuster, Dr. Jessica Schira, Brigida Ziegler and Dr. Jan Jadasz, who always supported me in my research work. Thank you for a cooperative and helpful working atmosphere, for your support, interest and precious hints. I want especially thank Marion for expert advice on cell culture methods, for your perpetual encouragement and friendship.

I certainly owe many thanks to the members of the Institute for Anatomy II. Especially to Angelika Hallenberger, Hanna Bellert, Ulla Lammersen, Ralf Faßbender, Dr. Amira Ali, Dr. Marion Viktor, Dr. Anna Stahr, Dr. Marc Ingenwerth, Dr. Julian Lommen and Anne Lembach. Your support during the doctoral study is of invaluable estimation. You are not my colleagues, but a part of my family. I love you. Thank you for always being there and accompany me during the good and bad days of this journey, encouraging me every day.

Thank you Anna, for having taken me by the hand without never leaving it, boosting me with self-confidence and positive energy to accomplish the journey that we all dream of. Thank you for listening to me, for providing me with expert advice whenever necessary, for the scientific discussions, for Chicago, your constant support and friendship.

Thank you Amira for you incitation to continue, for believing in me, motivating me and for your friendship.

Vero, Anna and Amira, thank you for offering suggestions for improvement by the correction of the final version of this thesis.

Particular appreciation goes to all my friends, Manu, Elli, Lara, Isa, Lili, Ayse, Angelo, Beate, Aphrodite & Family, Mirela & Almir and Basti & Danica for their tolerance during the writing of this thesis. Your words gave me the necessary energy to go on in my work. Thank you for your support and for distraction whenever it was necessary.

Finally, but first in my heart, I would like to take this opportunity to dedicate this work to my beloved parents: Luigi and Maria Antonietta and my sisters Isabella and Ilenia. You have been always besides me, giving me moral support and helping me emotionally, physically and materially to overcome all the obstacles I faced throughout my studies. I am particularly indebted to you for your never-ending encouragement and ongoing support. I love you!

Also I would like to thank all my relatives, especially my cousins Mari, Anto, Anna and Lia, who are always there whenever I need them as well as my newly gained family, especially Giacoma Lavalle, Lidia Lavalle, Sebastian Straßburg, Giuseppe Lavalle and family and Roberto Lavalle and family.

To my angels, the ones who are looking at me every day from above and stand by me step by step. Thank you, because you are the reason of my motivation and the origin of this journey.

All my love and thanks go to my husband, Daniele Lavalle for his invaluable support and encouragement during the most difficult periods of my work. He gave me the opportunity to find my way and he always believed in me. I cannot put it into words how grateful I am. Sei la mia forza e la mia più grande motivazione. GRAZIE, perché questo traguardo non è solo il mio, ma anche il tuo. Ti amo!